THERMAL MANAGEMENT AND OPTIMIZATION OF HEAT TRANSFER FROM DISCRETE HEAT SOURCES

by

Jean-Marc Katumba Mujanayi

Submitted in partial fulfilment of the requirements for the degree

Masters of Science in Engineering

in the

Faculty of Engineering, Built Environment and Information Technology

University of Pretoria

2016

ABSTRACT

Title : Thermal Management and Optimization of Heat Transfer from Discrete Heat sources

Author : Jean-Marc Katumba Mujanayi

Supervisors : Prof. Tunde Bello-Ochende and Prof. Josua P. Meyer

Department : Mechanical and Aeronautical Engineering

University : University of Pretoria

Degree : Masters of Science (Mechanical Engineering)

These days, the cooling of new generation electronic servers is a challenge due to the immense heat generated by them. In order to avoid overheating caused by the important rise in temperature appropriate cooling procedures must be used in order to meet the thermal requirement. The current study aims at addressing the issue of overheating in this field, and focuses on the thermal management of electronic devices modelled as a discrete heat sources (mounted in a rectangular cavity) with uniform heat flux applied from the bottom. A review of the literature published regarding the convective heat transfer from heated sources as well as a thorough background on the theory of the cooling of discrete sources by forced convection in rectangular channel is provided in this study. It was showed that the heat transfer performance in channel is strongly influenced by the geometric configurations of heat sources. Therefore, the arrangement and geometric optimisation are the main considerations in the evaluation of thermal performance. Unlike experimental methods that were carried out widely in the past, which provided less cost-effective and more time-consuming means of achieving the same objective, in this study we first explore the possibilities and the advantages of using the CD-adapco's CFD package Star-CCM+ to launch a three dimensional investigation of forced convection heat transfer performance in a channel mounted with equidistant heat-generating blocks. Numerical results were validated with available experimental data, and showed that the thermal performance of the heat transfer increases with the strength

of the flow. The second objective was to maximise the heat transfer density rate to the cooling fluid and to minimise both the average and the maximum temperature in the channel by using the numerical optimisation tool HEEDS/Optimate+. The optimal results showed that better thermal performance was not obtained when the heated sources followed the traditional equidistance arrangement, but was achieved with a specific optimal arrangement under the total length constraint for the first case. Subsequently, for the second case study, on the volume constraints of heat sources, the results proved that optimal configurations that maximise the heat transfer density rate were obtained with a maximum of either the height-to-length ratio or the height-to-width ratio. It was concluded that the heat transfer rate to the cooling fluid increases significantly with the Reynolds number and the optimal results obtained numerically are found to be fairly reliable.

Keywords: *Thermal management, discrete heat sources, CFD package, forced convection, numerical optimization, maximise heat transfer, optimal configuration, volume constraints*

ACKNOWLEDGEMENTS

My infinite gratitude goes straight the Almighty God Yahweh, the Master of the times and the seasons who has allowed the realization of this work.

Acknowledgement and thanks are given to my supervisor Prof Tunde Bello-Ochende for suggesting the topic for my dissertation and for his guidance, continuous understanding and encouragement in this project.

My sincere gratitude is expressed co-supervisor and head of the department, Prof Josua P. Meyer, for his technical and financial support during this period of my postgrad studies, which allowed the successful completion of this study.

Recognition and thanks are also due to all my fellow students and the Staff members of the Department of Mechanical and Aeronautical Engineering, especially those of the Thermofluids Research Group for their willingness to help.

Great appreciation goes to the University of Pretoria and the Gauteng Social Development Department for the funding granted for my studies.

Deep thanks are addressed to Aerotherrm for the training and assistance which set me on my way in making the most of the CFD software.

Very special thanks go to my wife Lisette Mwanza, to my mother Julienne Mbiye and to my family members and friends for their continuous encouragement, consistent assistance and prayers throughout the course of my studies.

TABLE OF CONTENTS

LIST OF FIGURES

LIST OF TABLES

NOMENCLATURE

A	surface area, m^2
B	heat source height, m
C	heat source span-wise length, m
$\boldsymbol{C}$	Global thermal conductance
C_p	Specific heat capacity, $J.kg^{-1}$
con	Constraint
D_h	enclosure hydraulic diameter, m
$f(\boldsymbol{x})$	Objective function
G	heat source streamwise length, m
Gr	Grashof number
g	Standard acceleration gravity, m/s^2
H	enclosure height, m
h	heat source height, m
h	Heat transfer coefficient, W/m^2K
k	Thermal conductivity, W.m-1K-1
L	Length, m
N	Dimensionless Normal
n	normal direction
Nu	Nusselt number
obj	Objective
P	dimensionless pressure
p	Pressure, Pa
Pr	Prandtl number
Q	Heat transfer, W
Q’	Rate of heat transfer, W
q	Rate of heat transfer, W
q''	Heat flux, W/m^2
$\tilde{q}$	Dimensionless heat transfer rate

Ra	Rayleigh number
Re	Reynolds number
S	side-to-side distance between consecutives blocks, m
T	Temperature, ºC
t	Time, s
u, v, w	velocity components, m/s
V	Volume, m3
V	Velocity vector
W	Enclosure width, m
X, Y, Z	dimensionless Cartesian coordinates directions
x, y, z	Cartesian coordinates directions
x+	dimensionless distance along the wall

Special characters

α	Thermal diffusivity, m^2/s
δ	Kronecker delta function
∂	Derivative
γ	standard convergence criterion
ν	kinematic viscosity, m2/s
Θ	Dimensionless temperature
Δ	Difference
∇	Gradient function
ψ	Stream function
Φ	Dissipation function
ρ	fluid density, kg/m^3
μ	Dynamic viscosity, $kg.m^{-1}.s^{-1}$

Subscripts

ave	Average
c	characteristic

ch	Channel
cond	Conduction
cons	Constant
conv	Convection
f	Fluid
f	Function
h	Hydraulic
in	Inlet
max	Maximum
min	Minimum
norm	Normalised
dev	Fully developed
opt	Optimum
s	Solid
w	Wall

Superscript

*	Non dimensionalized

CHAPTER 1: INTRODUCTION

1.1. BACKGROUND

Worldwide, the need of better productivity has led to place employees in good working conditions. To increase performance related to the theories of content, based on the needs of the worker according to Maslow in order to achieve effective results, it is so imperious that the working environment must be very comfortable for human being.

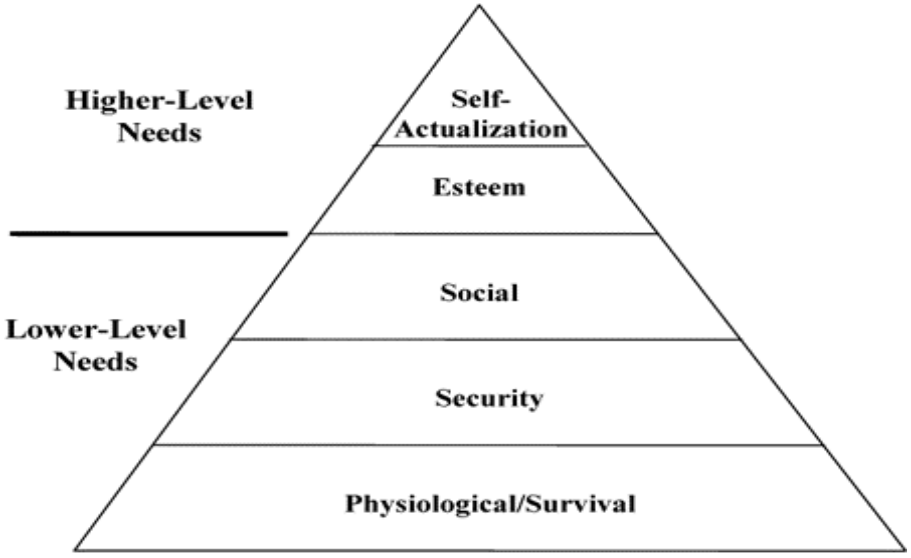

Figure 1-1: Abraham Maslow's hierarchy (pyramid) of needs [1]

The state of comfort in a work area depends on several important factors including the quality of the ambient air: temperature and relative humidity as well as the noise of the environment. As shown on the pyramid of Maslow Figure 1-1, the two first needs for a human are based on the comfortableness of the workspace and therefore depend on the ambient air quality which must follow the standard requirements: 20 to 24°C for the temperature and the relative humidity between 45% and 55% in the ambient air [1].

This present work consist in an approximated study of the only thermal state comfort in a working area wherein there are a defined number of servers or devices that generate heat. The study will focus on a similar thermal management of these heat-generating sources modeled as discrete sources in order to keep the temperature distribution in a certain and acceptable range within the workspace assumed to be an enclosure, emphasizing on the flowing fluid resistance. In this similarity, we suggest that the thermal behavior of a server is identical to that of a heat generating source. Regardless the fact that micro-modeling study carried out on macro phenomenon predicted similar results as seen the literature [2, 3], it has the great advantage of saving time as well as low cost for the study.

The trend in the evolving technology is the continuing increase of power densities and miniaturization in electronics configuration in order to improve the performance of computers as well as electronics, the need of an enhancement of the methods of cooling of electronic components or any other discrete heat source is the focus of several thermal management studies. Over the years, researches have shown how the integrated circuits performance was related to the number of components per each circuit [4].

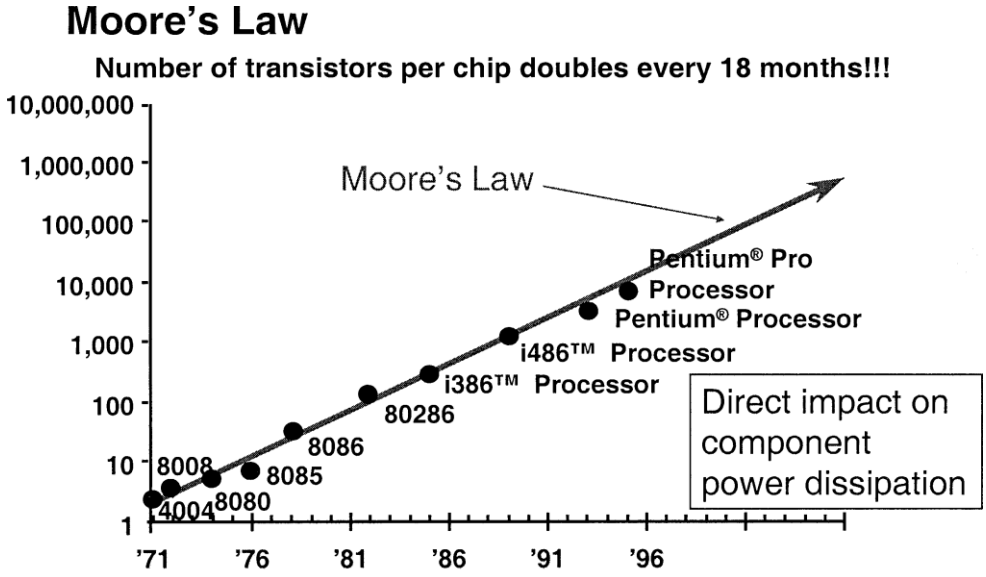

Figure 1-2: Moore's Law: Number of transistor double every 18 years [5]

Table 1-1: Technology roadmap for semiconductors [5]

Characteristic	1997	1999	2001	2003	2006	2009	2012
Process technology (nm)	250	180	150	130	100	70	50
No. of logic Transistor (millions)	11	21	40	76	200	20	1400
Across chip Clock speed (MHz)	750	1200	1400	1600	2000	2500	3000
Die area (mm^2)	300	340	384	430	520	620	750
Wiring levels	6	6-7	7	7	7-8	8-9	9

Although this had firstly led to better application for high performance computers and devices, nonetheless one other main issue kept on rising: the high rate of heat generated from each electronic component because its compactness and miniaturization. This aspect will lead thermal engineers to improve the cooling methods for discrete heat sources because the overheating causes the unit to malfunction and decrease its lifetime by degradation or material fatigue.

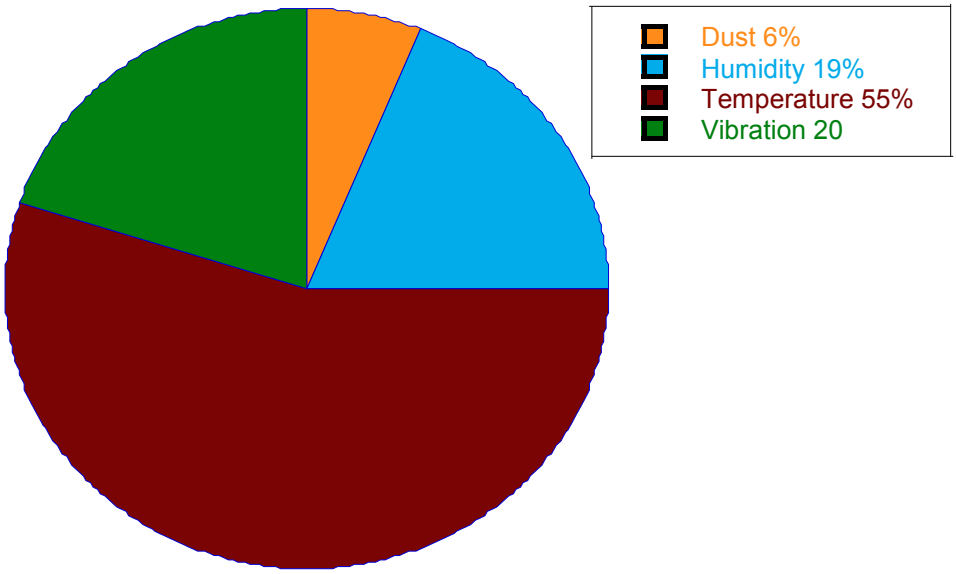

Figure 1-3: Major cause of electronic failure

This being, the overheating temperature is therefore the most important factor of failure for electronic equipment as shown on the figure above. As temperature and heating were noticed as being the predominant factors for reliability and effectiveness of electronic equipment, the major concern of scientists have been to find a reliable way to apply the cooling method. In the design of electronic equipment, permanent cooling remains a major concern in full operation as the released heat reaches up to 400w/cm2 [5-7] despite all the precautions that have been taken.

Cooling means transfer of heat from a heat source to a cooler one. This can be done in various ways or mode of heat transfer:

1. Conduction: is the transfer of energy as a result of interaction between adjacent particles due to the fact of thermal difference between them. it occurs in fluids and solids;

2. Convection: the transfer of energy occurs between a solid surface and the flowing fluid around it. Convection results of a combination of conduction and fluid motion;

3. Radiation: it happens when the energy is transferred (because of temperature difference) in the form of electromagnetic waves and therefore radiation does not require any medium to occur.

Several studies using different methods and systems have been investigated in order to perform effective cooling of heated sources in channels according to the thermo-physical configurations and based on the mode of use of different equipment. In this context of electronic equipment the most encountered in the literature are heat sinks, micro heat exchanger, and thermoelectric coolers, spray cooling and direct convective cooling methods.

Speaking of cooling of electronics by fluid flow, the two methods are convection heat transfer by gases and by liquids. We will conduct the air cooling by forced convective heat transfer in this study as the physical model being studied is a modeling of servers in a room that cannot be cooled by liquid. In order to enhance heat transfer from discrete sources, a forced convection heat transfer will be carried out in order to maintain components temperature at a satisfactory level required for reliability. In this regard, we can describe the thermal management as the fact of applying the most efficient cooling mean in other to keep the studying area in a satisfactory thermal environment, as well as to control of the flows patterns and the thermal characteristics variation: temperature gradient, thermal resistance and conductance, streamlines, and heat fluxes variation.

Cooling of electronics packages by free or forced convection emphasizing on thermal considerations and geometric constraints have started since the eighties with Pantakar, Incropera and others researchers. Earlier studies were basically experimental and analytical, gradually and as the years pass and possibly under the effect of miniaturization and complexity of electronics packages, until today we are experiencing the use of very powerful numerical methods implemented in software using Computational Fluid Dynamic (CFD) codes. It has been proven that, under general physical and thermal considerations, most recent numerical results related to cooling of heat-generating sources in channel are in good agreement with those previously predicted.

1.2. CONVECTION MECHANISM OVERVIEW

Convection is a mode of heat transfer between a surface (of a solid) and the surrounding and flowing fluid (liquid or gas) that occurs at their interface. It is also the mechanism of thermal interaction between both a solid and the surrounding fluid that is in motion or between two fluids. The factors that mainly influence convection heat transfer between a solid and the adjacent fluid are the thermo-physical characteristics of the fluid such as the temperature gradient, type of fluid, velocity and so forth. When the bulk motion of the

fluid is caused by an external agent (fan, pump...), the mode of heat transfer is called Forced convection. But when the fluid motion is only due to buoyancy forces because of temperatures gradient that produces differences in densities, the mode is said to be Natural or Free convection. In any of these two case or more, in the case we have both modes in during the mechanism called mixed convection. The rate of convection heat transfer was earlier expressed by Fourier [8] and later on, it was published as Newton's law of cooling [9]:

$$Q''_{conv} = hA_h\left(T_h - T_f\right) \tag{1-1}$$

Where T_h is the surface temperature and T_f is the temperature of the fluid sufficiently far from the surface. h is the coefficient of heat transfer by convection between the surface (solid) and the adjacent fluid; h depends on all the variables influencing the convection such as the surface geometry as well as the thermo-physical properties of the cooling .

At this stage we can also define mathematical expressions of important parameters or basic dimensionless numbers which thoroughly describe thermal and physical behavior of the convective heat transfer mechanism [9].

Those are:

- Grashof number Gr represent the ratio between thermal buoyancy forces and viscous forces in natural convection:

$$Gr = \frac{g\beta\left(T_h - T_f\right)L_c^3}{\nu^2} \tag{1-2}$$

  L_c is the characteristic length of the geometry

- Prandtl number Pr that describes the ratio of sensitivity to convective or diffusive of momentum to the diffusivity of heat transfer in a material. For a material, the higher is Pr, the greater significant changes in the fluid flow no matter the flow velocity:

$$\mathrm{Pr} = \frac{\mu C_p}{\alpha} = \frac{\nu}{k} \tag{1-3}$$

- Rayleigh number Ra, it is the ratio between thermal buoyancy forces and viscous forces:

$$Ra = Gr\,\mathrm{Pr} = \frac{g\beta\left(T_h - T_f\right)L_c^3}{\nu^2}\mathrm{Pr} \tag{1-5}$$

- The Reynolds number Re, expresses the ratio of the dynamic forces in the fluid to the viscous forces. It is given by:

$$\mathrm{Re} = \frac{UL_x}{\nu} = \frac{\rho UL_c}{\mu} \tag{1-6}$$

- The Richardson number *Ri*, defined as the ratio of Buoyancy to the vertical shear effects

$$Ri = \frac{g\beta\left(T_h - T_f\right)L_c^3}{U^2} = \frac{Gr}{\mathrm{Re}^2} \tag{1-7}$$

- The Nusselt number Nu, which is the ratio of the coefficient of convective heat transfer to the coefficient of conductive heat transfer; its basic expression is :

$$Nu = \frac{hL_c}{k} = -\frac{1}{\theta_h}\frac{\partial\theta}{\partial N}\bigg|_h \tag{1-8}$$

Where θ is the dimensionless temperature, it will be defined later in this work in Eq. (4-6). And N is the dimensionless normal.

- The local and average Nusselt number over a heat source will be given respectively by [10]:

$$Nu(x,y) = \frac{d\theta}{dZ}\bigg|_h \tag{1-9}$$

$$Nu_{ave} = \frac{1}{A}\int\int_{A} Nu(x, y)dxdy \tag{1-10}$$

1.3. DISSERTATION OUTLINE

During the last few decades, the search of significant performance of computer systems, commercial and military power supplies as well as telecommunications modules had led to a conception of higher transistor integration densities, faster electronic chips and therefore miniaturization of integrated circuits (Printed circuit Board) [4]. However, the improvement of performance level of microelectronic devices increase power dissipation and therefore enhances the chip level heat fluxes (critical heat flux CHF) and have the potential to reach the higher value, up to 400W/cm^2.

As mentioned previously, this work focusses on the study of thermal patterns and geometric characteristics of servers in room modeled as discrete heat sources (electronic) in a rectangular enclosure. In this purpose according to a chosen set of thermo-physical considerations, a theoretical and numerical method will be carried to simulate the cooling of the aligned discrete sources in the enclosure with air in the Reynolds numbers range from 250 to 1000, based on hydraulic diameter. Thereby, with an emphasis on the geometric and thermal considerations such as dimensions and arrangement of discrete sources, generated heat, gradient temperature in the enclosure, flowing fluid resistance, simulations results from this work suggest that the contribution of natural convection (buoyancy factor) is negligible compare to forced convection which will only be considered in this study.

In this regard, the numerical optimization methodology will consist in finding the optimal blocks configurations that will improve the global thermal conductance between the heat-

generating sources and the cooling fluid, meaning maximize the heat transfer density rate to the cooling fluid by forced convection. The flow is limited to a laminar flow regime, and the configuration of the model will consists in five identical and equi-spaced heated blocks mounted on the bottom wall of a rectangular enclosure.

Convection heat transfer which is the only heat transfer mode in presence is basically expressed by Newton's law of cooling [9] as already given by in Equation 1-1 in Section 1.2. Thus the convection mechanism depend essentially on the rate at which heat convection is transferred between a solid and a fluid per unit surface area per unit of difference in temperature; on the total heat transfer surface area and on the difference between the temperature of the surface and the surrounding fluid. However, it may be expressed otherwise: in a differential and integral formulation because of the thermo-physical properties of the model. It turns out that results of this thermal mechanism (convective heat transfer) is mainly interpreted in accordance with the resulting Nusselt number and temperature contours that vary with the Reynolds numbers which depend on the flowing fluid characteristics.

Convection being a mechanism of heat transfer between a solid and the surrounding fluid at different temperature may be free or forced. In the first case the fluid is stationary meaning no motion. In the second one, the rate of heat transfer is very significant as the fluid motion is driven by an external agent (fan, pump…). However in this last case, there is usually a non-negligible amount of heat transfer by free convection, such phenomenon are commonly known as mixed convection. During this type of mechanism, the cooling fluid is described by a set of four partial differential equations named as governing equations for fluids. It appear that solving mixed convective heat transfer equations coupled with governing equations in which are related thermal properties to physical characteristics is quite complex to be done manually because of the non-linearity.

Table 1-2: General typical values of h [11]

Process	Free Convection		Force Convection		Phase Change
	Gases	Liquids	Gases	Liquids	Boiling and Condensation
h (W/m^2 ^{o}C)	2 - 30	10 – 1000	25 – 250	50 – 20,000	2500 – 100,000

That why the need of using analytical methods or numerical procedures (Finite methods, numerical algorithm…) implemented in computer-based simulations codes such as Computational Fluid Dynamics CFD (Star-CCM+, Ansys-Fluent, Open Foam…) are required.

1.4. OBJECTIVE OF THE WORK

The objectives of this study are:

a. to geometrically optimize the heat-generating blocks in such a way that the global thermal conductance or the heat transfer density rate from the heated blocks to the cooling fluid is maximized leading to the minimization of the peak temperature in the enclosure

b. to conduct this optimization using a multidisciplinary automated algorithm implemented in the new numerical optimization tool add-on to a computational fluid dynamics (CFD) Package.

1.5. SCOPE OF THE STUDY

In this dissertation, a CFD code is used in three dimensions to conduct simulation for a laminar forced convection within a rectangular enclosure mounted with in-line heat generated blocks on its bottom wall. From this simulations results a numerical optimization design code that uses automated and multidisciplinary optimization algorithm which is efficient and robust is thereafter applied to computational domain in

order to maximize the heat transfer density rate depending on design variables and subjected to various constraints. In order to maximize the removal of heat from heated blocks and to minimize the peak temperature in the enclosure, the scope of this study will consists in these two cases:

a. to find the optimal blocks arrangement (optimal spacing)
b. to find the optimum blocks' geometry (optimal shape)

1.6. ORGANISATION OF THE DISSERTATION

For a better understanding of our work, this dissertation is divided in seven chapters that are also subdivided into different sections and subsections. Besides this present introduction, our study is organized as follows:

- Chapter Two consists in five sections whose contents provide review of relevant literature that summarises works related to numerical modelling studies and especially to thermal performance investigations emphasising on important factors in optimization of the cooling of heat-generating sources in channel.

- Chapter Three describes the flowing fluid motion and computational domain for the forced convection simulation. In this chapter the mass, momentum and energy conservation equations governing the transport of mass and heat are detailed. This chapter also defines the iterative method of coupling these governing equations.

- Chapter Four presents the applied CFD Code Star-CCM+ and provides the simulations results of the forced convection heat transfer in the enclosure.

Validation of the numerical procedure is done in this third chapter by comparing simulations results with experimental data.

- Chapter Five outlined with the Numerical Optimization Code HEEDS-Optimate+ to be applied. This chapter highlights the guiding principles of this optimization code that uses the SHERPA Algorithm.

- Chapter 6 performs the geometric optimisation by applying the numerical optimisation methodology presented in Chapter Five to two optimisation case studies. The first Study case deals with optimal spacing between heated blocks while the second one focuses on three-dimensional optimal blocks' geometry. Comparison with results from similar investigations documented in the literature is also done in this chapter.

- Chapter Six provides a general summary, gives conclusions and suggests recommendations for future work.

CHAPTER 2: LITERATURE REVIEW

2.1. INTRODUCTION

The cooling and the control of electronics equipment look very complex and require certain tact in the way to apply the suitable cooling method in order to stay below a given peak of temperature for the all system regarding the geometry of the set up. According to reliability considerations, this issue led thermal engineers to study and investigate the fundamentals mechanisms of fluids flow and heat transfer from discrete heat sources flush mounted on a flat plate or in a rectangular enclosure either on a vertical wall or on a horizontal (as well on inclined plane) in one-, two- , and three-dimensional direction .The cooling fluids used are: air (mainly), water, the fluorocarbon FC-77 or FC-72 and FC-87(rarely) as well as R-113. After a complete thermal modeling of equipment, the studies were carried out considering the conduction, the convection (natural, forced, mixed) as well as the radiation heat transfer.

2.2. MICRO-MODELING SIMILARITY AND VALIDATION

Generally experimental research investigations in industries are very expensive costing and are time consuming because of several factors including environmental constraints such as human and material resources. Thereby, scientists while seeking to preserve their envisaged results effectiveness, they are always trying to reduce the effort to achieve their goals in less time over the miniaturization of the model and using appropriate software for the phenomenon being studied. In this context, several investigations based on miniaturization of the model and on the simulation of mechanism of phenomena have led to very similar results to real model.

Chen and Xu [2] presented a new zero-equation CFD model that uses less computer memory and run ten times faster than the standard k-e model to perform three dimensional numerical simulation for distributions of the velocity and temperature of the air and contaminants concentration in a room, For natural, forced and mixed convection, the results agreed reasonably with those obtained using the k-e model as well as with experimental data.

In the same way, Li *et al.* [11] carried out micro-scale climate numerical simulation using new two-layer zero-equation turbulence where the turbulence viscosity is assumed to be a function of the velocity deformation rate, the mean velocity as well as the length scale in both the inner and the outer layer. The results were similar to wind-tunnel experimental data and matched with using standard k-e model.

In [3] McCarthy micro-modeled and used Particle Dynamics Simulations method to describe an experimental and computational investigation of the effects of cohesion on mixing and on segregation in simple flows. He showed how cohesion may increase the rate of mixing in tumbler devices and predicted the macroscopic behavior of cohesive materials to the relevant inter-particle forces together with the effect of cohesion on segregation, more complex than originally.

A three dimensional numerical study was carried out in by Feurish and Olsen [12] to find the free surface of supercritical flows location using Star-CCM+ as CFD codes for different cases. In order to validate their results, they used two idealized channel geometries from literature: one with a channel expansion and another with a channel junction. In both cases, oblique standing waves occurred as the numerical model reproduced the geometry of the waves. The third case was a complex study that modeled physical laboratory study of natural river geometry upstream of the dam of a hydropower. After visualization, the numerical model of this unusual case showed supercritical flow

and oblique standing waves that occurred upstream of the dam also gave reasonable results for the location of the free water surface.

2.3. THERMAL MANAGEMENT OF ELECTRONICS

The need of thermal management of electronics has increased because of overheating issues in electronics. Previous investigations and performance comparison studies have been carried out on forced-convection heat transfer with emphasis on the critical heat flux (CHF) of microelectronic heat sources. Analytical, experimental and numerical procedures using different cooling fluids have therefore been conducted.

Bar-Cohen [13] in his study on the cooling phenomenon and elimination of thermal contact resistances at highly-loaded solid interfaces through the use of direct liquid cooling by convection, impingement forced convection, and boiling incipience, observed that using a dielectric liquid (FCs) was most efficient than water in cooling of electronics.

Bergles and Ma [14] utilized a specific test apparatus to study heat transfer characteristics for cooling of simulated microelectronic chips by boiling jet impingement using saturated or sub-cooled R-113 based on the jet velocity to accommodate the heat fluxes from heated chips electrically at power levels well above those expected during normal operation. Taking the free convection boiling data as reference, for several jet velocities directed at two positions on the heated sources, they observed that the burnout heat flux was proportional to the cube root of the jet velocity.

Suresh V. Garimella [15] reviewed recent advances in several applications for cooling high-performance emerging electronics. In this work the author discuss both experimentally and theoretically modeling the applicability as well as the efficiency of

each of the cooling method regarding thermal management of electronics such as micro-channel transport and micro-pumping techniques, jet impingement, miniaturized heat pipes, transient phase change energy storage systems, smart piezoelectric fans, and enhancement of interface contact conductance.

Performances comparison studies have been conducted in two-dimensional on forced-convection regarding thermal management of microelectronics heat sources emphasizing on the between theoretical and experimental methods using FC-77 by Incropera *et al*. [16], using FC-72 [17] as well as between numerical and experimental procedures using water or FC-77 [18]. After analyzing final results for an array of twelve heated sources in four rows mounted on a rectangular horizontal wall, considering the Reynolds number ranged from 1000 to 14000, in terms of the Nusselt number and thermal characteristics their observed that experimental data were found to be in good agreement with theoretical or numerical predictions.

2.4. EXPERIMENTAL FORCED CONVECTION HEAT TRANSFER FROM DISCRETE SOURCES

And as far as the years went, thermal control of equipment had become a very imperious concern. On a thermal management point of view which aims for the maximization of heat removal in order to keep the element under an allowable temperature for functional reasons, forced convection was unable to reach proper cooling performance because of the excess heat generated. However, for reasons of power consumption, reliability, reasonable cost, air forced convection was found to be more advantageous from cooling methods for electronics equipment [19]. Avoiding cumbersome equipment in thermal control studies of heat from discrete sources was the reason why researchers focused on air cooling of microelectronics heat sources by natural, force and mixed convection as well as conjugate heat transfer.

Chadwick *et al.* [20] undertook experimental and theoretical study of natural convection (2-D) of discrete heat sources fixed in a rectangular enclosure on vertical wall and proved by the mean of numerical solution using SIMPLER algorithm, that lower heat source was marginally influenced by the above on .

Sultan [21] experimentally studied the passive cooling of multiple protruding heat-generating sources in a horizontal channel with perforated holes are arranged in the base of channel in a staggered manner in two rows between heat sources. After analysing the forced convection heat transfer mechanism, they found that increasing holes-open area ratio β enhances the thermal performances such as it decreases the maximum surface temperature and improves local Nusselt with a maximum increase of 33.15% which corresponds β = 0.0589. However the best holes/open area ratio is found to be β = 0.0409 with 16 holes of 2.5 mm of diameter.

Mc. Entire and Webb [22], investigated both experimentally and numerically in two dimensions the local forced convective thermal characteristic of the cooling of heat sources flush mounted as well as protruding on the bottom wall of a channel. For Reynolds number ranged from 1000 to 10000, their results show how the thermal characteristic were strongly influence by the geometric parameters such that the The amount of the increase varied between 5 and 50% for the range of Reynolds number and dimensionless wall spacing investigated. Indeed, the observed a heat transfer enhancement from heater to heater due to the interruption of the thermal boundary layer in the intervening adiabatic spacing while the flow separation and associated vena contracta effects enhanced the heat transfer particularly for subsequent heaters downstream. From Re = 2000 flow visualization results illustrated the fact that the flow separation and the onset of turbulent flow increased heat transfer for protruding heat sources. Furthermore they show also how decreasing the channel wall spacing decreased the heat transfer rate because of a decrease in the effective measured flow area.

2.5. NUMERICAL FORCED CONVECTION HEAT TRANSFER FROM DISCRETE SOURCES

Similar investigations as in the previous Section were also conducted using different numerical methods to study as well as to enhance thermal performances of cooling mechanism of heat-generating sources in channels by convection. On a thermal management point of view, simulations results were found to be in good agreement with experimental data and showed that the overall thermal performance of electronic equipment depends not only on its thermal characteristics of the equipment but also on the geometric configuration of the heat sources .

In [23] Choi and Ortega presented after numerical procedure important and fundamental aspects of mixed convection on an inclined plate mounted with discrete heat sources. The investigate the effects of laminar forced flow on buoyancy-induced natural convection cells throughout the regions of natural, mixed, and forced convection for $10^3 \leq Gr \leq 10^5$; $0.1 \leq Re \leq 500$ at Pr = 0.7 1. At low Re and high Gr they observed that flowing air from the exit section changes the flow and temperature fields significantly but the flow reversal does not noticeably influence the heat transfer coefficient on the module. It was also seen that the overall heat transfer performance varies with the inclination angle with a maximum at an angle equals to 0 (vertical orientation).

Premachandran and Balaji [24] numerically reported in 2-D results of their numerical investigation of conjugate mixed convection with surface radiation from a horizontal channel mounted with four aligned heated parametric. They study the effect of the Reynolds number, Grashof number and thermal characteristics on the heat transfer flow characteristics of sources in a channel. Keeping the geometric parameters such as spacing between the channel walls, size of the protruding heat sources, thickness of the substrate and the spacing between the heat sources are fixed unchanged, they showed that the convective as well as the radiative thermal effect varies with the Reynolds

number. They also developed a correlation for the non-dimensional maximum temperature using the method of asymptotic expansions.

Alves *et al*. [25] worked out the average Nusselt numbers for a laminar airflow convection of three discrete heat sources flush mounted to a wall of parallel plates channel for a developed flow and for a developing flow. A numerical procedure was applied to evaluate the convective heat transfer coefficient for each source. As a result, they found that, based on a constant Prandtl number, the average Nusselt number for each heater was in fact function only of the Reynolds number however the overall Nusselt number for the three heaters depended also on the heat flux distribution in both cases. They then deduced that the resulting values of a single heater could be applied to predict the average temperature for any other thermal condition with a larger numbers of active heaters.

Yutaka and Mohammad [26] simulated the cooling of a printed circuit board by computing the periodic fully developed heat transfer characteristics for laminar convection cooling flow throughout an array of square blocks uniformly heated from the bottom that are deployed along one wall of a parallel-plate channel. For a specific range of Reynolds numbers close to 1000 Results showed that he Nusselt number can be predicted by a two-dimensional model depending on the geometric parameters. For high values of thermal conductivity, they observed surface temperature of each block was almost uniform and the maximum values heat flux occur at the corners of the top surface.

The Micro Electronic Thermal Analyzer (TEMA) was implemented in by Culham *et al.* [27] to analyze thermal characteristics of a conjugate heat transfer model for air cooling of circuit boards with arbitrarily located heat sources. For the studied model, investigation results show non-negligible effect of heat conduction through the substrate

and significant radiation heat transfer contribution to the global heat transfer. The resulting thermal flow characteristics were in good agreement with experimental data.

Cheng *et al.* [28] investigated a three dimensional numerical analysis of laminar mixed convection of four heat sources flush-mounted on the horizontal wall of a rectangular utilizing the SIMPLEC algorithm. They showed that the enhancement of convective heat transfer depended not only to the velocity field and temperature field but was related to the field synergy which strongly affected the thermal performance. It includes these four parameters: Richardson number, heat source distribution and channel height and inclination angle.

Cheng *et al*. [29] performed with a 3-D numerical method using the newly proposed algorithm CLEARER on collocated grid to simulate the cooling of electronics. They focused on the influence of openings on the substrate, heat source height and their distribution along the substrate on the maximum temperature and overall Nusselt number. In the results it was noticed that the Nusselt number increases with the Reynolds number, was further improved up to 10 %. Global thermal performance can be greatly improved both by a specific arranging the heat sources and by better synergy between the velocity and temperature which can guides in the design of electronic.

In their study Hung and Fu [30] analyzed and compared the effect of natural, forced and mixed convective heat transfer from heat sources mounted on parallel plates and cooled by air. They numerically carried out the solution from discretization of the governing partial differential equations followed with simulations using the CFD Package PISO. Based on the grids points' configuration and the artificial geometrical modification, the resulting flow characteristics and the temperature distribution revealed an optimal configuration due to the global heat transfer which depends of the local Nusselt number

along the surface where the forced convection is dominant. They concluded that the forced convection is decreasing from the inlet to the outlet, while the natural convection is increasing in the same direction with the flow.

An invariant descriptor was developed by Alves *et al*. [31] based on conjugate influence coefficients g+ which were grouped in a square matrix G+ for the conjugate cooling of discrete heaters to evaluate distinct convective heat transfer coefficients of three heaters in a channel . Considering the Reynolds number in the range from 600 to 1900, for the heaters′ height in the channel ranged from 0.05 to 0.35 of the channel height and assuming a thermal conductivity equal to 500 that of the air their results showed that the resulting values of a single heater could be applied to predict the average temperatures for any other thermal condition with a larger numbers of active heaters. They also observed that the adiabatic heat transfer coefficient depends solely on the flow and the geometry.

Young and Vafai [32] reported in two dimensions experimental and numerical investigations of the forced convective heat transfer of individual and arrays of multiple for Reynolds varying from 800 to 13000. For input heat flux of $950 \leq q'' \leq 20200$ W/m2 they analyzed the effects of parametric changes in the Reynolds number, channel height, geometric configuration on the Nusselt numbers and heat obstacles temperature variations. From their results they established a set of correlations characterizing the heat transfer from the protruding heat sources based on the various pertinent thermo-physical parameters. The mean heat transfer from heated obstacles within the channel which is correlated with the airflow Reynolds number and the experimental mean Nusselt numbers were found to be in good agreement with the numerical model. It was learned that taller obstacles were found to enhance the thermal transport from obstacles further downstream by increasing the mixing and impingement as the core flow expands and reattaches.

A numerically study was conducted by Zeng and Vafai [33] to analyse the Reynolds number, channel clearance height-to-element length ratio, spacing-to-channel height

ratio, geometric ratio of the blocks, and total number of obstacles variation effects on the forced convective cooling of an array of heated obstacles. After several simulations, considering four heated blocks and Reynolds number in between 200 and 2000, they came up with comprehensive correlation representing convective cooling of the heated obstacles and incorporating all the above pertinent thermo-physical parameters. This correlation gave a comprehensive average error less than 10% against all of the numerical simulation data. They also found that for $Re_{Dh} \leq 1500$, obstacles enhanced the heat transfer when there were taller and slender.

Ghasemi and Aminossadati [10] carried out a two dimensional numerical investigation to model thermo-physical air characteristic for a mixed convection heat transfer from discrete heat sources based on the heat dissipation and the temperature distribution. Analyzed results concluded that the thermal performances depended on the number as well as the geometric arrangement of discrete heat sources such as at any Rayleigh number, placing less heat sources on the bottom wall results in a higher heat transfer however at high Rayleigh numbers, the influence of the position of the heat sources on the maximum surface temperature was negligible. It was seen that increasing the Rayleigh number increasing heat transfer rate and decrease the maximum temperature which also varied with flow.

M. El Nakla [34] studied the effects of Reynolds number, element (rib) height, element width, element-to-element spacing and the variation of heat flux distribution of the elements on the average Nusselt number and heat transfer coefficient in two dimensional using a commercial CFD package. Simulations results showed that global thermal performance is strongly affected by the geometric characteristics and it varies with the flow turbulence and mixing characteristics that increase with the Reynolds number. The average Nusselt number was thereby correlated to each variable parameter using regression analysis. Indeed they observed an enhancement of the heat transfer rate due to the increasing of both the spacing and the height of the heated elements. However the heat transfer enhancement was limited by spacing-to channel height ratio value of 0.4 and by specific element height-to-channel height ratio depending on the compromise between

the pressure drop and the supplied fan power. Finally, major finding of the numerical study was the negligible effect of heat flux profile on the average Nusselt number.

2.6. OPTIMIZATION OF HEAT TRANSFER PERFORMANCE FROM DISCRETE SOURCES

So far it has been seen that the global heat transfer from discrete heat sources was not only a function of thermo-physical properties of the equipment but also depended on the geometrical arrangement as well as the aspect ratio. Thus in order to optimize the rate of heat from sources, thermal engineers emphasized on the geometric aspect ratio as the thermal and physical material were already know and for some time in industry the growing need to achieve better performance has always led researchers to come up with effective processes.

In order to prevent or to avoid limitations shown by air convection method, the need of optimization of some pertinent geometric parameters was inevitable to reach better cooling performance. That is how some researchers have begun to focus more on optimization studies of geometric parameters to improve the cooling mechanism in electronics equipment using different method.

An optimal spacing of four heated chips mounted on a conductive substrate of a horizontal channel was numerically investigated by Y. Liu *et al.* [35], in order to improve e the global thermal performance. The utilized an Operator-Splitting Pseudo-Time-Stepping Finite Element Method to solve the problem using the Boussinesq approximation where the density in the buoyancy term is temperature dependent . Their observed that the equi-space arrangement was not the optimal one, however when the center-to-center distances ratio between two consecutive heated elements was larger than 1.2, there was a significant decrease in the maximum temperature and increase in global thermal performance compared to the ratio of 1.0.

Similarly, an optimization investigation related to spacing between simulated electronics entities in channels was experimentally executed by Chen and Liu [36], for cooling of nine (three-by-three) resistors mounted on a substrate by forced convection. From the results, it was concluded that the conventional equi-spaced arrangement is not an optimum option for cooling electronic packages as the temperature of heated sources strongly depended on the spacing arrangement with specific results such the thermal performances varied with the geometric series arrangements of center-to-center distances of resistors. They showed that for a fixed Reynolds number of 800, when the side-to-side distance of two consecutive elements follow a geometric ratio range from 1.6 to 1.8 a good cooling performance is reached.

A.K. da Silva *et al.* [37] observed that the spacing between heated sources has a strong effect on the global thermal performance and there is an optimal non-uniform distribution to allocate discrete heat sources to the space on a wall cooled by forced convection. These results were also confirmed after a comparison with those obtained from numerical simulations.

A theoretical and numerical analysis of the distribution of heat sources on a horizontal wall of a convergent duct was carried out by Jassim and Muzychka [38].They observed that the model that optimized the density of heat transfer by forced convection regarding geometric properties together with free stream velocity was a non-uniformed distribution of the heat sources on the wall. Then the performance of the process could be improved by reducing sources right after the leading edge.

Nowadays, numerical optimization tools are added-on to numerical methods process in order to performed automated design (in minimizing or maximizing objectives functions). This presents important advantages such as multidisciplinary design optimization, varieties of constraints, simple and easy to use, fast procedure compare to experimental

and analytical methods as illustrated [39, 40] where the computational results showed very good agreement with experimental data with reliable optimal results.

It should also be noted that recently, constructal theory was also used to perform optimization studies in thermal sciences [41-46]. It is a powerful method in particular for forced convection heat transfer mechanism as it helps to optimize geometries together with spacing between heated elements in order to get maximum thermal performances.

A dual effect of size and spacing of a finite number of heat sources on the heat transfer characteristics of heat-generating mounted on a the horizontal wall of a channel was studied by Hajmohammadi *et al.*[47]. By solving governing equations numerically and using Constructal theory they showed that the global performance depends on the sizes and the number of heat sources as well as on optimal adiabatic spacing between heated sources.

Bello-Ochende et al. in [46] used constructal theory to conduct numerical procedure to determine the optimal configuration of a two rows of pin-fins that maximizes the total heat transfer rate by laminar forced convection. The optimal configuration obtained numerically was found to be in good agreement with scales analysis predictions since conduction along the fins and convection transversal to the fins were well balanced.

2.7. CLOSURE

All the literature we have covered so far show us some related and important work done as well as investigations undertaken regarding the cooling of discrete heat sources mounted on a flat wall. Numerical Optimization presents a comprehensive and up-to-date description of the most effective methods in continuous optimization. It responds to the

growing interest in optimization in engineering, science, and business by focusing on the methods that are best suited to practical problems.

Looking through all our literature we saw that in order to achieve optimal thermal performance of cooling of heat-generating sources, different studies have been conducted experimentally, theoretically, analytically and numerically using different procedures. It follows that, in most of the case the resulting thermal profiles together with the flow characteristics under the same considerations (assumptions, thermo-physical properties and geometric configuration) were found to be in good agreement for different methods applied. In conclusion, based on general thermo-physical considerations, the thermal performance characteristics and optimal configurations were deducted accordingly.

CHAPTER 3: NUMERICAL MODEL AND MATHEMATICAL FORMULATION

3.1. INTRODUCTION

This chapter describes the heat transfer phenomenon that occurs within our computational/numerical model. A three-dimensional fluid flow and heat transfer form heated blocks mounted on a horizontal wall of a rectangular enclosure under forced convection in the laminar regime will be analyzed. A commercial CFD code is used to discretize the computational domain as well as to solve the governing equation of transport for mass and heat transport.

1.2. NUMERICAL SOLUTION SCHEME

The study of fluid flow and heat transfer problems has recently been made easier by the implementing CFD software packages which use numerical method and algorithms in thermo-fluids analysis. CFD is a powerful engineering tool that helps by mean of computers to solve the governing equations of fluids flow. These equations are very complex and complicated to solve analytically because they are partial differentials equations (PDEs) while in numerical procedure, the PDEs are substituted by a system of algebraic equations easy to solve using a commercial CFD. Numerical procedure also shows a great advantage compare to experimental methods by the fact that experiments are very expensive and time consuming.

A standard procedure followed in CFD codes while proceeding with numerical solving of fluids flow problems consist in these three main stages [48].

1. Pre-Processing: this step involves:
   - Definition of the computational domain
   - Grid generation
   - Setting and modelling of the phenomenon as well as fluids properties
   - Specification of boundary conditions
2. Solving process: at this stage, the following operations are being conducted:
   - Integrations of the governing equations
   - Discretization
   - Solving of algebraic equations
3. Post-processing: by the mean of specific tools and others facilities different results are obtained:
   - Display of the computational domain discretized (grid)
   - Visualisation of solution
   - Various plots as well as particle tracking

The commercial CFD code Star-CCM+ 8.02 is used to discretize the computational volume with grid generation as well as to solve the PDEs together with the boundary and initial conditions that describe the forced convection heat transfer in the computational domain. These equations are being transformed in a set of algebraic equations using a finite method approach. The pressure-velocity coupling is solved using the Semi-Implicit Method for Pressure-Linked Equations (SIMPLE) [49] well explained by Patankar and Spalding [50].

3.3. COMPUTATIONAL DOMAIN AND MESH GENERATION

The computational volume is subdivided in a finite number of discretized control volumes which the physical solvers use to provide numerical solution of the governing equations. In the Star-CCM+ packages [49], different functions and mesher options, which consist in an automated grid generation tool, are implemented in order to unable the user to generate quality mesh according to the geometries and to the process (chemical, physical or thermal). In addition to the fact that meshing options are suitable for different applications, the mesher process within Star-CCM+ has the advantage of being flexible, repeatable, and easily applicable even for complex geometries.

The domain is discretized using a polyhedral meshing of the core volume obtained using a finite volume approach (which is a finite volume method FVM) for segregated flow where the second order upwind scheme is used for the diffusive terms and the convective terms in the momentum and energy equations. At this stage it's also important to point out that when using Star-CCM+, the user must decide in choosing the mesh model (trimmed, polyhedral or tetrahedral) depending on several parameters such us:

- The available time for building the specific mesh on the model
- The tagged accuracy and convergence rate for the solution
- The available computer memory
- The type of mesh: single or multi-region
- The quality of the starting surface mesh and
- The size of the geometry: thin or not

3.4. MATHEMATICAL FORMULATION OF GOVERNING EQUATIONS

The generalized mathematical expressions that govern the fluids hydrodynamics as well as the heat transfer process are known as governing equations. These equations are non-linear and partial differential equations (PDEs) and they describe the three following fundamental laws:

1. Conservation of mass (Continuity equation)
2. Conservation of momentum (Navier Stokes or momentum equation)
3. Conservation of energy(Energy equation)

In the Cartesian coordinate system the non-dimensional equations of continuity, momentum and energy conservation [51] using the enclosure hydraulic diameter D_h as the characteristic length are:

3.4.1. Conservation of mass

The conservation of mass is governed by general form of the continuity equation

$$\frac{D\rho}{Dt} + \rho div\vec{V} = 0 \tag{3-1}$$

Here t represents the time; ρ and $\vec{V}$ are respectively the density and the velocity vector of the fluid.

As we assumed the fluid to be incompressible, therefore the density ρ is being constant the continuity equation is reduced to:

$$\rho div\vec{V} = 0 \tag{3-2}$$

3.4.2. Conservation of Momentum

The conservation of momentum is governed by the momentum equation also called Navier Stokes equations derived from the Newton's second law for Newtonian fluids. Using the Kronecker delta function δ_{ij} and λ is the vexing coefficient associated with volume expansion [52].

$$\rho\frac{D\vec{V}}{Dt} = \rho g - \nabla P + \frac{\partial}{\partial x_j}\left[\mu\left(\frac{v_i}{x_j} + \frac{v_j}{x_i}\right)\right] + \delta_{ij}\lambda div\vec{V} \tag{3-3}$$

With g, the vector acceleration gravity; P, the hydrostatic pressure; x, the spatial coordinate; μ, the coefficient of viscosity and v, the velocity component

Based on the Stokes hypothesis, $\lambda = -\frac{2}{3}\mu$

As the flow is incompressible flow: ρ is constant, and because of the continuity equation, the vexing coefficient λ and $div\vec{V}$ vanish, therefore the Equation 3-3 is reduced to:

$$\rho\frac{D\vec{V}}{Dt} = -\nabla P + \rho g + \mu\nabla^2\vec{V} \tag{3-4}$$

3.4.3. Conservation of energy

The conservation of energy is governed by the conjugate energy equation derived from the first law of thermodynamics in a system. It is given by:

$$\rho\frac{Dh}{Dt} = \frac{DP}{Dt} + div(k\nabla T) + \Phi \tag{3-5}$$

With h, k and T are respectively the enthalpy, the thermal conductivity and the temperature of the fluid. Φ Is the dissipation function and it is expressed as follow:

$$\Phi = \mu\left[2\left(\frac{\partial u}{\partial x}\right)^2 + 2\left(\frac{\partial v}{\partial y}\right)^2 + 2\left(\frac{\partial w}{\partial z}\right)^2 + \left(\frac{\partial u}{\partial y} + \frac{\partial v}{\partial x}\right)^2 + \left(\frac{\partial w}{\partial y} + \frac{\partial v}{\partial z}\right)^2 + \left(\frac{\partial u}{\partial z} + \frac{\partial w}{\partial x}\right)^2\right] + \lambda\left(\frac{\partial u}{\partial x} + \frac{\partial v}{\partial y} + \frac{\partial w}{\partial z}\right)^2 \quad (3\text{-}6)$$

For an incompressible flow in the laminar regime (low velocity) and based on the assumptions made before: constant thermal conductivity and negligible viscous dissipation, Equation (3-5) is reduced to:

$$\rho C_p \frac{DT}{Dt} = k\nabla^2 T \quad (3\text{-}7)$$

Where C_p is the specific heat.

Applying this conjugate energy equation to both the liquid for convection heat transfer and the solid side for conduction separately, we have:

The energy equation for the fluid:

$$\rho C_p \frac{DT}{Dt} = k_f \nabla^2 T \quad (3\text{-}8)$$

The energy equation in the solid:

$$k_s \nabla^2 T = 0 \quad (3\text{-}9)$$

k_f and k_s are respectively the thermal conductivity of the fluid and the solid.

3.5. BOUNDARY CONDITIONS

Considering all the thermo-physical properties as well as the main assumptions made in Section 3-4 the boundary conditions equation are set as follow:

The continuity of the flux at the heated block-air interface is:

$$k_s \left.\frac{\partial T}{\partial n}\right|_s = k_f \left.\frac{\partial T}{\partial n}\right|_f \tag{3-10}$$

The continuity of the temperature at the heated block-air interface is:

$$T_s = T_f \tag{3-11}$$

The boundaries conditions for the thermal configuration of the fluid are described as follow:

No-slip and adiabatic conditions at the channel walls $y = z = 0$

$$\vec{u} = \vec{v} = \vec{w} = 0 \tag{3-12}$$

$$\frac{\partial T}{\partial \bar{x}} = 0 \tag{3-13}$$

And at the inlet (x = 0):

$$\bar{v} = \bar{w} = 0 \tag{3-14}$$

$$T = T_{in} \tag{3-15}$$

$$\bar{u} = \vec{V}_{in} \tag{3-16}$$

At the outlet (x = L_x):

$$P_{out} = P_{atm} \tag{3-17}$$

$$\frac{\partial T}{\partial \bar{x}} = 0 \tag{3-18}$$

3.6. STAR-CCM+ PROCEDURE

3.6.1. Star-CCM+ Methodology

Solving simultaneously these above equations that include governing equations and convection formulation of heat transfer from heat sources to the cooling fluid proves to be very complex because of the elliptic and partial differential form of governing equations. Implementation of numerical methods and mathematical formulations in CFD packages for solving complex equations in fluid flow as well as in heat transfer process using finite volume method (FVM) after discretization provides several result patterns that come from the modeled mechanism such as: displayer and visualization (flow, streamlines, temperature profile, etc.) in 2D or 3D, different plots etc. This requires basic information on different quantities that describe the fluid flow motion and the heat transfer phenomenon [49]:

- the velocity field: $V = [u(x; y; z; t); v(x; y; z; t); w(x; y; z; t)]T$
- the pressure field: $p(x; y; z; t)$
- Density distribution: $\rho(x; y; z; t)$
- Temperature distribution: $T(x; y; z; t)$

In this study Star-CCM+ 8.02 is being used as a commercial CFD code which is one of the latest and efficient CFD codes. It applies Finite Volume discretization to subdivide the solution domain is into a finite number of small control volumes, corresponding to the cells of a computational grid. This commercial CFD code solves The Reynolds Averaged Navier Stokes Equations (RANSE) in their integral form as a mathematical model to calculate the numerical simulations. It uses an iterative Semi Implicit Method for Pressure Linked Equations (SIMPLE) algorithm to coupled velocities and pressures solved separately. The Gauss-Seidel iterations method is also applied to solve the discrete or linear system of equations to get convergence and accelerated by algebraic multigrid method. Within the Star-CCM+ environment, the governing equations that are solved at each of this small discretized volume are specifically expressed as [47]:

- **Conservation of mass in discrete form**

$$\sum_f \overset{\circ}{m}_f = \sum_f \left(\overset{\circ *}{m}_f + \overset{\circ \bullet}{m}_f \right) = 0 \tag{3-19}$$

Where $\overset{\circ *}{m}_f$ is the uncorrected face mass flow rate with the flow correction $\overset{\circ \bullet}{m}_f$

- **Conservation of momentum discrete form**

$$\frac{d}{dt}(\rho X v V)_0 + \sum_f \left[v\rho(v - v_g).a \right]_f = -\sum_f (pI.a)_f + \sum_f T.a \tag{3-20}$$

Where X is the position vector, v the velocity and v_g the grid velocity; V represents volume, T is the viscous stress tensor, a is the face area vector and I the identity matrix.

- **Conservation of Energy discrete form**

$$\frac{d}{dt}(\rho E V_0) + \sum_f \left\{ \left[\rho H(v - v_g) + q''.a - (T.v) \right] a \right\}_f = (f.v + s) V_0 \tag{3-21}$$

3.6.2. Star-CCM+ Scheme

It is important to follow a standard workflow when proceeding with a numerical solution. Common CFD codes workflow consists in these following principal steps [48]:

1. Describe the physical flow:
   - describe main flow phenomena.
2. Construct a mathematical model:
   - analyze the partial differential equations.
   - fixe the physical boundary conditions.

3. Formulate the numerical problem:
    - construct a mesh.
    - choose a time differencing scheme.
    - choose a space differencing scheme.
    - set initial conditions.
    - fixe the numerical boundary conditions.
    - solve difference equations and check stability and consistency.
4. Implement the formulation in a computer code:
    - structured programming, environment.
5. Run code and obtain the solution:
    - computer system.
6. Analyze and interpret the obtained result:
    - flow visualization.
7. Draw conclusions:
    - answer practical hydrodynamic problems.

The discretization and the equation solver must be well defined as they are the main steps in the numerical process in order to get to better solution.

A typical flowchart of numerical solution using SIMPLE Algorithm is illustrated as follow:

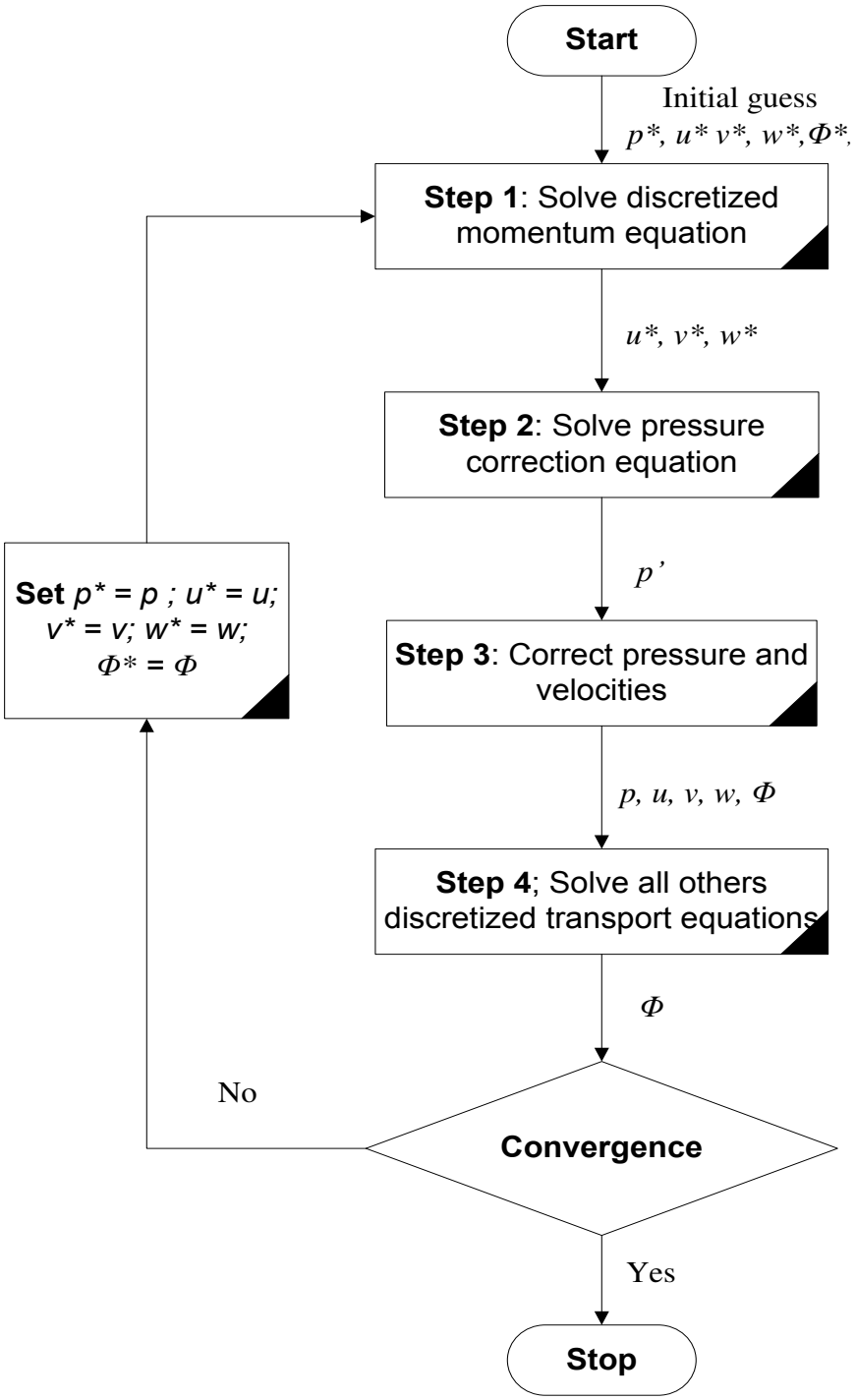

Figure 3-1: Flowchart of SIMPLE Algorithm

Numerical methods require basic properties to reach effective solutions from simulations; these properties which are:

1. Consistency:

There is constituency in a numerical solution when there is convergence in the limit between the discretized equations and the exact equations when the grid size tends to zero

2. Stability:

It is characterized by the Courant-Friedrichs-Levi condition CFL, and defined by the fact that a numerical solution is stable when errors occurring in the process don't amplify.

$$CFL = u\frac{\Delta t}{\Delta x} \tag{3-22}$$

Where u is the velocity, Δt is the time step and Δx is the grid size

3. Convergence:

A numerical solution is said to convergent when the solution of discretized equations tends to the solution of the differential equation as the mesh is being more refined. Consistency and stability are the main conditions for a solution converge.

4. Conservation:

It is defined by the fact that the discretized equations must also obey to the conservation laws that drives the differential governing equations describing the phenomenon occurring in the computational domain.

5. Accuracy:

For a numerical solution accuracy is evaluated according to the range as well as the rate of different kind of errors occurring during the process: modeling, discretization, iteration etc.

Star-CCM+ software is a powerful CFD package for solving engineering processes, this being so, it was built in a way that for any solution it always follows the implemented major steps or a determined workflow:

1. Import or create surface

2. Repair surface if required

3. Define boundary conditions

4. Set meshing models and properties

5. Set physics models and properties

6. Generate mesh

7. Define solver settings

8. Prepare post-processing

9. Run analysis

3.7. CLOSURE

In this chapter we have define the problems to be investigated numerically. A brief description of the numerical procedure followed in most CFD codes for solving fluid flow and heat transfer problems was also made. Basically numerical methods use different algorithms to discretize computational domains, to couple and solve partial

differential equations governing the mechanism in order to obtain better solutions regarding accuracy and convergence. We have thus given the main steps to follow when using Star-CCM+ software as the numerical solver for a forced convection heat transfer problem. Grid generation within Star-CCM+ is easily obtained from its various options, as well as discretization of the computational The pressure-velocity coupling and solution of partial differential equations are obtained using SIMPLE algorithm.

CHAPTER 4: CFD CODE VALIDATION AND SIMULATION RESULTS

4.1. INTRODUCTION

This section deals with three-dimensional numerical approximation to simulate forced convection heat transfer mechanism from identical and aligned heated blocks within a rectangular enclosure with the use of CFD. We started by defining the grid generation of the computational domain and we investigated the mesh independency.

The resulting profiles of pressure contours, average and maximum temperatures, velocity vectors and overall Nusselt number variations along the flow direction are presented to show the effect of the Reynolds number that varies with the inlet velocity of the cooling air in the enclosure. The validation of the numerical method used was carried out by comparing the overall Nusselt number obtained using this CFD code with its value obtained based on the experimental method described in the literature [53].

As mentioned before, in all simulations, thermo-physical properties of the air which are temperature dependent will be taken at the inlet air temperature considered as the reference temperature.

4.2. DESCRIPTION OF THE PHYSICAL MODEL

Our study built on the similar research models previously carried out on thermal management of five heat-generating blocks cooled by laminar forced convection [13, 24, 32, 33, 54-56]. The physical model is schematically shown on figure 4-1 and figure 4-2

(a) and (b) and it consists in five aligned heated blocks mounted on the bottom wall of a rectangular enclosure. The heated blocks are identical have a length *G*, a width *C* and a height *B*. The spacing between consecutive blocks is S_i. The enclosure has a total stream-wise length L_x, a span-wise width *W* and a height *H*.

To insure that the boundaries of the enclosure do not thermally influence our model, we set our model dimensions based on the theoretical considerations regarding forced convection within a rectangular channel mounted with heated blocks found the literature [9, 32, 35, 49] for similar studies.

In the channel flow , the upstream face of our first block is located at L_{in} = 5G (which is $\geq$ 3*G*) and the downstream distance after the fifth heat sources $L_{out} \geq 10G$, which is significantly long so that the recirculation flow remains within the computational domain. The lateral distances are set to be equal to 5*L* on both sides.

With all these considerations, let:

$$\frac{C}{G}=1;\frac{B}{G}=0.5:\frac{W}{G}=11;\frac{H}{G}=3;\frac{L_x}{G}=30;\frac{L_{in}}{G}=5;\frac{L_{out}}{G}=28 \tag{4-1}$$

$$G.C.B=V_i \tag{4-2}$$

$$\sum_{1}^{n}V_i=V_{tot} \tag{4-3}$$

$$L_{in}+\sum_{1}^{n}G+\sum_{1}^{n-1}S_i+L_{out}=L_x \tag{4-4}$$

Where V_i , V_{tot} and L_x are constants and n is the total number of the heated blocks which is 5 as described above.

Table 4-1: Thermo-physical properties of air at Tin = 20 °C, 1 atm [8]

Density ρ (kg/m^3)	Thermal diffusivity,α_f (m^2/s^2)	Thermal conductivity,k (W/m.K)	Dynamic viscosity, μ (Kg/m.s)	Kinematic viscosity,ν (m^2/s)	Specific heat,c_p (J/kg.K)	Prandtl number,Pr
1.204	2.074×10^{-5}	0.02514	1.825×10^{-5}	1.516×10^{-5}	1007	0.71

A uniform heat flux is applied from the bottom of the blocks that are being forced to cool by a steady and incompressible air flow whose temperature is fixed at 20 ºC at the inlet of the channel. This temperature is set as the reference temperature and so are its thermal properties as shown in Table 4-1.

To better analyse the fluid flow and the heat transfer characteristics in the enclosure that can really simulate the cooling of electronic entities in a channel or even better the cooling of servers in a room, we modelled the heated blocks as made with homogenous materials made by silicon, wafer, metal frame, and packaging materials with isotropic properties and having an assumed thermal conductivity of k_s = 2.63 W/m [35, 54, 57, 58] The flow is laminar and considered to be hydrodynamically and thermally fully developed within the computational domain, where the Reynolds number varies from 100 to 1000. All the thermo-physical properties are assumed to be constant. The enclosure walls are adiabatic and the radiative effect from heated sources is neglected. We will also neglect the buoyancy induced effects as well as the viscous heat dissipation when compared to convection in the process. In most practical applications of electronics systems cooling by air, we consider the buoyancy strength not to be very high [59].

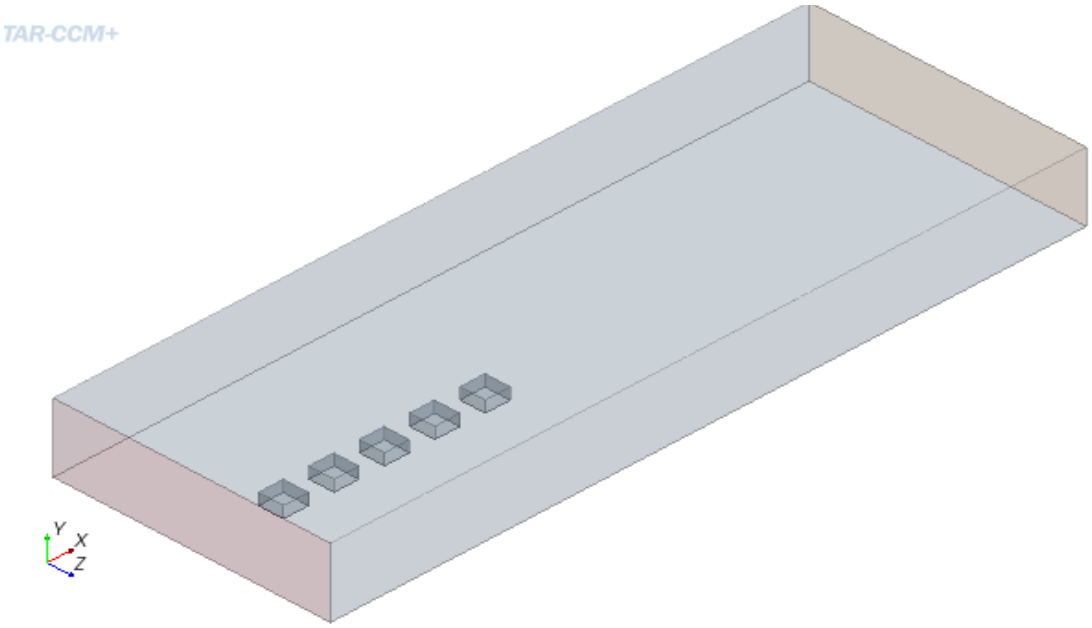

Figure 4-1: Computational domain in 3-D

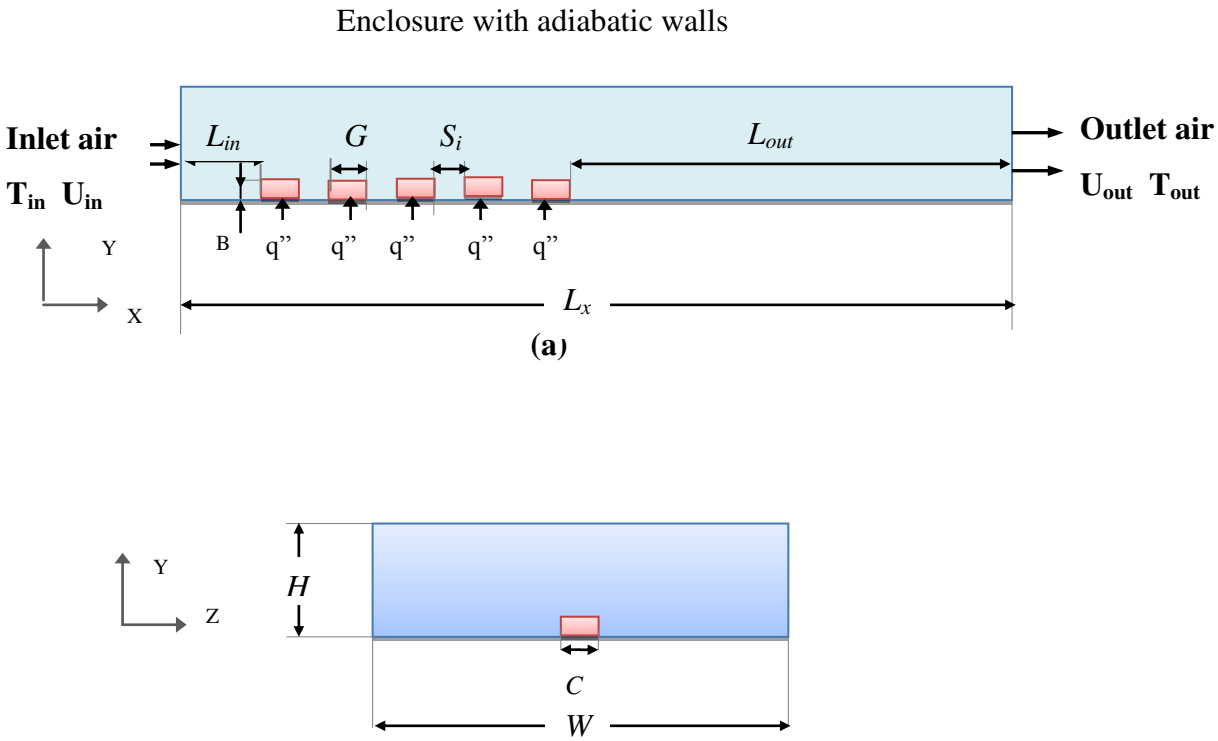

Figure 4-2: 2-D physical model: (a) X-Y plane; (b) Y-Z plane

4.3. THERMAL PERFORMANCE EVALUATION

In view of the flow fluid motion and heat transfer partial differential equations and their respective boundary conditions of heat transfer mechanism occurring within the computational domain as defined in Sections 3.4 and 3.5, we will analyze the thermal performance of the cooling process using specific non-dimensionalized parameters.

In fact, for different Reynolds number Re_{Dh} obtained from different inlet velocity V_{in} and based on the hydraulic diameter D_h of the enclosure as the characteristic length, we will focus on the following dimensionless numbers to measure the thermal performance of the heat transfer phenomenon:

- the Reynolds number

$$Re_{Dh} = \frac{V_{in} D_h}{\nu} \tag{4-5}$$

- the dimensionless temperature θ given by:

$$\theta = \frac{T - T_{in}}{(q'' D_h / k_f)} \tag{4-6}$$

- the overall or global dimensionless conductance is defined as:

$$\overline{C} = \frac{Q'' D_h}{k_f (T_{ave} - T_{in})} \tag{4-7}$$

$$Q'' = 5q'' \tag{4-8}$$

- the local Nusselt number that are evaluated using:

$$Nu_x = \frac{hD_h}{k_f} = \frac{-1}{\theta_s} \frac{\partial \theta_f}{\partial \theta_s} \tag{4-9}$$

Therefore we have:

$$\overline{Nu}_i = \frac{\int_{A_i} Nu_x dx}{A_i} and \tag{4-10}$$

$$\overline{Nu}_{ave} = \frac{\sum \overline{Nu}_i A_i}{\sum A_i} \tag{4-11}$$

For the mean or the overall Nusselt number for a single heat source Equation 4-10 and for multiple heat sources Equation 4-11.

- the Bejan number

$$Be = \frac{\Delta P D_h^2}{(\mu \alpha_f)} \tag{4-12}$$

$$\Delta P = P - P_{ref} = C_p \left(\frac{1}{2} \rho_{ref} v_{ref}^2 \right) \tag{4-13}$$

Where Ac_{ch} is the channel cross section, Nu_i the mean Nusselt number over a single surface, Nu_{ave}, the overall Nusselt number and C_p is the pressure coefficient, P_{ref} is the reference pressure which is the atmospheric pressure, ρ_{ref} and v_{ref} are the air reference density and velocity taken at the inlet condition. The enclosure walls are maintained adiabatic and the blocks are heated from the bottom face with a constant heat flux of 0.1 W/m^2.K.

4.4. CFD MODEL VALIDATION

4.4.1. Mesh generation

The mesh schemes and solver were presented in Section 3.3. The meshing process conducted within Star-CCM+ starts from the surface meshing over the computational domain in order to create a starting meshing surface required to generate the volume

meshing. The polyhedral volume meshing option is chosen in our present case to discretize the computational volume based on its advantages which are:

- best accuracy
- higher capturing flow
- conformal interfaces between multi regions

To improve and to optimize the meshing quality and accuracy of the flow solution for our computational model, the surface remesher and the trimmer option was applied for the surface quality. Thereafter, the curvature refinement together with proximity refinement and compatibility refinement option as well as the prism layers model was used to in the volume meshing generation.

Within Star-CCM+, volume meshing is obtained using a finite-volume method for segregated flow where the second order upwind scheme is used for the diffusive terms and the convective terms in the momentum and energy equations. The pressure-velocity coupling in governing equations is solved using the Semi-Implicit Method for Pressure-Linked Equations (SIMPLE) which was well explained by Patankar and Spalding [50]. The conjugate-gradient method where the Algebraic Multigrid (AMG) solver as the preconditioner, to accelerate the convergence of the iterative solution of the linear system in the pressure solver, for incompressible flows using the segregated flow model as the density was assumed constant.

4.4.2. Grid independence test

Referring to the dimensions of our computational domain , the grid independence test was conducted form an initial reference value of 0.1 m for the base side and fixing 100% of the maximum cell size; 50% and 100% respectively for the relative minimum and relative target surface size. We started grids generation by choosing an initial base size of 0.1 m. The base size is a characteristic length of the numerical model that is set before using any other relative values applied to the meshing generation process. This coincided

when the normalised simulation residuals fall below 10^{-7} for momentum and the energy equations, and 10^{-6} the continuity equation. The convergence criterion at each step for the overall temperature as the quantity monitored was:

$$\gamma = \frac{\left|T_{ave_i} - T_{avei-1}\right|}{T_{avei}} \leq 10^{-2} \tag{4-14}$$

Where *i* is the mesh index according to refinement obtain form varying the base size.

In order to make a suitable comparison with experimental data on a basis of a specific characteristic length *Lc* such as $2 \leq Lc/a \leq 20$ [60] Where a is the heated block height At this stage of our code validation, we would point out that both the Reynolds and the average Nusselt numbers are also evaluated based on the same the same characteristic length.

We refined the mesh by decrease the base size to satisfy the convergence criteria described by Equation 4-14 in order to ensure the accuracy of the results. The mesh refinement was made by reducing the base size with by a value of 0.01 after each simulation that drastically increased the grid density.

For our model of five aligned blocks mounted in the enclosure the convergence criterion was reached for a base size of 0.05 m, this model generated 138150 cells. After discretisation of the computational domain, it was found that a further increase in the grid density led to insignificant changes in both the maximum and the average temperature using Re_{Lc} = 500 as mean value Table 4-2.

Table 4-2: Grid independent study for the air cooling process in the channel for Re_{Lc} = 500

Base size	Cells	T_{max}	T_{ave}	$\gamma = \frac{\left\|(T_{ave})_i - (T_{ave})_{i-1}\right\|}{(T_{avex})_i}$
0.08	40370	132.46	112.86	
0.07	49172	133.01	116.11	0.027
0.06	91731	135.49	113.79	0.020
0.05	138150	133.32	112.23	0.014
0.04	186246	133.23	113.01	0.006

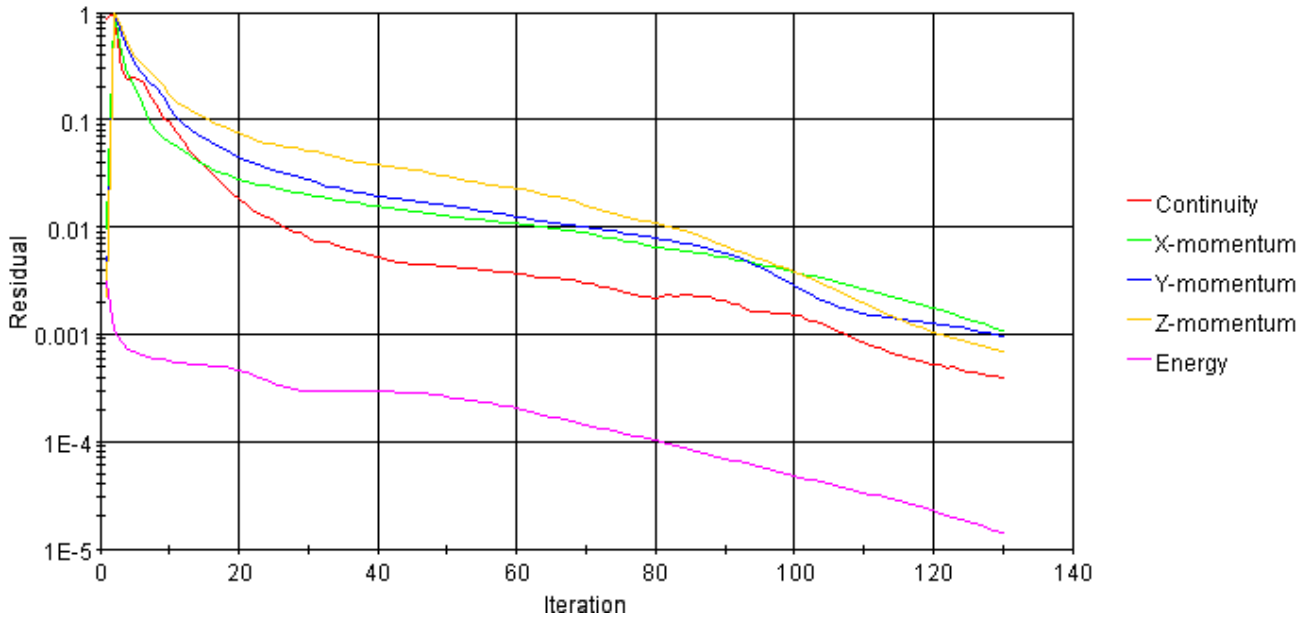

Figure 4-3: Generated residual plots describing simulation convergence for Re_{Lc} = 500

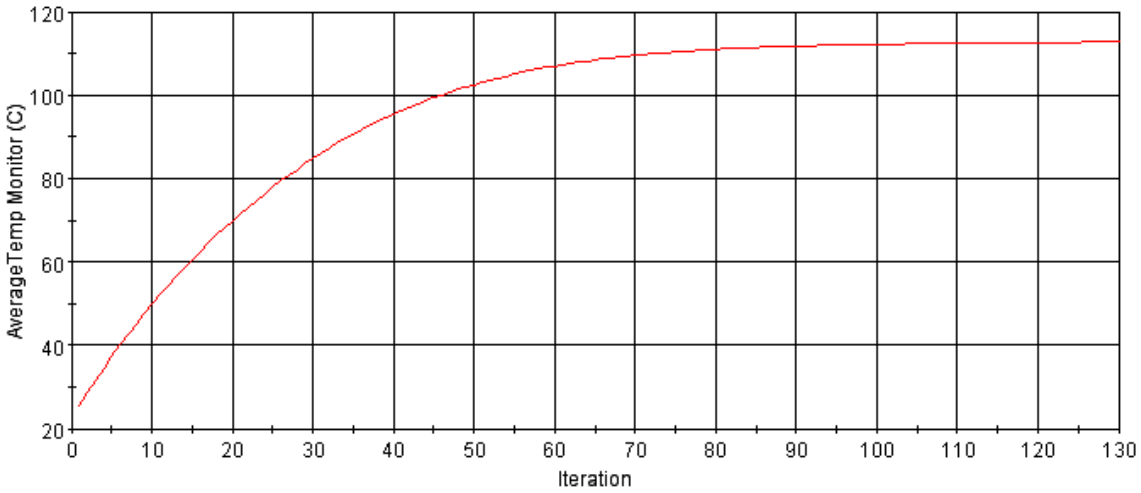

Figure 4-4: Average temperature plot indicating convergence for Re_{Lc} = 500

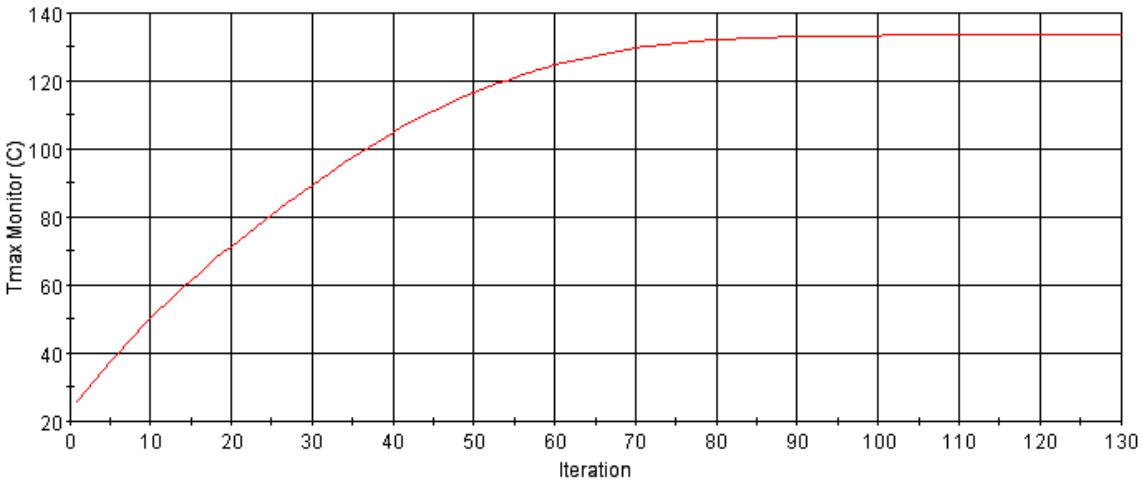

Figure 4-5: Maximum temperature plot indicating convergence for Re_{Lc} = 500

(a)

(b)

Figure 4-6: Discretised three-dimensional computational domain

4.4.3. CFD Code Validation

The present numerical code validation was evaluated by comparing the resulting overall Nusselt number generated numerically with available accepted experimental data. In this purpose, the Wirtz and Dykshoorn [60] correlation given by Equation 4-15 based on their experimentally results for cooling of in-line arrays of heated blocks in electronic packages was used against which to compare the numerical results obtained.

$$Nu_{Lc} = 0.6\,\mathrm{Re}_{Lc}^{1/2}\,\mathrm{Pr}^{1/3} \tag{4-15}$$

Where *Lc* is the specific characteristic length defined in the previous.

Figure 4-7 depicts similarity in the trend between the overall Nusselt numbers obtained with both methods for various Reynolds numbers.

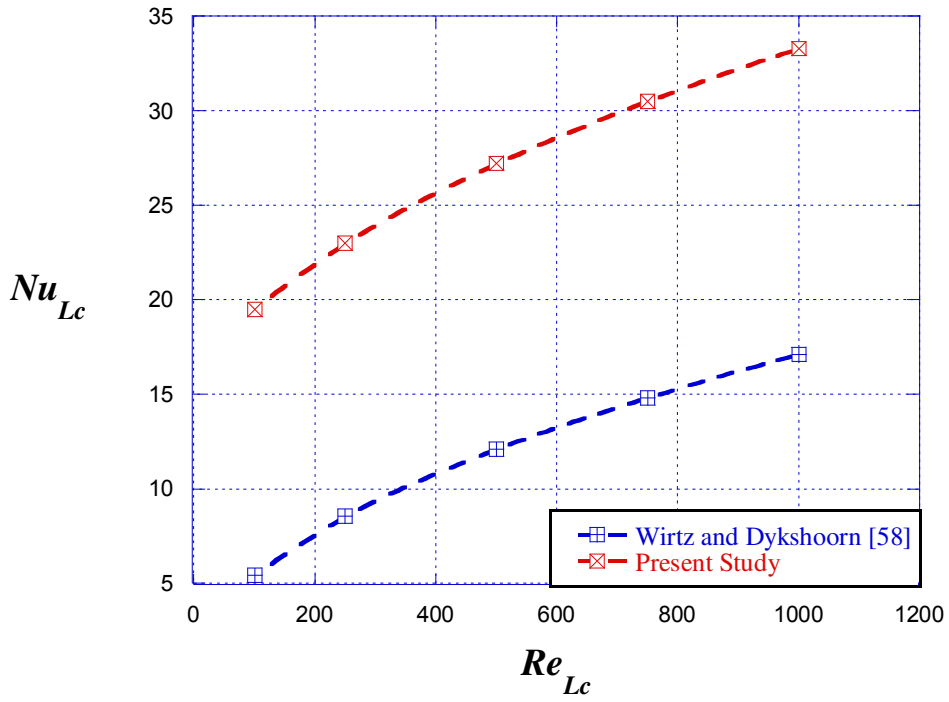

Figure 4-7: Numerical model validation using the resulting overall Nusselt based on the channel hydraulic diameter

4.5. SIMULATION RESULTS AND OBSERVATION

In this section, steady state numerical results of simulations will be presented for the five specific cases: Re_{Dh} = 100, 250, 500, 750 and 1000 which depend on the respective inlet cooling air velocities V_{in} = 0.00643 m/s, 0.01608 m/s, 0.03215 m/s, 0.04823 m/s and 0.06430 m/s. Similarly for the previous case (with Re_{Lc}), the convergence criterion was reached at the base size of 0.05 m for other values of Re_{Dh} (100, 250, 750 and 1000). Figure 4-3 shows how the Reynolds number varies with the inlet cooling air velocity.

Table 4-3: Grid independent study for the air cooling process in the channel for Re_{Dh} = 100

Base size	Cells	T_{max}	T_{ave}	$\gamma = \frac{\left\|(T_{ave})_i - (T_{ave})_{i-1}\right\|}{(T_{avex})_i}$
0.08	40370	384.49	329.33	
0.07	49172	383.12	328.02	0.004
0.06	91731	385.59	330.37	0.007
0.05	138150	384.17	329.80	0.002
0.04	186246	384.56	330.30	0.001

Table 4-4: Grid independent study for the air cooling process in the channel for Re_{Dh} = 250

Base size	Cells	T_{max}	T_{ave}	$\gamma = \frac{\left\|(T_{ave})_i - (T_{ave})_{i-1}\right\|}{(T_{avex})_i}$
0.08	40370	303.9	255.8	
0.07	49172	301.4	253.76	0.008
0.06	91731	308.09	258.63	0.019
0.05	138150	306.71	258.04	0.002
0.04	186246	307.12	258.66	0.002

Table 4-5: Grid independent study for the air cooling process in the channel for Re_{Dh} = 500

Base size	Cells	T_{max}	T_{ave}	$\gamma = \frac{\left\|(T_{ave})_i - (T_{ave})_{i-1}\right\|}{(T_{avex})_i}$
0.08	40370	248.85	206.80	
0.07	49172	241.86	202.40	0.0213
0.06	91731	249.92	207.21	0.0238
0.05	138150	248.73	206.50	0.0034
0.04	186246	248.49	206.83	0.0016

Table 4-6: Grid independent study for the air cooling process in the channel for Re_{Dh} = 750

Base size	Cells	T_{max}	T_{ave}	$\gamma = \frac{\left\|(T_{ave})_i - (T_{ave})_{i-1}\right\|}{(T_{avex})_i}$
0.08	40370	213.81	178.58	
0.07	49172	209.17	175.51	0.017
0.06	91731	216.67	179.16	0.020
0.05	138150	215.66	178.44	0.004
0.04	186246	215.13	178.68	0.001

Table 4-7: Grid independent study for the air cooling process in the channel for Re_{Dh} = 1000

Base size	Cells	T_{max}	T_{ave}	$\gamma = \frac{\left\|(T_{ave})_i - (T_{ave})_{i-1}\right\|}{(T_{avex})_i}$
0.08	40370	192.28	161.45	
0.07	49172	187.46	158.18	0.0205
0.06	91731	193.82	160.52	0.015
0.05	138150	192.97	159.80	0.004
0.04	186246	192.42	160.10	0.001

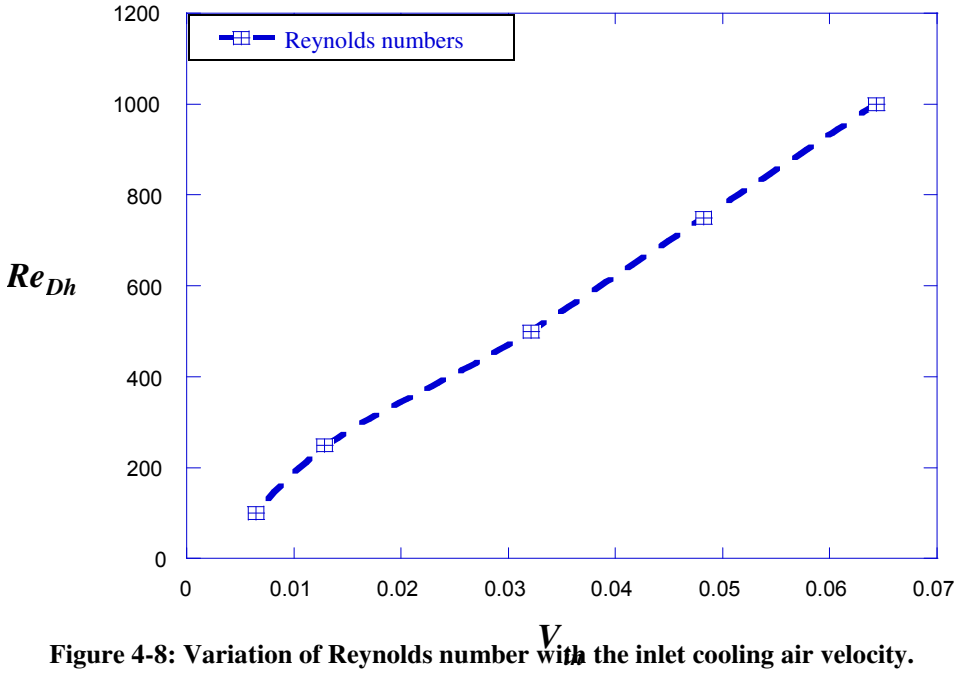

Figure 4-8: Variation of Reynolds number with the inlet cooling air velocity.

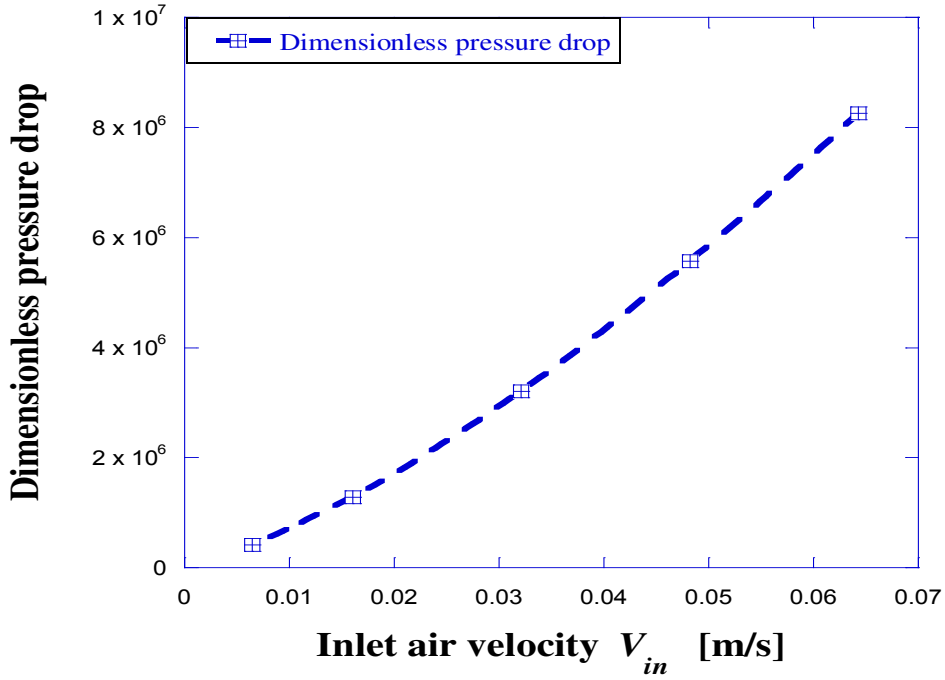

Figure 4-9: Variation of Pressure drop with the inlet cooling air velocity

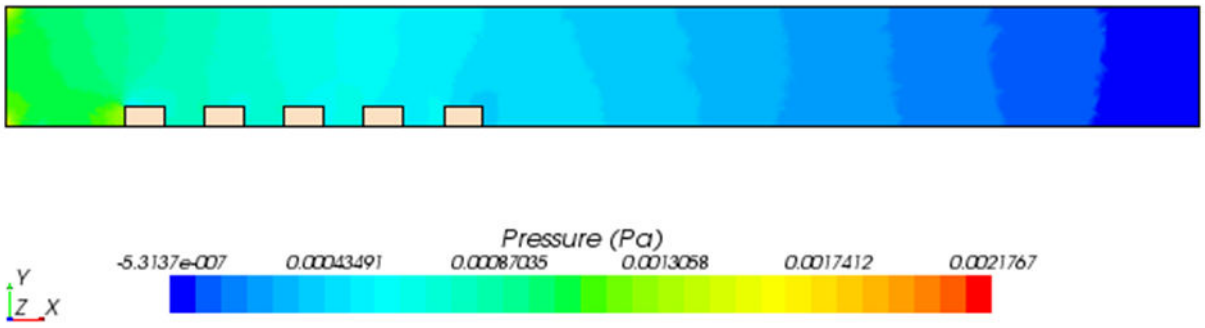

Figure 4-10: Pressure drop profile in the channel for Re_{Dh} = 500

The convergence criterion results obtained with Re_{Dh} = 500 as a mean value (for the code validation), is used for all simulations, while maintaining a constant generated heat flux of 0.1 W/cm^2 and keeping the geometry unchanged (B/G = 0.5 and S/G = 1). From these results, we observed how the convective heat transfer thermal performance is strongly influenced in the enclosure by the Reynolds number varying from 100 to 1000.

It must also be noted that the following profiles (temperature and velocity) of the cooling fluid inside the enclosure obtained after simulations are due to the assumption of hydrodynamic fully developed flow.

4.5.1. Temperature patterns

From a general point of view, the solution of the convection heat transfer shows from the plot of the temperature profile along the length of the channel shown in Figure 4-11, a gradual increase in temperature of the cooling air across the channel length from the inlet of the enclosure to its outlet. Along the streamwise direction there is a decrease in the temperature difference between the fluid and the heat blocks from the first one to the last.

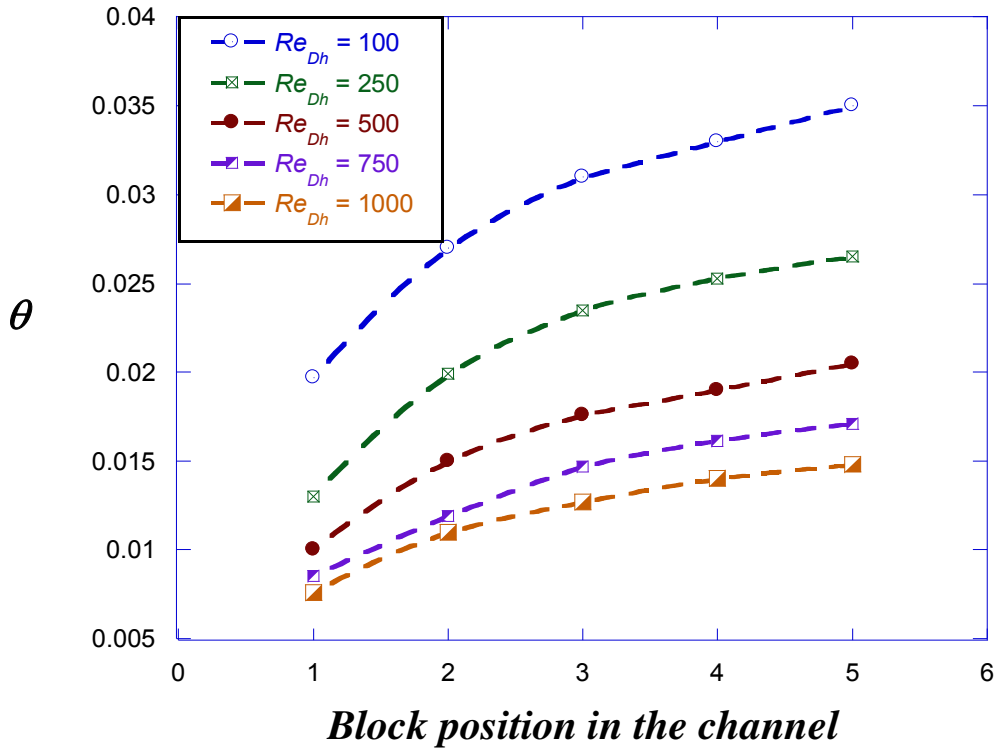

Figure 4-11: Influence of Reynolds number variation on different heated blocks temperature

Certainly regardless the Reynolds numbers, the temperature of any block downstream in the channel is higher than the previous blocks due to its self-heating and to the thermal wakes of upstream blocks: this phenomenon known as the principle of superposition of thermal wakes effect was previously observed [13, 61-63].This same effect was also proved numerically [34, 55, 57, 64]. This phenomenon is related to that previously described by Cess and Shaffer [65] as well as Kays and Crawford [53] from the principle of the temperature distribution caused by a specific heat flux distribution for internal flow.

Therefore the equation for the temperature of an element in the k^{th} row, T_k is the conventionally expressed as follow [13, 66]:

$$T_k - T_{in} = \left(\frac{q_k}{h_k A_k} \right) + \sum_{i=1}^{k-1} \theta_{k-1} (T_i - T_{in}), \; for: i \le k \qquad (4\text{-}16)$$

Where T_{in} is the inlet temperature, rows 1 to k-1 represent upstream rows, q_i is the heat flux of upstream component i, θ_{k-1} is the discrete kernel function (*DKF*), T_i is the bulk mean air temperature, q_k is the component heat flux, and h_k is the adiabatic heat transfer coefficient. The θ_{k-1} or *DKF* is the ratio of adiabatic temperature rise to mean temperature rise at row k that results from the application of heat flux on upstream row i. The adiabatic heat transfer coefficient, h, is defined such that the adiabatic, or unpowered, temperature is used as the reference temperature, instead of the mean temperature, as is common in internal flows. From Equation 4-16, it is apparent that the equilibrium temperature rise of a component in the k^{th} row is equal to the sum of the thermal wake influences from upstream components, as described by the *DKF*, plus the self-heating component governed by h [66].

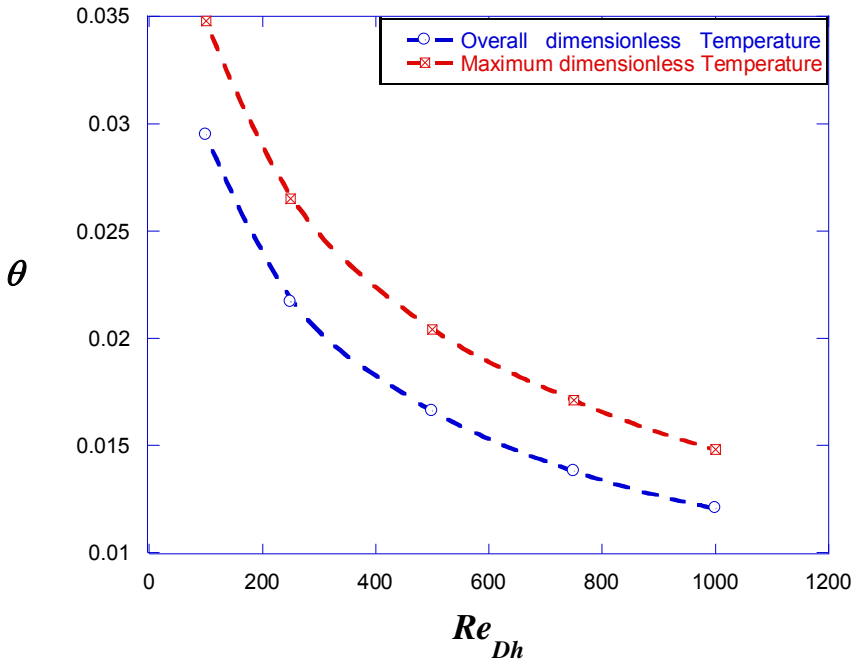

Figure 4-12: Variation average and maximum temperature of heated blocks with the Reynolds number

Actually, the inlet flow impacts on the left (front) face of the first block and create a small clockwise vortex at the lower left corner. In the cavities between heated blocks, a recirculation flow also occurs due to the under pressure induced by the flowing air over the heated blocks: this creates an insulating zone. Because of this phenomenon, over the adjacent heated faces (left and right) will occur a significant rise in temperature due to the fact that the heat is not remove as it is happened over the top and the side heated faces by the core flow because it's parallel to these faces. High temperature zones are therefore concentrated near the heat sources. Behind the last block a recirculation zone appears and affects the downstream flow field Figures 4-13. Due to these effects the highest temperature (peak temperature) is reached at the last block in in the channel.

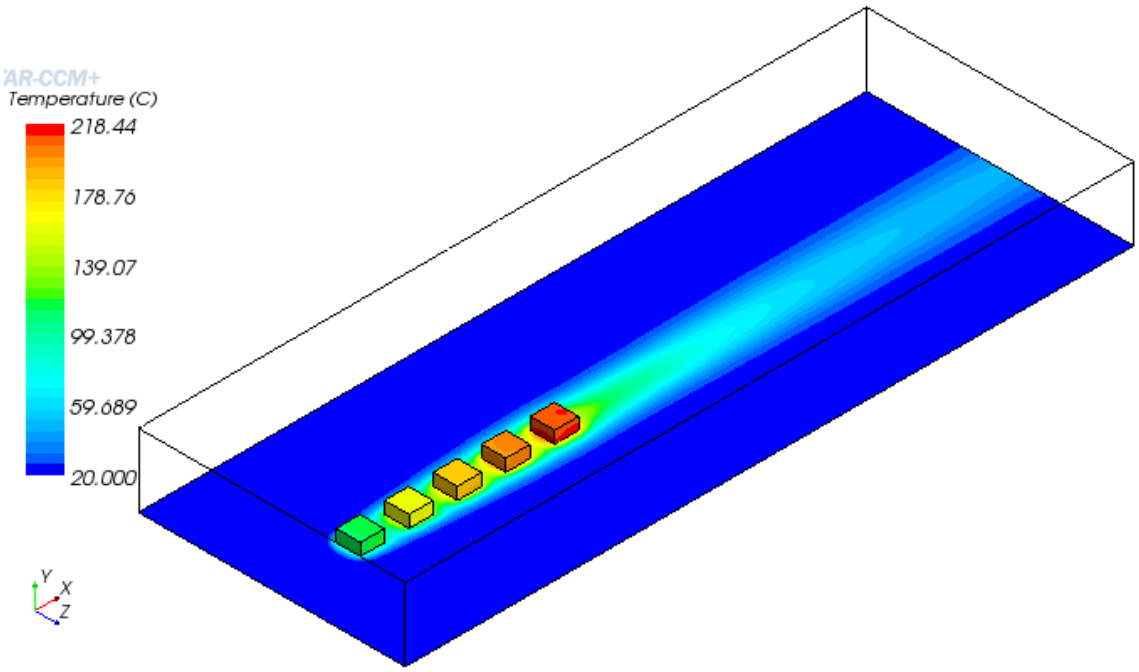

Figure 4-13: 3-D Temperature contour in the channel, Re_{Dh} = 500

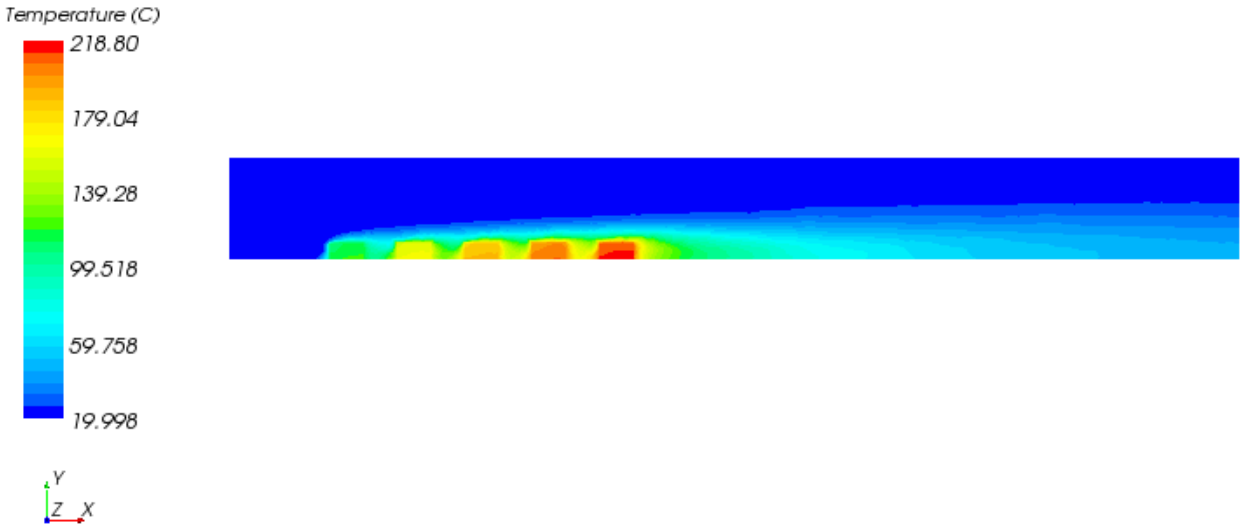

(a)

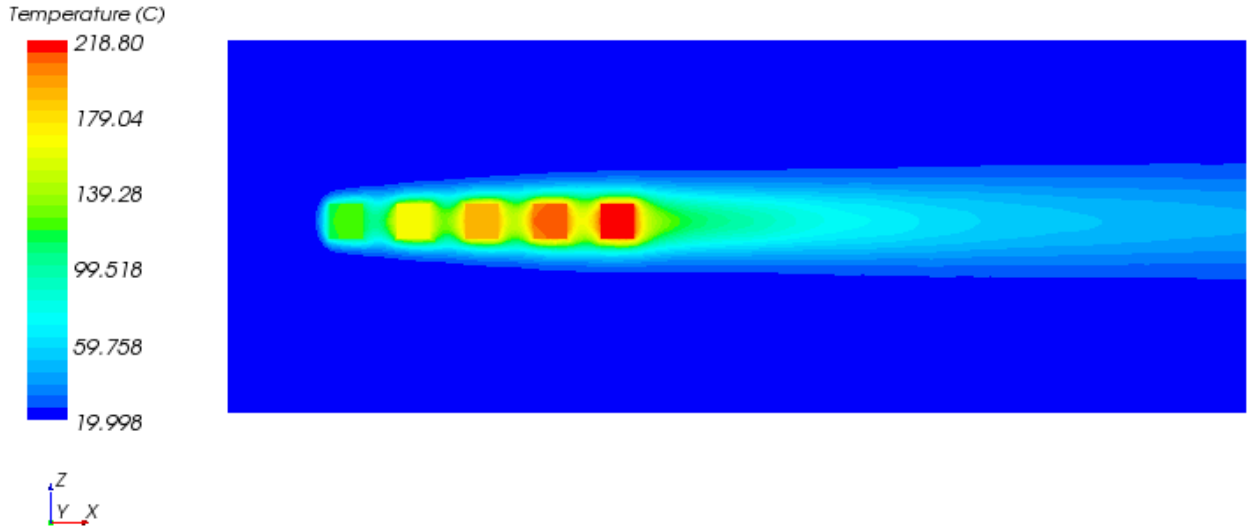

(b)

Figure 4-14: 2-D Temperature contour in the channel for Re_{Dh} = 500: X-Y plane (a) and X-Z plane (b)

4.5.2. Velocity profiles

The magnitudes of recirculation zones and vortex together with thermal performances are proportional to the Re_{Dh} and vary with the geometric ratios as well as to the spacing between heated blocks [33, 34, 55].

Figure 4-15: (a) to (e) display the effects of varying the Re_{Dh} on the fluid flow velocity. It showed that the strength or the magnitude of the small clockwise vortex at the lower left corner and the recirculation zone that appears behind the last block and affects the downstream flow field directly depend on the value of Re_{Dh}. However the magnitude of the vortex occurred in the inter-blocks spacing due to the creation of an under pressure zone induced by the flowing air above the blocks the in the cavities between heated blocks are inversely proportional to the Re_{Dh} magnitude.

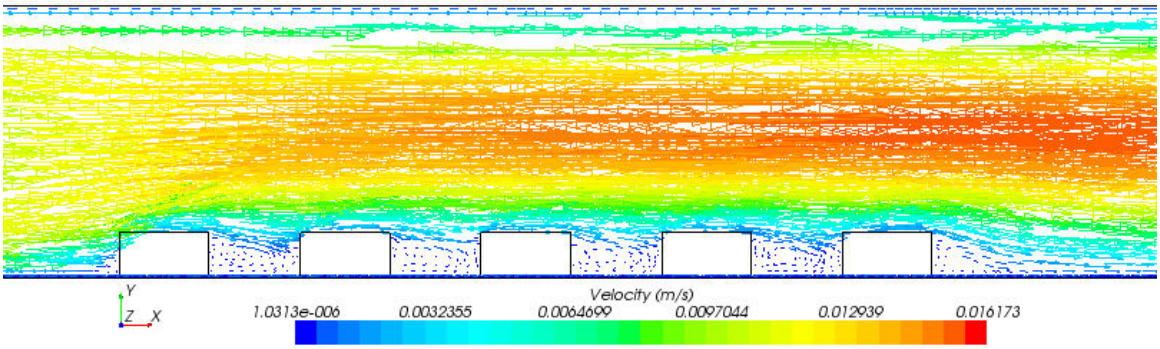

(a)

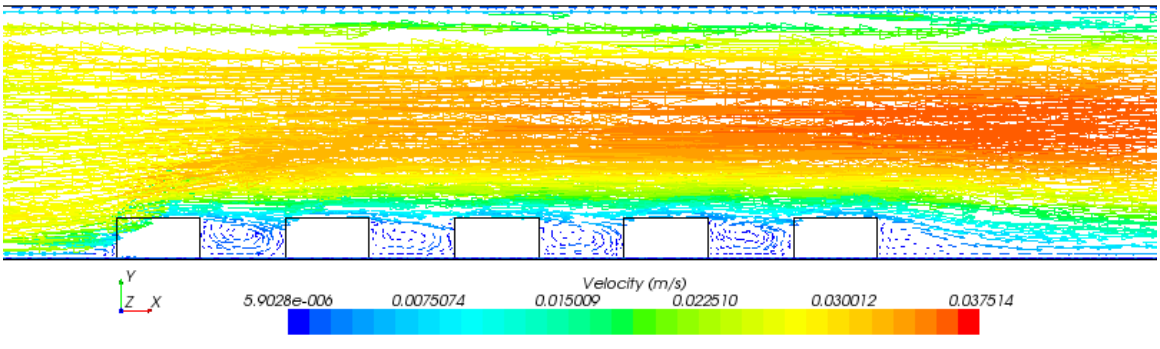

(b)

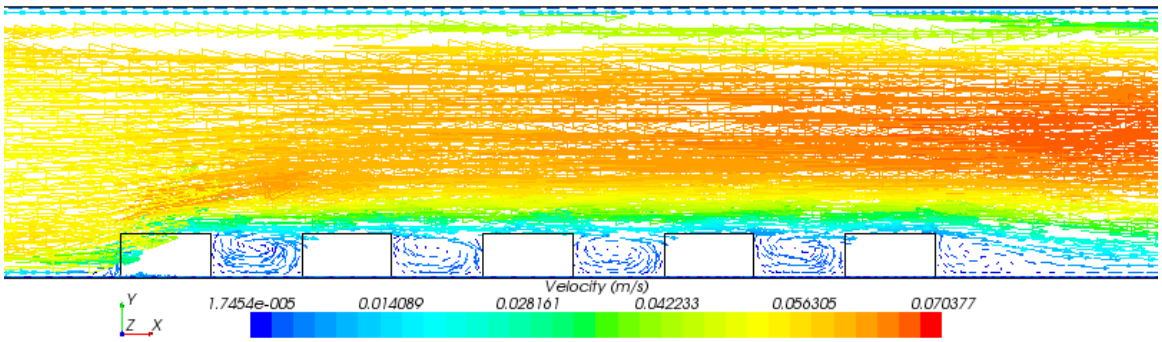

(c)

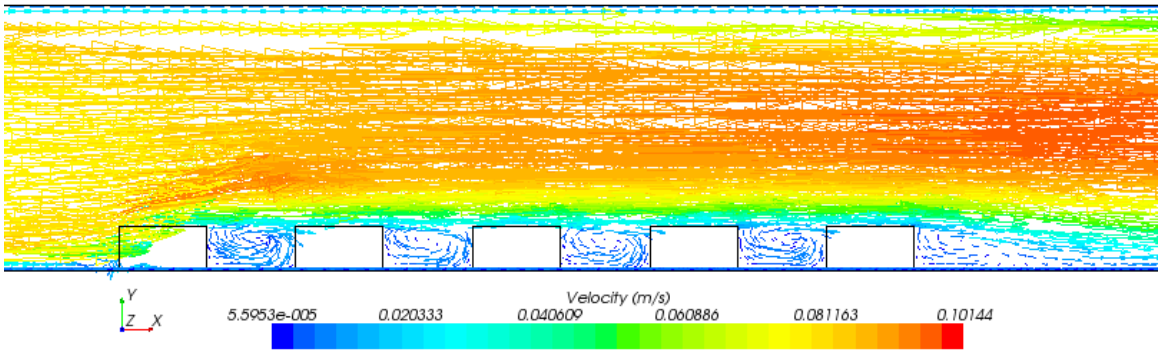

(d)

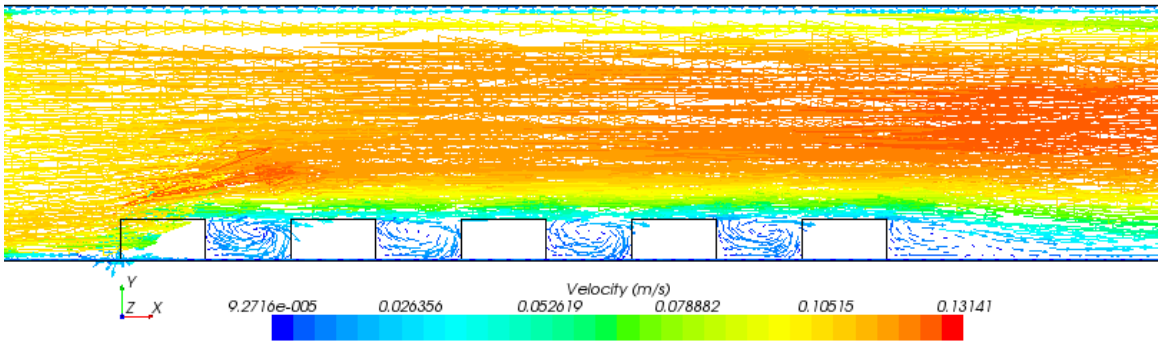

(e)

Figure 4-15: Velocity profiles variations with Reynolds number in the enclosure: Re_{Dh} = 100; Re_{Dh} = 250; Re_{Dh} = 500; Re_{Dh} = 750; Re_{Dh} = 1000

This phenomenon affects the thermal result and the velocity profile of the core flow such as the higher is the Re_{Dh} (high velocity magnitude in the enclosure), the stronger are the recirculation both up- and down-stream and the lower is the inter-blocks vortex as depicted in Figure 4-15(a) - (e).

4.5.3. Overall Nusselt number

The Nusselt number was early presented as a measure of convective heat transfer coefficient at the surfaces of heated blocks. Indeed in this section we illustrate the variation of resulting Nusselt number with the Reynolds numbers in Figures 4-16 and 4-17.

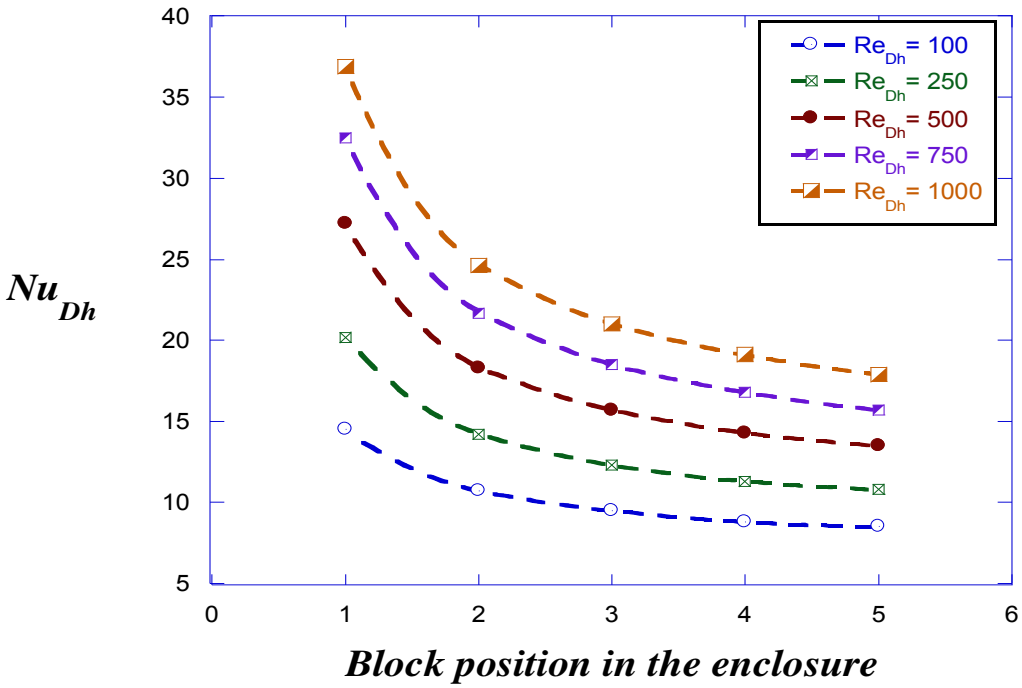

Figure 4-16: Average Nusselt number variation with blocks position in the enclosure

The thermal and hydrodynamic phenomena occurring in the flow, as explained in the previous sections justify the fact that the overall Nusselt number of the heated blocks increases when the Re_{Dh} increases while the average Nusselt number of each single block decreases as the position moves away in the stream-wise direction with the downstream block location in the enclosure because the difference of the heat transfer rate between consecutive heated blocks is not constant.

That said, an increase in Reynolds number enhances the mixing in the enclosure as it is due to the increasing of the flow velocity which would result in improving the removal of the heat as circulation zones are fully develops and rotates faster while the free stream flow moves faster. The buoyancy effects become stronger as the Reynolds number decreases and longitudinal vortices may occur after the flow is heated but with an increase in the Reynolds number, the forced convection transport is enhanced, and more heat is dissipated directly into the fluid, as observed figures 4-15.

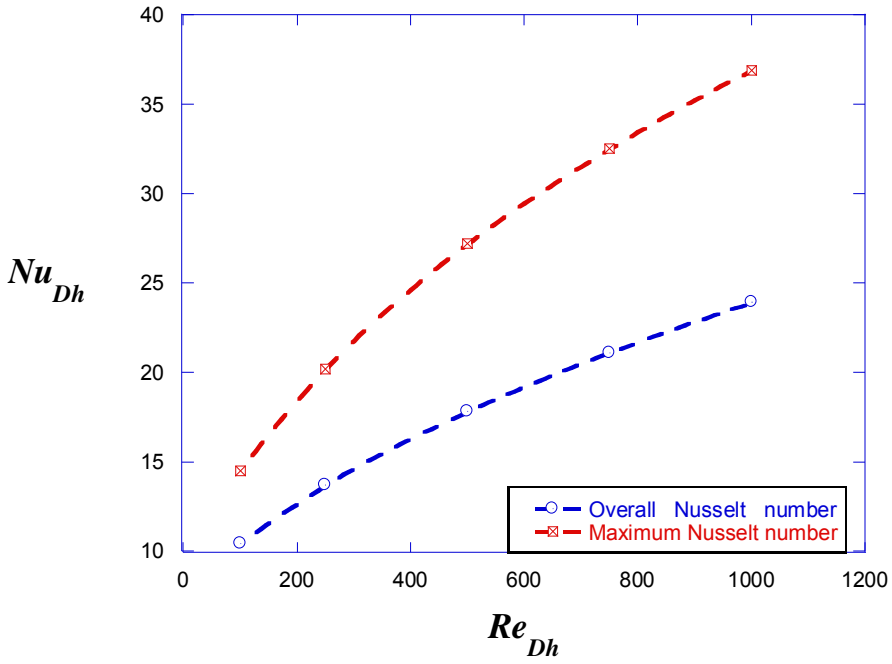

Figure 4-17: Variation of both Overall and Maximum Nusselt numbers in the enclosure with Reynolds number

.

4.6. CLOSURE

A three dimensional numerical analysis has been conducted to simulate the forced convection heat transfer to cool heated blocks in a rectangular enclosure with an emphasis on the thermal performances while varying the Reynolds number with a laminar regime.

Regarding thermal performances, simulations gave understanding results which has lead to the following conclusions:

- increasing the Reynolds number decreases both the overall and the maximum surface temperature of the heat sources, increases their overall Nusselt number and improves the enclosure heat transfer process

- heat transfer from upstream heated block is greater than that from the second and subsequent ones, this is due to fact that the fluid temperature in the wake of the first heat source is higher than that in the entrance region of the enclosure

- the temperature contours move slightly inside the enclosure, showing a gradual growth along the flow direction with high temperature zones near the heat sources and quite uniform temperature profile in the rest of the enclosure

In a general way, these numerical results are comparable in their trend with those provided or already predicted in the literature either experimentally or numerically [56, 67] as well as by analysis based on synergy principle [28, 29] for similar physical and thermal configurations.

CHAPTER 5: NUMERICAL OPTIMIZATION

5.1. INTRODUCTION

This chapter presents the Optimization CFD software used in our study. Actually the principle behind the numerical optimization process implemented to the numerical simulations conducted in chapter 4 will be described. Objective functions will also be selected as required in the optimization process.

5.2. NUMERICAL OPTIMIZATION OVERVIEW

Automated procedures had been found to be very efficient for solving industry challenges. Therefore numerical optimization or mathematical optimization methods are nowadays accepted industry practice to identify best solutions that are being maximized or minimized according to the design specifications. However we should point out that the first optimization method called the steepest descent was used to solve very simple problems in the 1940s [68].

In this study numerical optimization method is being conducted using HEEDS-Optimate CFD code to find optimal blocks geometry which implies blocks aspect ratio or blocks arrangement modification in order to maximize the heat transfer density rate and to minimize the temperature in the enclosure.

5.3. OPTIMIZATION PROBLEM FORMULATION

5.3.1. Objectives functions

The aim of our study is to find optima configurations. Therefore in order to minimize the peak temperature, we will conduct a numerical optimization procedure that minimizes the overall temperature from all heated elements. This will consequently maximize the overall thermal conductance.

As the numerical optimization procedure is based on two objective functions that are the minimization of the overall temperature which minimizes the peak temperature and the maximization of the overall Nusselt number. This will be obtained via a CFD simulation using Pareto Multi-Objective optimization mode in Optimate+ code [67].

5.3.2. Pareto Optimization Mode

In Pareto Optimization mode, the weighting for competing objectives does not need to be defined a priori. The study will return a set of all optimal designs that lie on the Pareto front. The optimization algorithm being used is the MO-SHERPA search.

5.3.3. Design variables

In Pareto-Optimization mode, design variables are those that are allowed to vary in order to reach the desired optimum results and must be defined as minimum and maximum method.

5.3.4. Constraints

The constraints are the limitations you want to place on the design. They may specify how big the part must be, how it must connect to various other objects, what the most extreme operating conditions that it can tolerate without failing must be, how much it can cost, etc. The best possible design will be the one that most effectively meets the objective while staying within the constraints [69].

5.4. OPTIMIZATION ALGORITHM USED

The numerical optimization is performed using Optimate+ CFD code, which is as an add-on for STAR-CCM+ that allows us to setup multiple STAR-CCM+ runs without scripting. By using this tool we have the ability to perform design exploration, optimization, and design of experiment and robustness studies without leaving the STAR-CCM+ environment. Optimate+ uses the HEEDS SHERPA search algorithm provided by Red Cedar Technology [69].

HEEDS (Hierarchical Evolutionary Engineering Design System) is a Multidisciplinary Design Optimization (MDO) method that uses the SHERPA algorithm, which works on the principle of Simultaneous Hybrid Exploration that is Robust, Progressive and Adaptive. It is based on simultaneous multiple search method instead of sequential method used by many others algorithms.

SHERPA has a very notable exception of not needing tunable parameters. Moreover, because of the high quality of its hybrid adaptation that allows an automatic adjustment of all the parameters in this process as it controls the type and direction of the search at each iteration step while several optimization algorithms are sensitive to the initial guesses of design variable values and other methods are relatively insensitive to these values.

Speaking of its robustness, compared to others optimizations algorithms, SHERPA is found to be very efficient as ideally, the performance of an optimization algorithm should be similar under all sorts of different starting conditions. Such an algorithm is said to be robust. This property is important for instilling confidence in the results of an algorithm and for approximating the number of evaluations needed to identify a good design [69]. This is surely one of the main advantages of this numerical optimization method as the time saving is very large compare to many others method where the user must conduct a number of trial-and-error simulations to obtain optimum results.

HEEDS MDO works on a basis of the design's performance value. When all constraints are satisfied for a good rating on the design's objectives, we have a high performance design. All designs that satisfy the chosen constraint essentially ignore by what margin they meet those constraints. Thereafter once the constraints are satisfied, only the objectives contribute numerically to the performance whose value is obtained using the following equation:

$$\sum_{i=1}^{Nobj}\left(\frac{L_{in}Wt_i * Obj_i}{Norm_i}+\frac{QuadWt_i * S_i * Obj_i^2}{Norm_i^2}\right)-\sum_{j=i}^{Ncon}\left(\frac{L_{in}Wt_j * ConViol_j}{Norm_j}+\frac{QuadWt_j * ConViol_j^2}{Norm_j^2}\right) \quad (1)$$

Where *Nobj* and *Ncon* are respectively the number of objectives and the number of constraints. *Linwt* represents the linear weight of the i^{th} objective, the default value is 1 and *S,* the sign for the i^{th} objective: -1 when minimizing and +1 for maximizing. Obj_i is the response value of the i^{th} objective for that design and *Norm*, the normalizing value for the i^{th} objective or constraint. $ConViol_j$ amount by which the j^{th} constraint is violated, it is 0.0 when the constraint is met and *QuadWt*, quadratic weight, the default value is 0 for objective and 10^4 for constraint

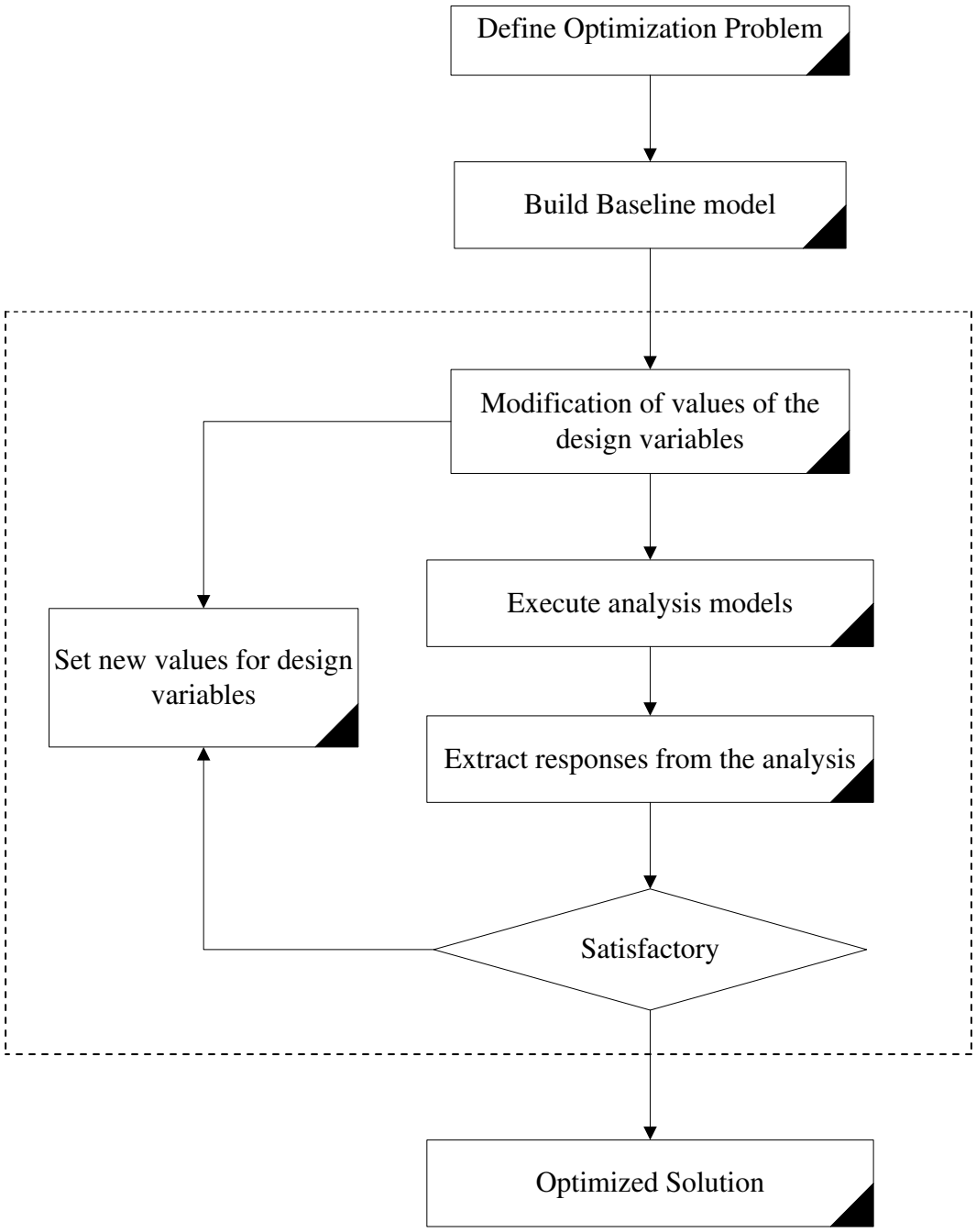

Figure 5-1: Flow chart of an optimization design process using SHERPA algorithm

However when the linear and quadratic weight variables are set to their default values, Eq. (32) becomes:

$$\sum_{i=1}^{Nobj}\left(\frac{L_{in}Wt_i * Sign_i Obj_i}{Norm_i}\right) - \sum_{j=i}^{Ncon}\left(\frac{QuadWt_j * ConstrntViol_j^2}{Norm_j^2}\right) \qquad (2)$$

During the optimization process, the computational domain is automatically remeshed at each run according to the geometry.

5.5. CLOSURE

This chapter emphasized on the importance of the numerical optimization Optimate+ Code conducted in terms of the efficiency as well as the robustness of its hybrid adaptive algorithm. Despite those two major advantages, SHERPA algorithm was showed to be very effective compare to many others optimization algorithms because of its several advantages including facts such as it:

- is easy to learn and to use
- doesn't required any expertise
- helps to save operating time and cost.

CHAPTER6: OPTIMIZATION RESULTS AND DISCUSION

6.1. INTRODUCTION

In this section we focused on the optimization of heat transfer density rate from heat-generating blocks using the CFD code detailed in the preceding chapter. In order to perform a better thermal management of heated blocks mounted on a horizontal wall of a rectangular enclosure and subject to forced convection, SHERPA numerical optimization algorithm is conducted to obtain the best heated blocks configuration (arrangement or geometry) that enhances the heat transfer density rate for two case studies.

In the automation process, the numerical optimization solution is conducted automatically according to design variables and constraints that implicitly influence the objective functions using by Optimate+ whose process was describe in Section 5.4. Thereby, we do not have to write and to implement a specific optimization code.

The first is the optimal distribution of heated blocks in the enclosure while the second and the third will be the geometric optimization of the blocks shape under specific constraints. Afterwards comparison of results will be made between obtained optimal configurations and initial configurations of heated sources.

It was proved that global thermal performance for cooling aligned heated sources depend not only on the thermal characteristic of the equipment, however it is strongly affected by the physical parameters such as number of elements and more importantly their geometry ratios as well as the arrangement or spacing between them [36, 57, 70-72]. The optimisation technique described above was applied to the model schematically described in Figures 4-1 (a) and (b) in Chapter 4, which is our reference model.

6.2. OPTIMIZATION OBJECTIVE AND MATHEMATICAL FORMULATION

The first objective function (to be minimized) is the overall temperature of all blocks faces which is obtained from the wall boundary heat transfer coefficient h whose equation is:

$$h = \frac{\left(q''_{conduction} A\right)}{\left[\left|A\right|\left(T_{ref} - T_f\right)\right]} \tag{6-1}$$

With:

$$T_{ave} = \frac{\sum T_{f,i} A_i}{\sum A_i} \tag{6-2}$$

Where T_f is wall boundary temperature; T_{ref}, the specified reference temperature in the enclosure and A is the heat transfer area.

The second objective function is the overall Nusselt number Eq. (27) which will be maximized. It was already defined in section 4.3

$$Nu_{ave} = \frac{\sum Nu_i A_i}{\sum A_i} \tag{6-3}$$

As mentioned in section 6.1, a formal mathematical optimization formulation of the problem is not needed to run the automated process and optimal results will be post processed by HEEDS Post option.

6.3. CASE STUDY ONE: OPTIMAL ARRENGMENT OF HEATED SOURCES

The effect of the spacing between heated obstacles on the thermal performance of the air forced cooling mechanism is the focus of this first case studied. As described in Section 4.5.1 by the discrete Kernel function from the superposition of thermal wakes equation

(Equation (4-16)) for aligned heated elements [56, 66] as shown in Figure 4-11, the maximum temperature occurs at the last heated element such as the temperature of each subsequent heated element is higher than the preceding one. This temperature is not only a function of temperature of each upstream element but is also a function of the global arrangement of these elements.

6.3.1. Optimization problem formulation

In present case, the aim is to find an optimum arrangement of heated blocks that will lead to a maximization of the global heat transfer rate density while keeping the peak temperature to its minimal value as it was already proved that the principle of non-uniform distribution of heat generating sources in channel increases thermal performance of the cooling mechanism [35, 54, 70-72].

6.3.2. Objectives functions

The objectives functions are already defined in section 6.2

$$f_1(x) = T_{ave} \tag{6-4}$$

$$f_2(x) = Nu_{ave} \tag{6-5}$$

6.3.3. Setting design variables

In literature it is showed that increasing separation distance between heated blocks under forced convection in channel improved considerably the global thermal performances Thus we set the spacing S_1, S_2, S_3 and S_4 as design variables.

For our model the range of the design variables is set according to the data obtained from experimental work conducted by Bar-Cohen and Kraus [56] using blocks' height as a scaling factor. They observed that increasing the spacing-to-block height ration from 2.5

to 4.0 enhanced the heat transfer density rate to the cooling fluid and further increase in the ration show slight change in Nusselt number.

Thus we chose a reasonable range of variation for the spacing between heat blocks such as:

$$1 \le \left(S_i + G\right)/B \le 4 \tag{6-6}$$

$$0.05 \le S_{1,2,3,4} \le 0.20 \tag{6-7}$$

6.3.4. Constraints

The constraints for this optimization process are taken as described in Section 4.2 from Equations 4-1 and 4-4 such as:

$$L_{in} \ge 5.G \tag{6-8}$$

$$L_{out} \ge 10.G \tag{6-9}$$

$$\left(L_{in} + L_{out} + 5G + S_1 + S_2 + S_3 + S_4\right) = L_x \tag{6-10}$$

6.3.5. Optimization results

The numerical optimization process has been conducted for each Reynolds number (100, 250, 500. 750, 1000). Optimal distances between consecutives heat-generating blocks obtained are listed in Table 6.1. As one can see, optimal spacing for Re_{Dh} = 100 and the 250 are almost identical and there are similarities in the optimal arrangements when Re_{Dh} = 500, 750 and 1000.

The resulting temperature contours in Figures 6-1 and 6-2 show that optimum configurations of heated blocks' arrangement are such as any downstream spacing is larger than the subsequent one except for the last spacing. Figures 6-3: (a) to (e) indicates how the optimum arrangement compare to our initial one strongly influences the heat transfer to the cooling fluid. This phenomenon of non-uniformity of spacing reflects the

fact that the optimal arrangement must basically lower the strong thermal interaction between heated elements which tends to increase considerably both the overall and the peak temperatures in the enclosure due to the equi-spaced arrangement. Thus optimum location of each downstream block is such that it must minimize the thermal effect of the flow induced by the upstream heated blocks.

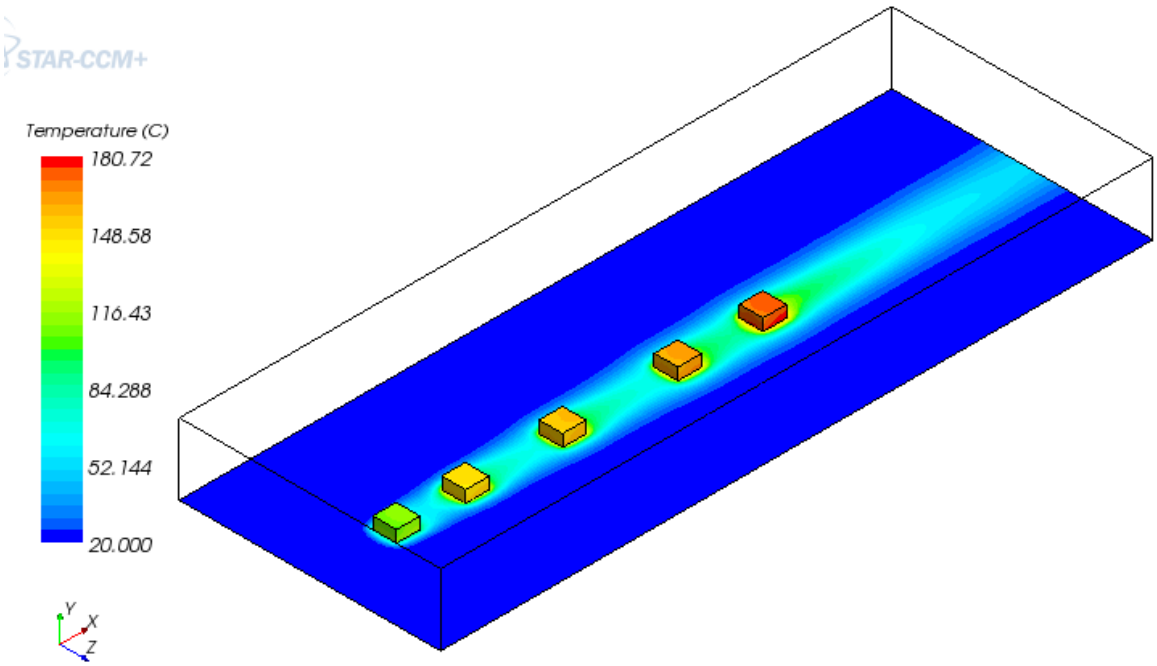

Figure 6-1: 3-D Temperature contour optimal blocks arrangement, Re_{Dh} = 500

Table 6-1: Resulting optimal spacing between consecutives heated blocks

Re_{Dh}	S_{1opt}	S_{2opt}	S_{3opt}	S_{4opt}
100	0.125	0.163	0.180	0.140
250	0.127	0.160	0.164	0.138
500	0.075	0.1295	0.227	0.160
750	0.104	0.134	0.223	0.150
1000	0.120	0.128	0.194	0.170

Through the principle of superposition of thermal wakes effect in the streamwise direction as it was clearly shown in Section 4.5.1, because of the important contribution in thermal energy from upstream heat sources that must be reduced, the optimal arrangement consists in a trade-off location of heat generating sources that provide an important heat removal by allowing important flow mixing around heated elements which transports more thermal energy to the cooling fluid. Since the air is gradually heated from the first blocks to the last one and the temperature of the air increases accordingly, so the greater the spacing between blocks, the lower the upstream thermal effect on subsequent blocks and the smaller the temperature gradient from the first to the last block.

Table 6-2: Resulting optimal spacing ratio for consecutives heated blocks

Re_{Dh}	S_2/S_1	S_3/S_2
100	1.30	1.10
250	1.26	1.02
500	1.73	1.75
750	1.29	1.66
1000	1.07	1.51

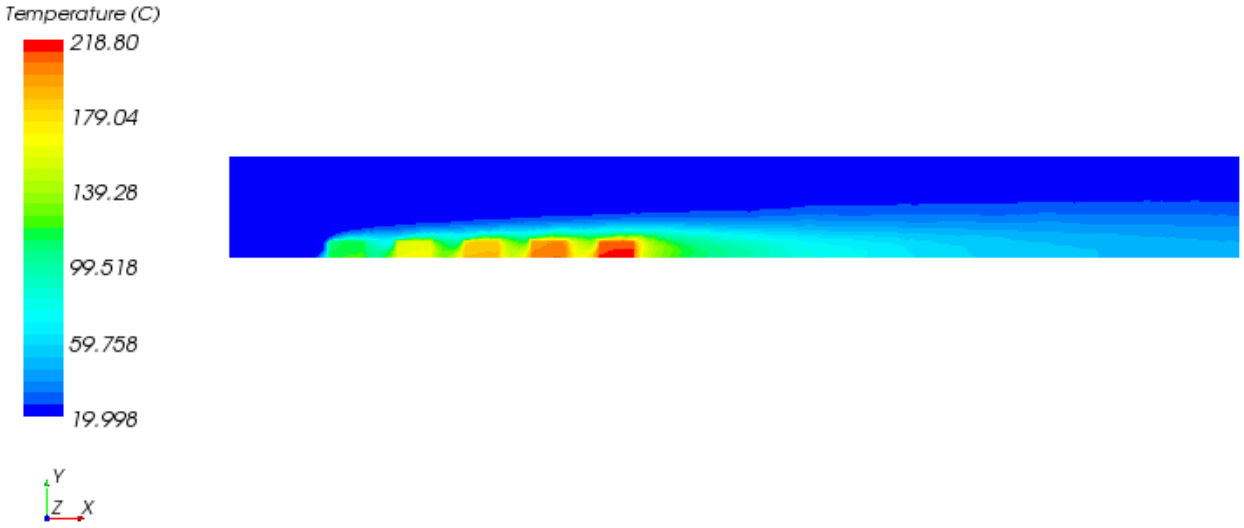

(a)

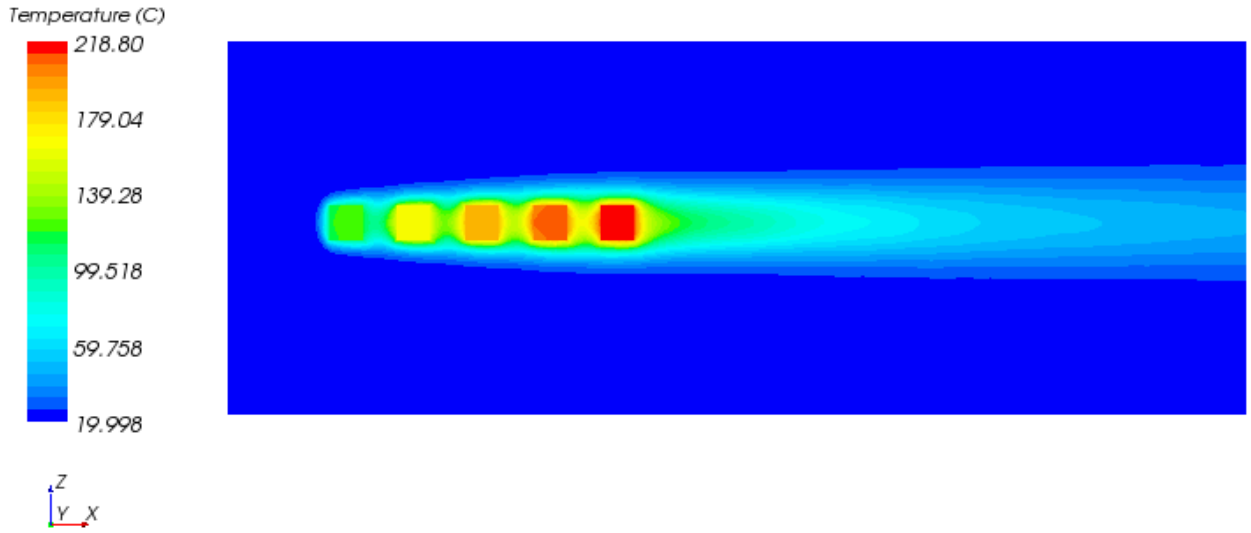

(b)

Figure 6-2: 2-D Temperature contour of the initial arrangement, Re_{Dh} = 500: X-Y plane (a) and X-Z plane (b)

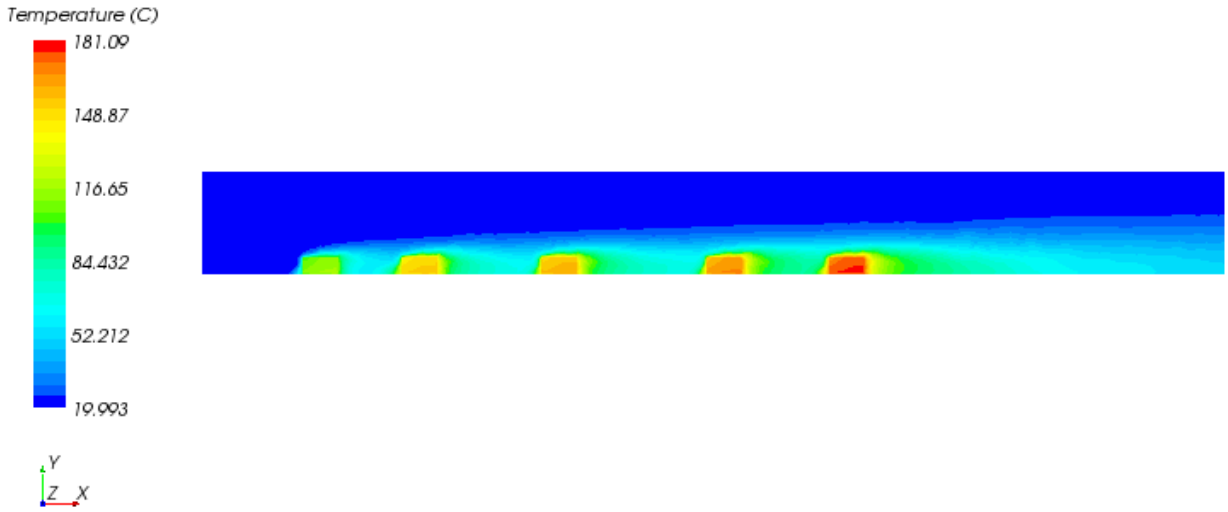

(a)

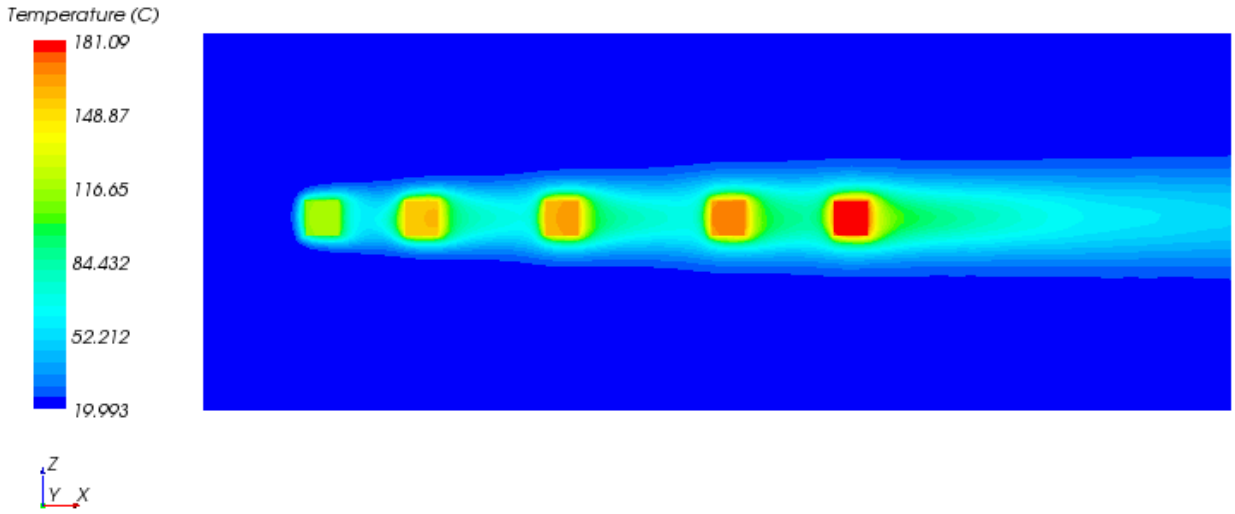

(b)

Figure 6-3: 2-D Temperature contour of the optimal arrangement Re_{Dh} = 500: X-Y plane (a) and X-Z plane (b)

Actually, for any Reynolds number, the heat transfer density rate from the first block is the same for both initial and optimal configuration, however from the second block when the separation distance increases, Figures 6-2 (a) and (b) show that the heat removal from downstream blocks is enhanced for the optimal arrangement as optimum spacing are found to be larger than the initial so that more upstream flow can penetrate the cavities in between blocks in order to decrease the thermal boundary thickness of vertical faces while mixing with the vortex and then reduces the isolating level the of recirculation flow. This has an effect of removing further the heat form blocks and reducing the surface temperature.

The peak temperature (temperature of the last block) depends on the temperatures as well as the distances away from upstream blocks. It depicts that, no matter the Reynolds number the heat removal from the first and any upstream block is greater than from the subsequent ones. Figures 6-3: (a) to (e) clearly illustrate that the enhancement in heat transfer rate cause a gradual temperature decrease of about 9% for the second block up to 20 %, for the last block as well as an average decrease in the temperature gradient between the first block and the last one of about 45%.

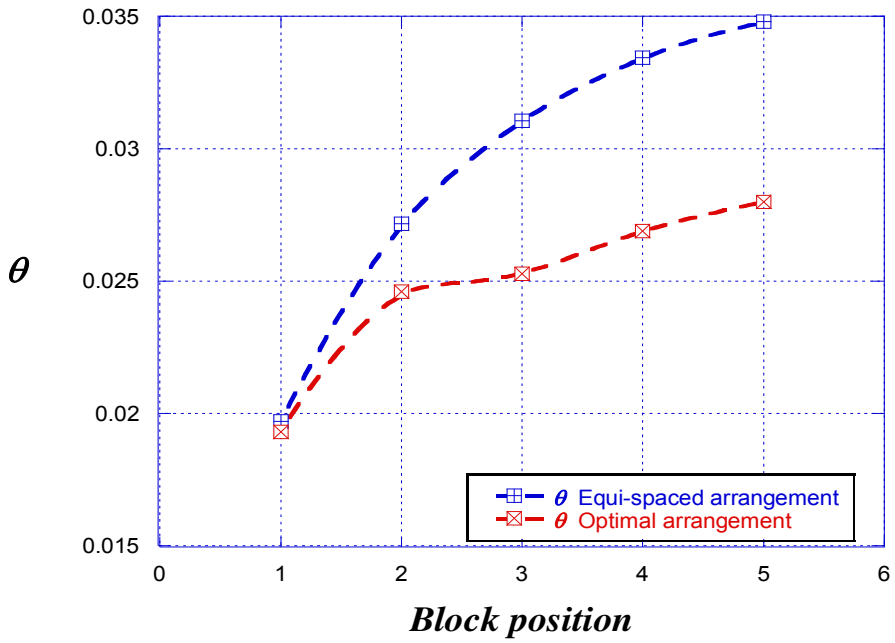

(a)

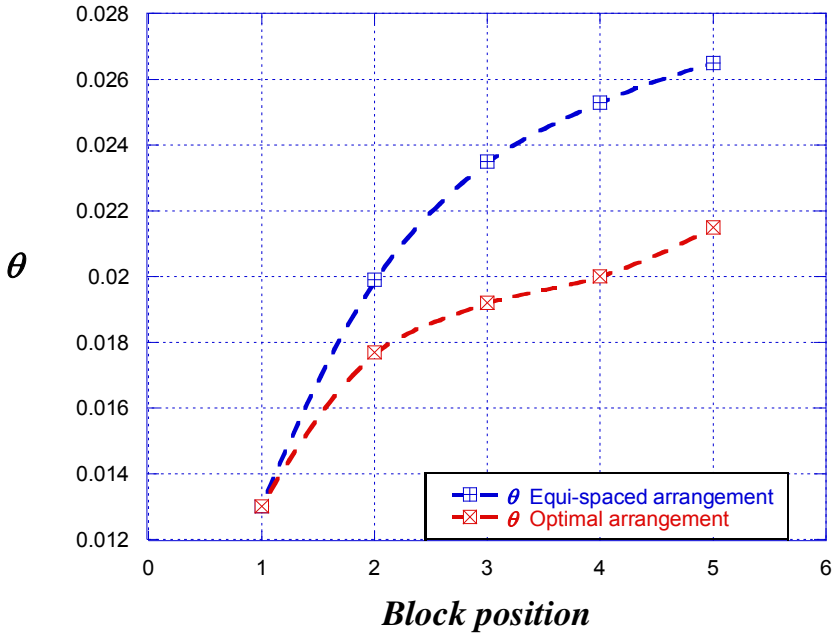

(b)

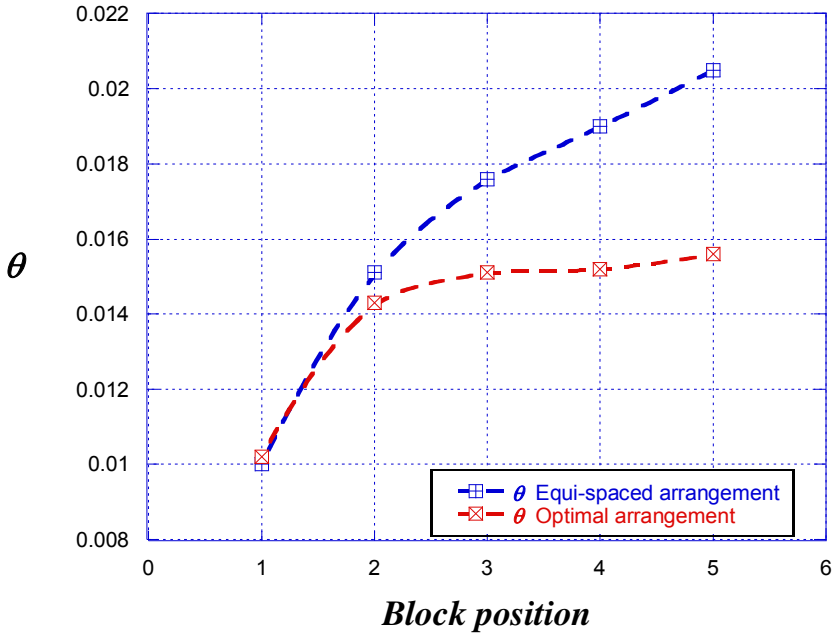

(c)

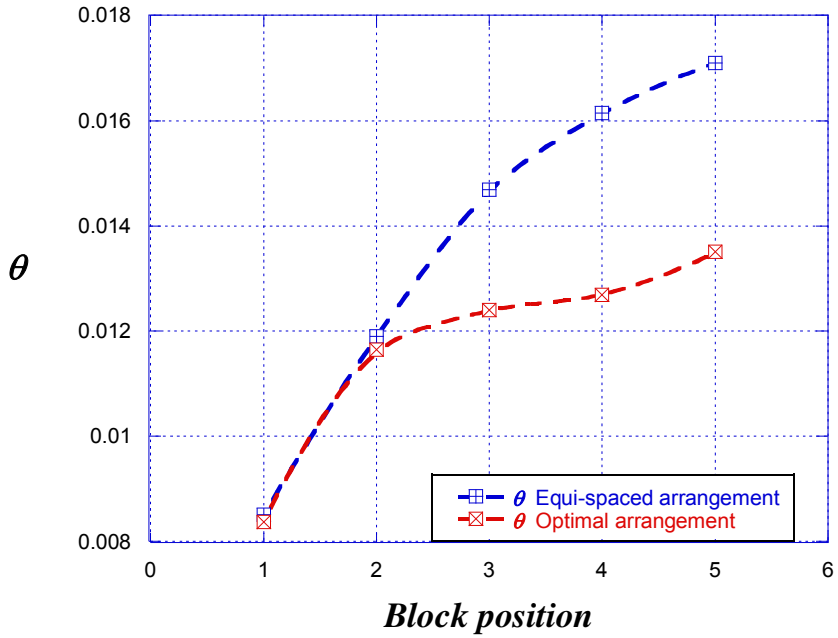

(d)

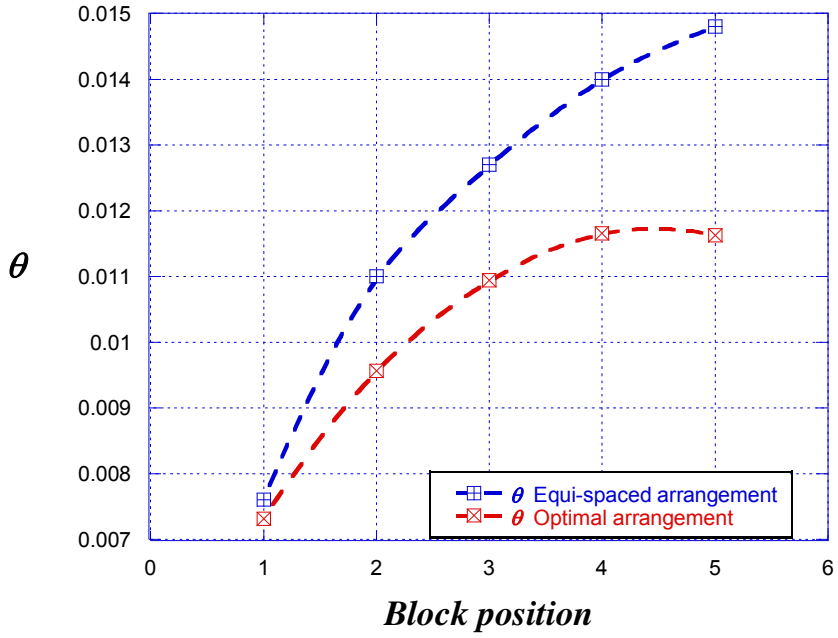

(e)

Figure 6-4: Comparison of the temperature between the optimal blocks configuration and the equi-spaced arrangement: (a) Re_{Dh} = 100; (b) Re_{Dh} = 250; (c) Re_{Dh} = 500; (d) Re_{Dh} = 750; (e) Re_{Dh} = 1000

Figures 6-5 to 6-7 illustrate that the optimal arrangement gave a significant decrease of 20% in the peak temperature and an important increase of 15% and 17% in the overall Nusselt number and the overall dimensionless conductance respectively in the enclosure. These results confirm that increasing the spacing is more favourable to improve the heat transfer density rate from the subsequent blocks. Moreover, heat transfer at the last block is further enhanced by the flow rate as the thermal transport due the downstream recirculation increases.

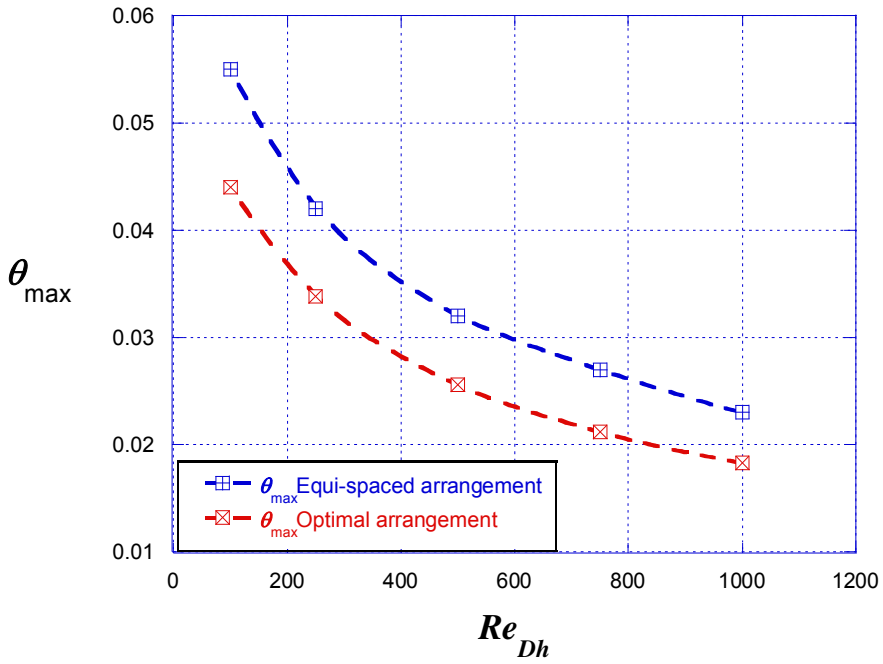

Figure 6-5: Dimensionless maximum temperature comparison between the optimal blocks configuration and the equi-spaced arrangement

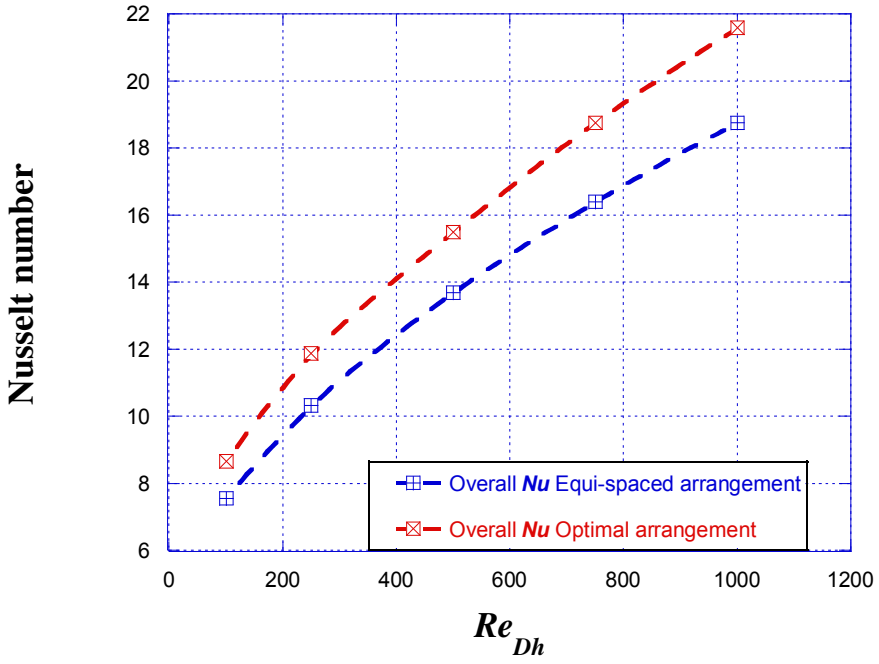

Figure 6-6: Overall Nusselt number comparison between the optimal blocks configuration and the equi-spaced arrangement

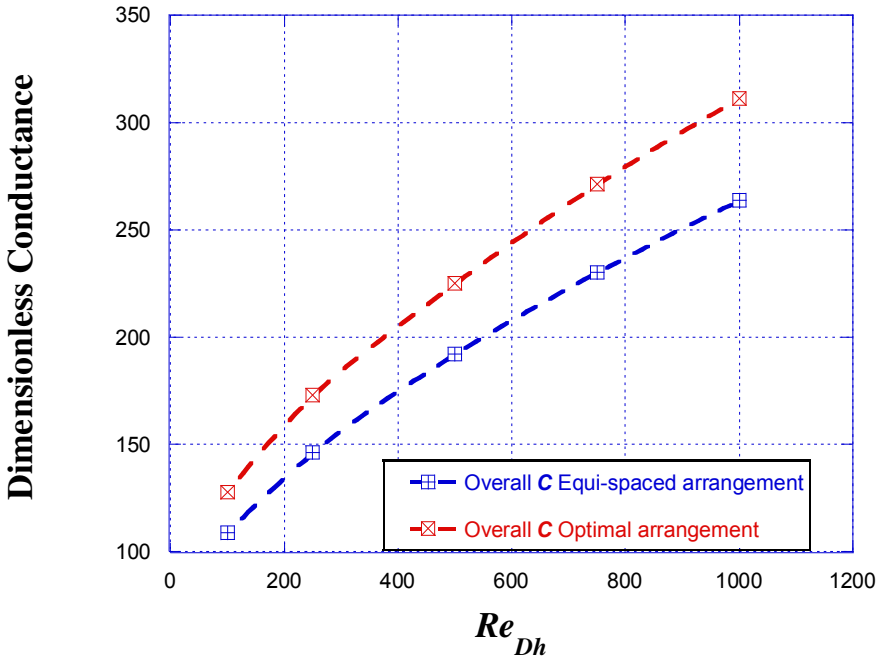

Figure 6-7: Dimensionless overall conductance comparison between the optimal blocks configuration and the equi-spaced arrangement

The results showed that better thermal performance for the cooling mechanism is not reached with the equi-spaced arrangement but when the spacing ratio of consecutive heated blocks is greater than 1, more precisely: $1.02 \leq S_{i+1} / S_i \leq 1.6$. However in the optimal arrangement, the spacing between the two last blocks ($S_{4,opt}$) for any Reynolds numbers range was almost equal to 3 x G.

It is of interest to note that optimal results found here tend to confirm data obtained in literature regarding similar investigations. It has been proved either experimentally or numerically that best thermal performance concerning the cooling of heated sources in cavities can be achieved if all the center-to-center distances ratio follow the geometric series and especially when the geometric ratio is 1.618 named as the Golden mean or Golden ratio [35, 54, 57] , the maximum temperature reaches its lowest value. More preferably when the side-to-side distance between the two last heated sources are fixed and others follow a geometric series arrangement, a much better thermal performances could be obtained [54].

Ultimately, considering optimal results, thermal performance of the convection mechanism depends more on the heated sources' general configuration than on the flow condition and the thermal specification.

6.4. CASE TWO: 3-D OPTIMAL GEOMETRY OF HEATED BLOCKS

In this section an attempt is made to find the optimal blocks' shape that maximizes of the overall heat transfer rate to the cooling air in order to reduce the peak temperature in the enclosure is discussed. This would allow for comparison with investigation data provided found in the literature.

It was clearly observed in [33, 34, 55] for two dimensional investigations on cooling of heat generating blocks that their geometry ratio strongly affected the thermal performance of the convection heat transfer.

6.4.1. Optimization problem

The heated blocks follow equidistant arrangement and are subjected to the numerical optimization in order to enhance the effect of variations in the shape of the blocks on the heat transfer density rate. The geometric parameters that are allowed to vary are the length of each side of the heated blocks. This being so the spacing between blocks might also vary according to optimal blocks shape.

6.4.2. Objectives functions

The objectives functions are already defined in section 6.2

$$f_1(x) = T_{ave} \tag{6-1}$$

$$f_2(x) = Nu_{ave} \tag{6-2}$$

6.4.3. Setting design variables

Here the length of each side of the block (*G, B, C)* is chosen to be design variable such that the geometry of the blocks can morph in three dimensions in order to reach an optimum shape for a maximum heat transfer density rate.

According to our computational model, variables ‘ranges are as follow:

$$0.02 \le G \le 0.05 \tag{6-11}$$

$$0.02 \le H \le 0.05 \tag{6-12}$$

$$0.02 \le C \le 0.05 \tag{6-13}$$

6.4.4. Constraints

Unlike to first study case, for geometric optimization, in addition to the three length constraints, we also have the volume constraint expressed in Equations 4-2 and 4-3 in Section 4.2.

Hence we deduce:

$$L_{in} \geq 5G \tag{6-14}$$

$$L_{out} \geq 10G \tag{6-15}$$

$$L_{in} + 5G + \sum_{1}^{4} S_i + L_{out} = L_x \tag{6-16}$$

$$G.C.B = V = Const \tag{6-17}$$

6.4.5. Automation and optimal results

Similarly to the first case, a three-dimensional geometric optimization of blocks' shape, subjected to both the total length and the global volume constrains, was carried out numerically at the same specific Reynolds numbers of 100, 250, 500, 750 and 1000 in order to maximize the heat transfer density rate.

Optimal blocks dimensions that maximize the rate of heat transfer and minimize peak temperature in the channel are listed in table 6-3. Optimal geometries are unique and identical when Re_{Dh} = 250 and 1000 while for Re_{Dh} = 100, 500 and 750, it was observed that good thermal performance is obtained with two very different and specific geometries that gave the same average Nusselt number for each Reynolds number. However for these last three cases, best thermal results, in term of both average and maximal temperature were achieved with geometry identical to the other two such as the block height is maximal while its length is minimal.

The temperature contours of the optimized geometries differences for Re_{Dh} = 500 is shown as an illustration of this results in Figures 6-8 (a) and (b).

Table 6-3: Optimal heated blocks dimensions for different Reynolds numbers

Re_{Dh}	**100(a)**	**100(b)**	**250**	**500(a)**	**500(b)**	**750(a)**	**750(b)**	**1000**
G_{opt}	0.050	0.025	0.025	0.041	0.025	0.050	0.025	0.025
B_{opt}	0.036	0.050	0.050	0.040	0.050	0.050	0.050	0.050
C_{opt}	0.039	0.050	0.050	0.038	0.050	0.025	0.050	0.050

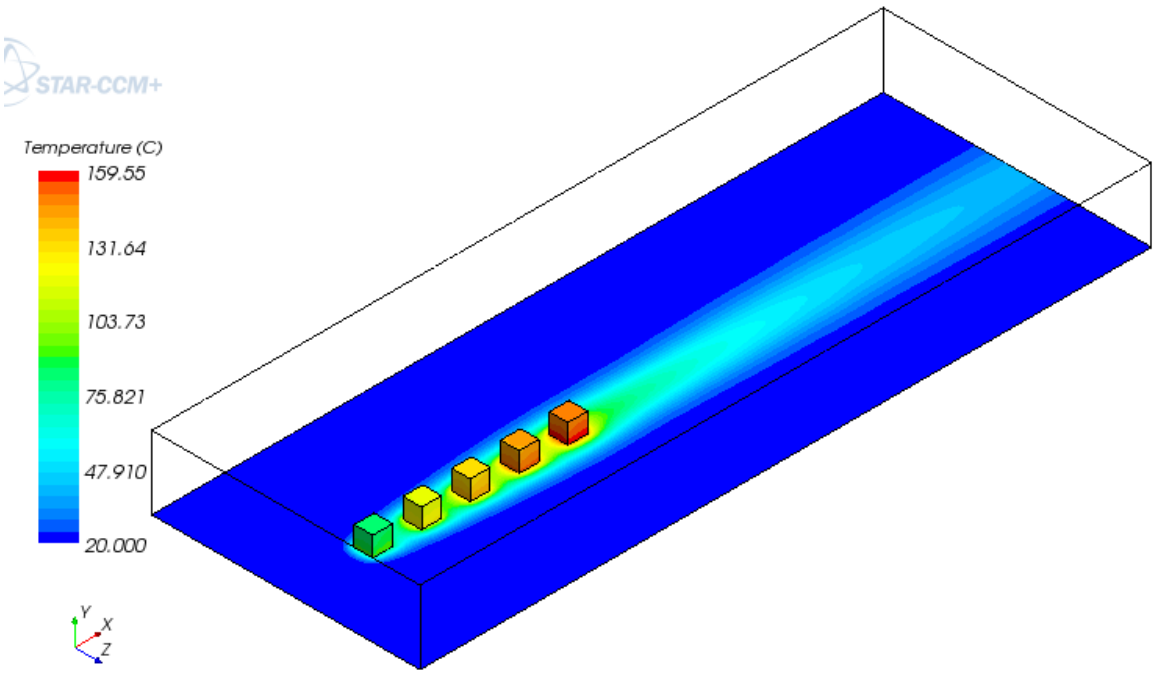

(a)

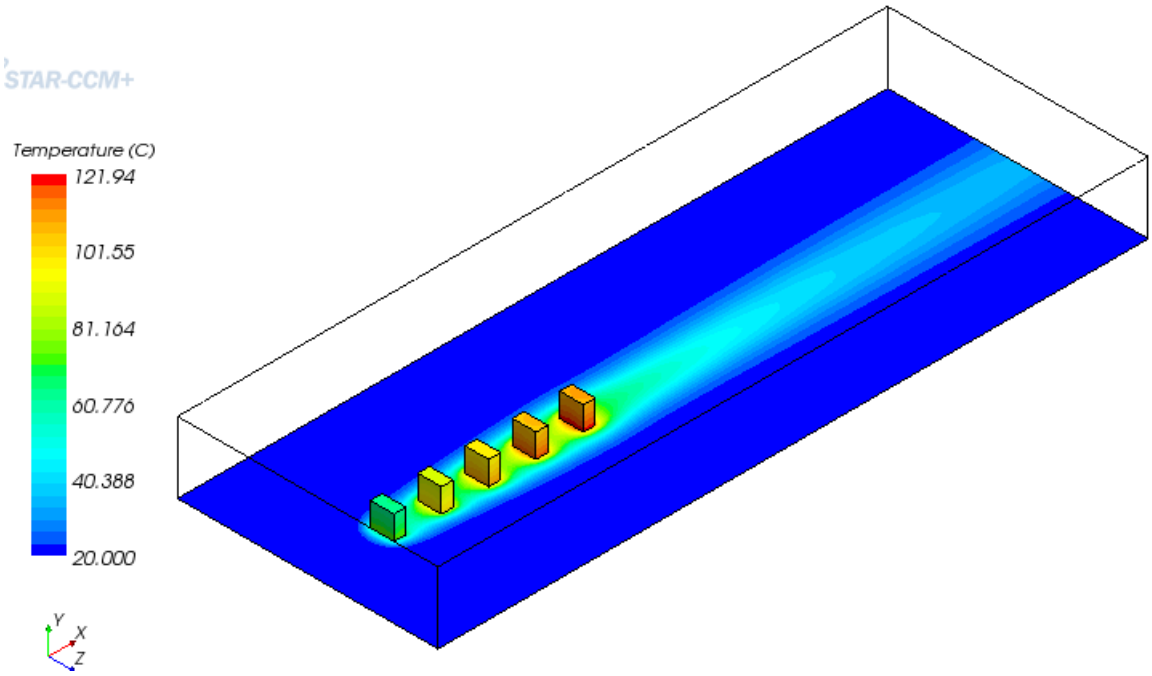

(b)

Figure 6-8: 3-D Temperature contour optimal blocks' geometry, Re_{Dh} = 500: (a) and (b)

Therefore it is clear to note that the optimal shape is the one whose blocks height (B) is maximum. We then infer that tall and slender blocks are found to be more advantageous compared to the initial configuration in term of enhancing the heat transfer to the cooling fluid.

Base on this observations we can confirm that besides the Reynolds number and the spacing of heated blocks effect on the heat flow rate, their shape strongly affects thermal performance of the convection mechanism. Indeed, the heat transfer is improved when the blocks height-to- length ratio is greater than 1. Since the optimal blocks ratio are very similar for selected values of Reynolds numbers in the range of 100 to 1000, this results are in good agreement with data obtained experimental and numerical investigations found in the literature [33, 34, 55] which reported that within the laminar regime, specifically when $Re \leq 1500$, the slender-taller obstacles produced a larger mean Nusselt number compare to the flatter-shorter ones.

The optimal configuration being as described, the geometric arrangement is such that the spacing between consecutive blocks that plays also a major role in the resulting thermal performance of the array is greater compare to initial configuration. Therefore it further improves the heat transfer rate as already explained previously in the first study case.

When the height-to-length ratio increases (tend to its maximum value), the blocks are taller, the inlet flow improves the rate of heat transfer of the heated blocks as their upstream face are larger. Notably this effect is more significant for the first block that benefits from the inlet cold flow impact which enhances the rate of heat transfer.

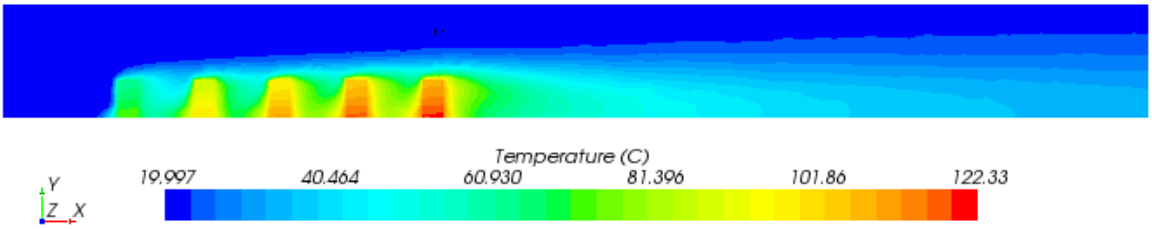

(a)

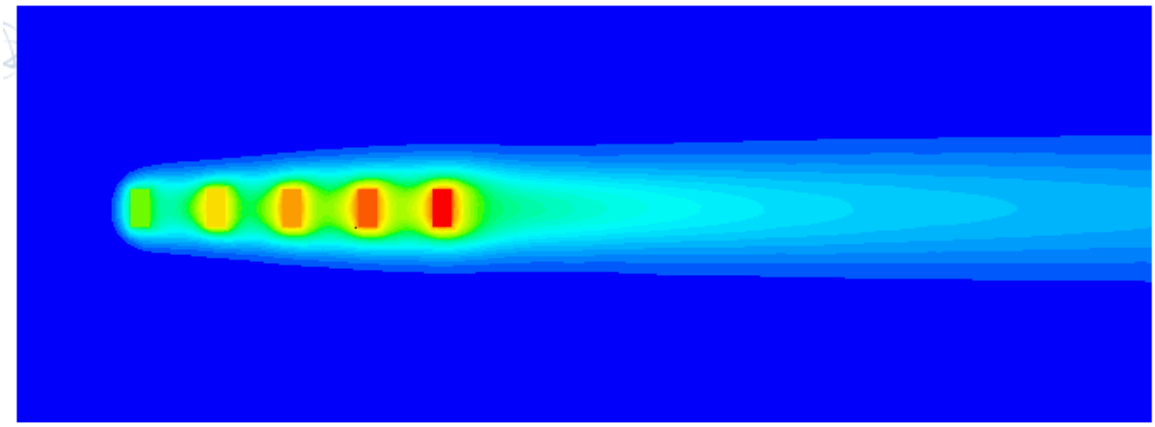

(b)

Figure 6-9: 2-D Temperature contour of the optimal blocks geometry, Re_{Dh} =: X-Y plane (a) and X-Z plane (b)

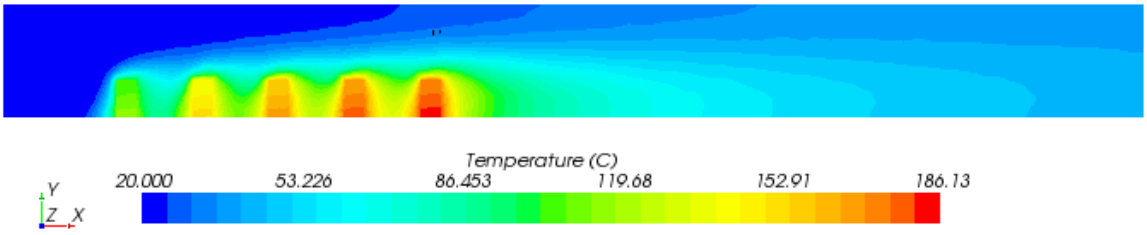

(a)

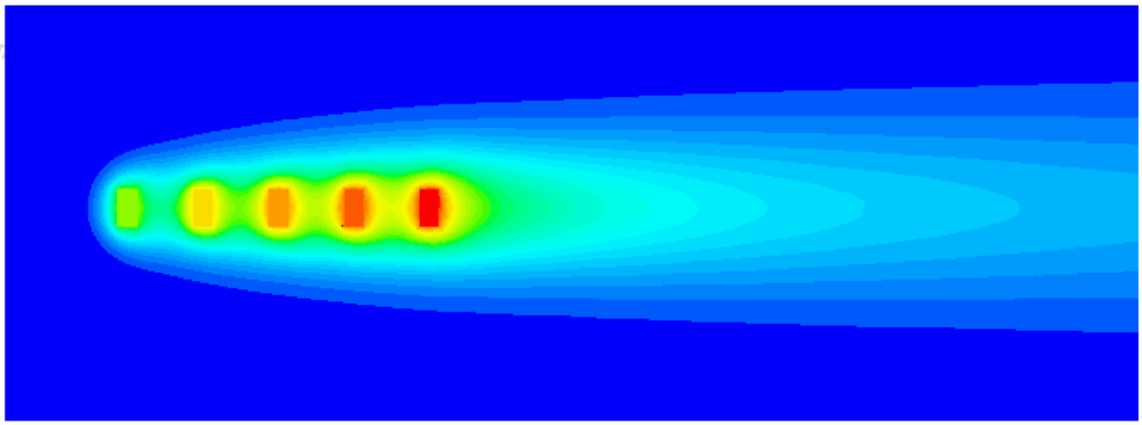

(b)

Figure 6-10: 2-D Temperature contour of the optimal blocks geometry, Re_{Dh} = 100: X-Y plane (a) and X-Z plane (b)

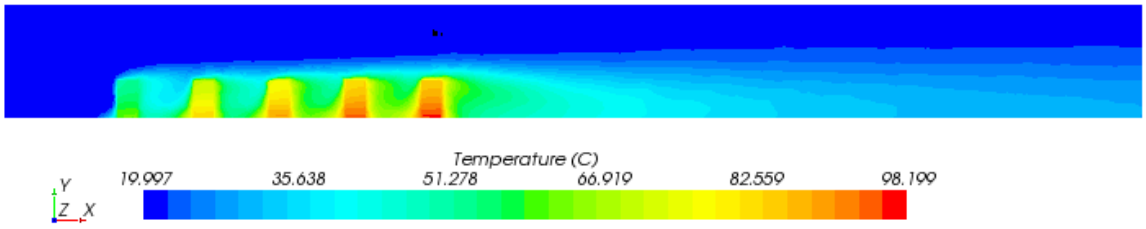

(a)

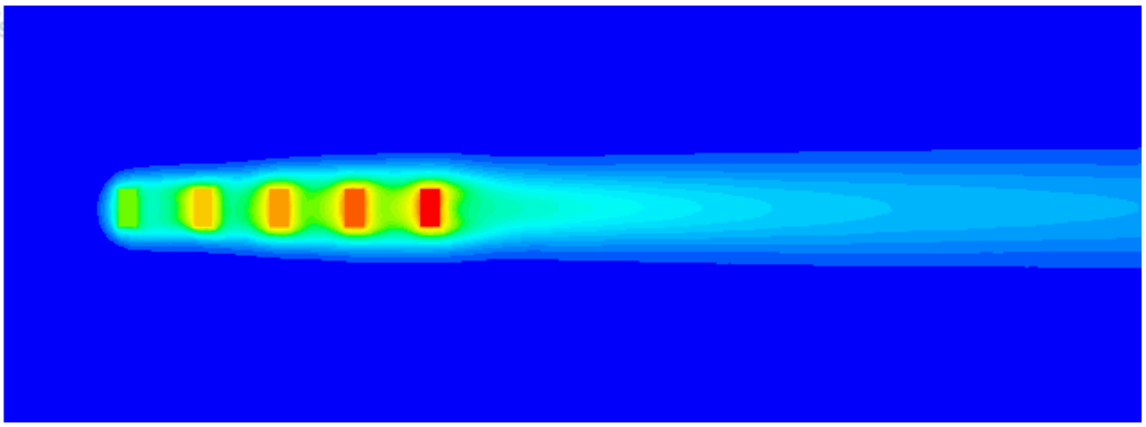

(b)

Figure 6-11: 2-D Temperature contour of the optimal blocks geometry, Re_{Dh} = 1000: X-Y plane (a) and X-Z plane (b)

Indeed, heat transfer from subsequent blocks downstream is enhanced by an acceleration of the flow air velocity on top the blocks due to the fact that taller blocks decrease the bypass region and therefore increase the recirculation above the block. As the blocks are slender the recirculation zone might be moved from the top of the blocks into the downstream spaces which are larger so that more flow can penetrate the cavities in between blocks. As a result it decreases the thermal boundary thickness of vertical faces while mixing with the vortex and then reduces the isolating level the of recirculation flow. This has an effect of removing further the heat form blocks and reducing the surface temperature. Heat flux rate at the last block is further enhanced by the flow rate as the thermal transport due the downstream recirculation increases.

The gap between the temperature profiles obtained from the initial geometry and from the optimal shape in Figures 6-8 to 6-11 corroborates that for all considered values of Reynolds number, the rate of heat transfer from each heated block is improved in the optimal configuration as the temperature of every heated block decreases significantly. The average increase in the heat transfer rate is about 35% compare to its value obtained with the initial value, which leads to a decrease of more than 50% for both the overall and the peak temperature as well as to a significant increase of 100% for the global conductance. At this point we can affirm that the average rate of heat transfer is enhanced with the increase of the block height-to-length ratio in the laminar regime when $Re \leq 1000$.

Optimization results showed that the best global thermal performance is not achieved when these two other sides of the blocks have the same length. However we observed that for some specific length-to-height aspect ratio of the blocks, we have significant enhancement of heat transfer rate to the cooling fluid and therefore this result reduces both the overall and peak temperature in the channel. Very similar results were also observed in the literature for two-dimensional numerical investigations [33, 34, 55].

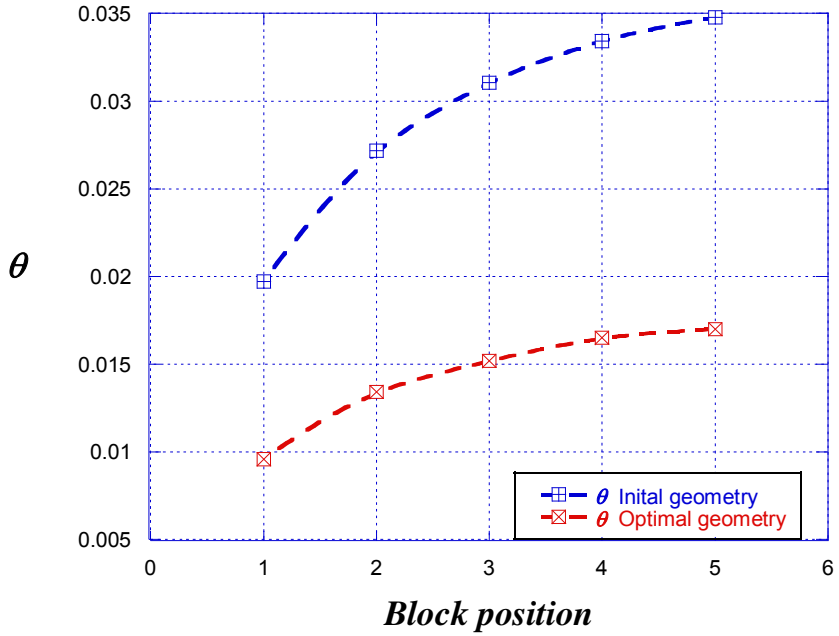

(a)

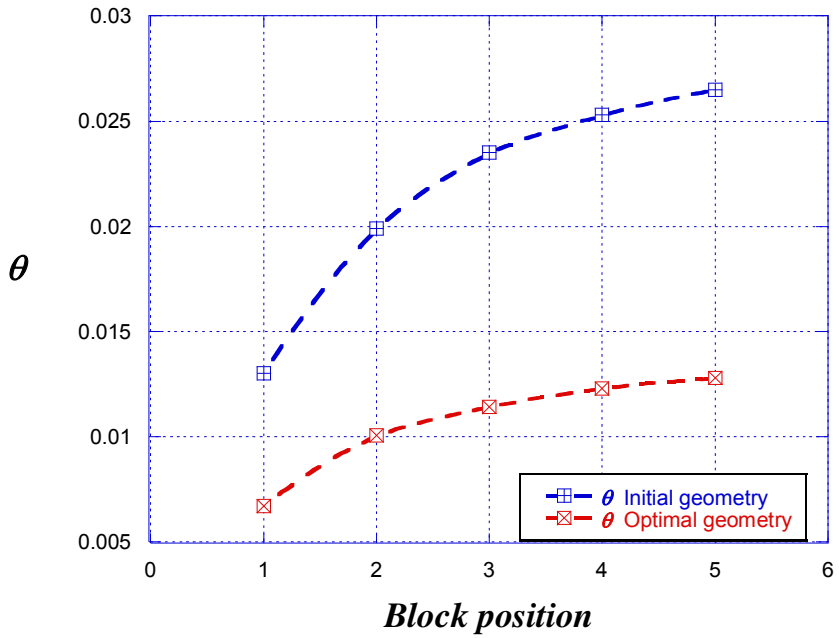

(b)

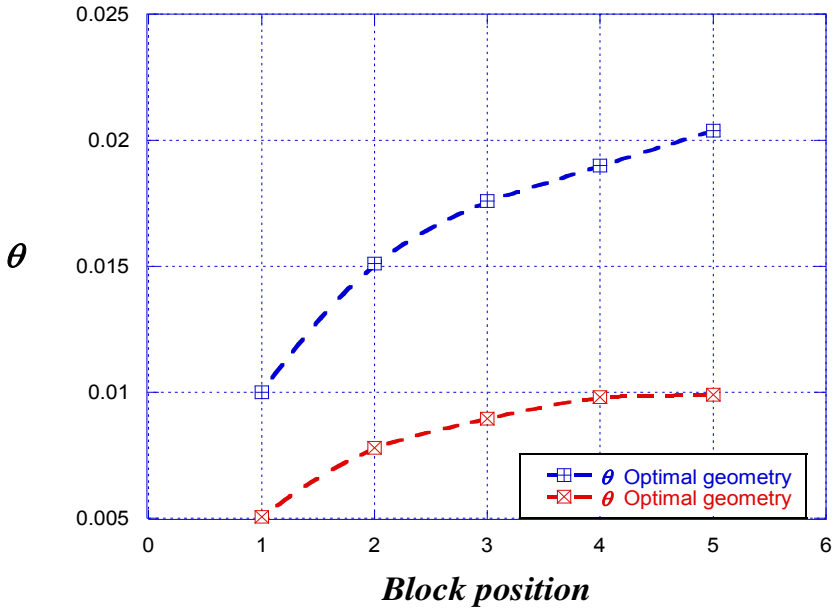

(c)

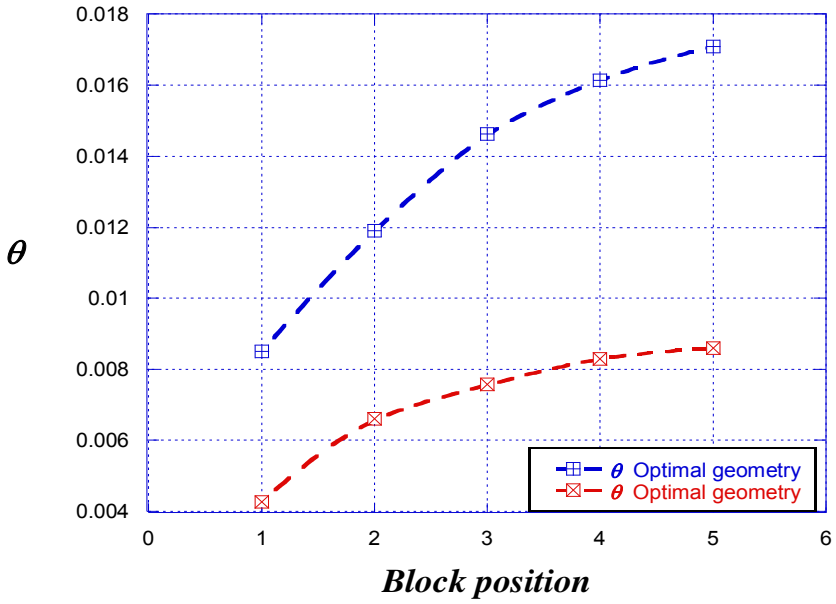

(d)

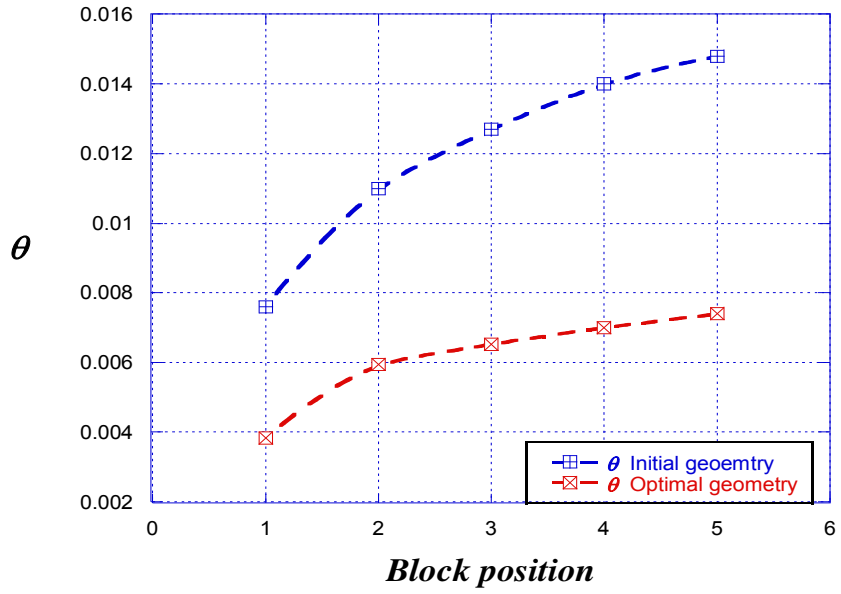

(e)

Figure 6-12: Comparison of the temperature between the optimal blocks geometry and the initial geometry: (a) Re_{Dh} = 100; (b) Re_{Dh} = 250; (c) Re_{Dh} = 500; (d) Re_{Dh} = 750; (e) Re_{Dh} = 1000

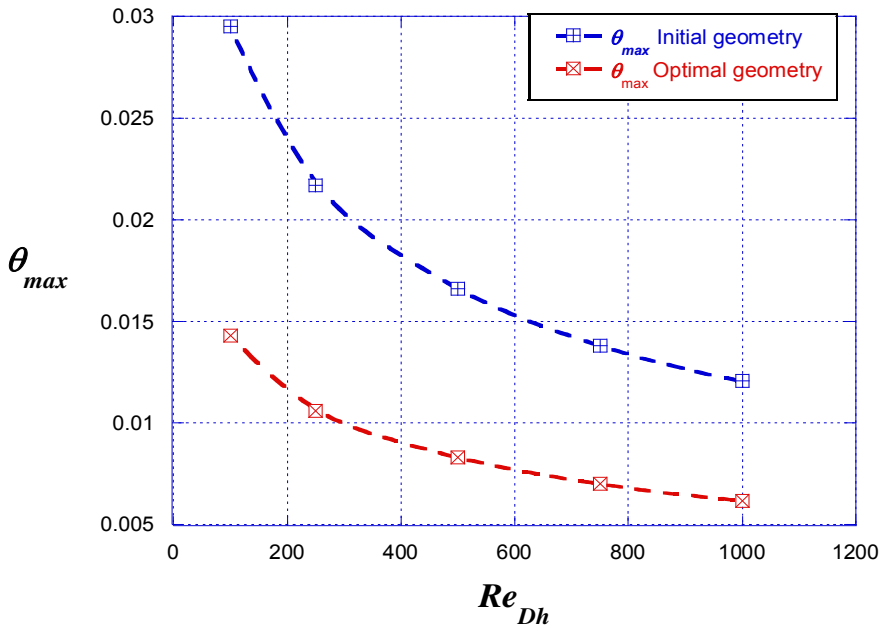

Figure 6-13: Dimensionless maximum temperature comparison between the optimal blocks geometry and the initial geometry

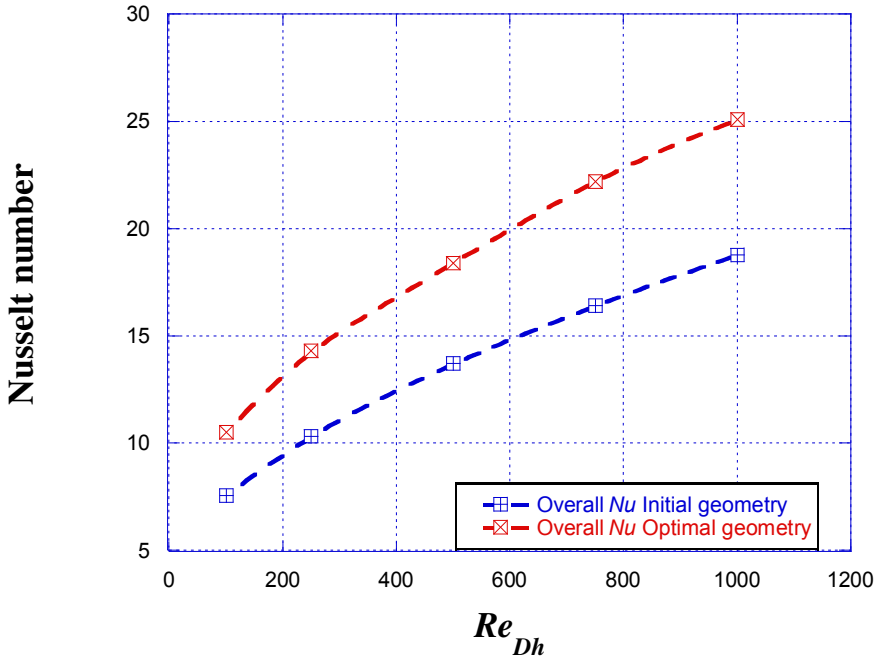

Figure 6-14: Overall Nusselt number comparison between the optimal blocks geometry and the initial geometry

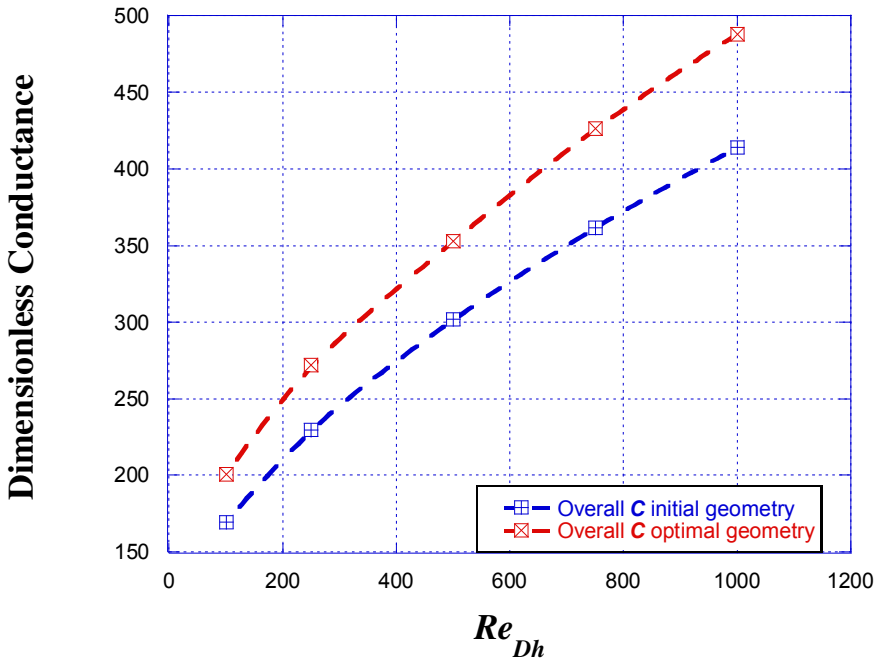

Figure 6-15: Dimensionless overall conductance comparison between the optimal blocks geometry and the initial geometry

6.5. CLOSURE

In this Chapter a three-dimensional geometric optimization has been numerical carried out to minimize the peak temperature as well as to maximize the heat transfer density rate in the enclosure mounted on its bottom with heat generating blocks whose thermo-physical specification were previously described in chapter 4. During the optimization procedure the objective functions are the overall temperature to be minimized and the overall Nusselt number to be maximized in the enclosure.

For specific Reynolds numbers range from 100 to 1000, optimized results using the HEEDS-SHERPA optimization algorithm were presented in terms of overall Nusselt number, the dimensionless temperature and the global dimensionless conductance in the channel. The geometric parameters on which the optimization procedure was focused were the global arrangement in the first study case followed by the shape of the heated blocks within the enclosure for the second case.

By varying the spacing between heat generating blocks in the optimization process in the first case, the results showed that the traditional equi-spaced arrangement of heated elements is not the optimal option. However a better thermal performance was achieved when the ratio of spacing between consecutive heated blocks was greater than 1. This revealed that increasing spacing between blocks result in significant enhancement of the heat transfer density rate up to 15%.

It is of interest to note that the results obtained in this first study confirmed those provided in the literature which obtain that better thermal performance for the cooling mechanism is not reached with the equi-spaced arrangement but when the spacing ratio of consecutive heated blocks is greater than 1 and more precisely when the center-to-center distances follow the geometric series and the geometric ratio is 1.618, known as the

golden ratio .Moreover when the side-to-side distance between the two last heated blocks are fixed and others follow a geometric series arrangement, a much better thermal performances could be obtained .

In Study Case Two where the geometric blocks dimensions were set as design variables and each block volume was fixed as a constraint, the numerical optimization has led to particular results such as the higher the block height-to-length ratio, the better the global thermal performance of the heat transfer in the enclosure. It was found that the taller and slender blocks give a maximum density of the heat transfer rate.

It can be concluded that for all the geometric parameters studied, the design variables had significant effect on the thermal performance of heat-generating blocks inasmuch as optimum results obtained in these studies have confirmed the existence of both an ideal configuration and an optimal shape of heat generating blocks that improve the global thermal performance of the heat transfer mechanism within the enclosure regardless the Reynolds number.

CHAPTER7: SUMMARY CONCLUSION AND SUGGESTIONS

7.1. SUMMARY

The need of thermal management of heat generating entities has increased because of overheating issues in electronics. Both natural and forced convection mechanism heat transfer are being widely conducted using various methods such as experimental investigation, numerical simulation, analytical procedure to investigate the influence of different thermo-physical factors of equipment on the cooling of heat sources flush mounted or protruding on a wall as well as in a channel.

In this dissertation relevant results provided in the literature about some of these studies were presented in chapter 2 after basics of heat transfer mechanism together with the limitations in the flow regimes considerations were provided in Chapter 1. The physical model as well as mathematical formulation of the governing equation describing the fluid and heat transport that takes into account the convective heat transfer from in-line arrays of heated blocks in a rectangular cross section channel was clearly presented in Chapter 3.

An attempt was made in Chapter 4 by simulation using an efficient and robust CFD Package Star-CCM+ 8.02 to show the impact the Reynolds number on the thermal performance of the heat transfer from discrete heat-generating blocks under laminar force convection in a rectangular enclosure. Simulations were conducted for specific values of Reynolds range from 100 to 1000 after a validation of this procedure on the basis of the similarity in the trend between the number of Nusselt obtained numerically and that calculated from an experimental method provided in the literature.

From a fundamental point of view the objective of this study was to conduct a numerical optimization method in order to maximize the heat transfer density rate and to minimize

the peak temperature in the enclosure, that's why in Chapter 5 an overview of the Star-CCM+ add-on Optimization Algorithm HEEDS-Optimate+ to be used was given. In order to achieve better global thermal performance, the numerical optimization algorithm named above was carried out in Chapter 6 to perform geometric optimization by varying the spacing between heated blocks in the first study case and then by varying the blocks' shape for the second one, under constant volume constraint for each bloc.

7.2. CONCLUSION

After conducting several simulations, the thermal performance of the cooling mechanism was found to be depended of the Reynolds number such as with the same heated blocks configuration (initial arrangement), the stronger the flow velocity, the better is the heat transfer rate density. A great improvement of heat transfer is achieved for higher Reynolds number and the recirculation zone adjacent to the blocks are also proportional in magnitude with the Reynolds number that varied in between 100 and 1000.

Subsequently, with regard to the optimization process no matter the Reynolds number, results from both cases clearly bear out that general configuration and arrangement of heat sources have a significant effect on the heat transfer performance. In the Study Case One, compare to the traditional equi-spaced arrangement of heated blocks the optimal arrangement increased the heat transfer density rate up to 15 % while in the second one, changing the blocks geometry improves the global performance of the heat transfer mechanism such that it gave a substantial decrease in the temperature of up to 50% both for the mean and the overall temperature and an increase in the overall Nusselt number in the channel of 5%.

These optimum results obtained in this study have confirmed the existence of an ideal configuration of heated sources that would minimize both the overall and the maximum

temperatures within the enclosure regardless the Reynolds number as it was experimentally proved in the literature.

In conclusion, when comparing optimal configuration to the optimization, results revealed that besides the Reynolds number influence on the heat transfer density rate, the blocks arrangement as well as their shape strongly enhances thermal performance of the convection mechanism.

7.3. SUGGESTIONS

The numerical procedure of optimization conducted in this study emphasised on the minimization of the peak temperature together with the maximization of the heat transfer density rate from in-line heat generating blocks protruding on the bottom wall of a rectangular enclosure. Although the presented results were found to be acceptable and coherent considering a simple forced convection and assuming constant thermo-physical cooling air properties at the inlet temperature, additional aspects could be the subjects of further investigations including these:

1. It would be important on a physical point on view to extend the geometric optimization process on a greater the number of in-line heated blocks or an array of staggered heated blocks in channel

2. it might be advantageous to take into account the effect of thermo-physical properties variations with the fluid temperature on the peak temperature as well as on the overall heat transfer density rate in the enclosure

3. It could also be interesting to study the contribution of natural convection or the radiation phenomenon to the overall heat transfer mechanism in the channel by considering the buoyancy or the radiative effect on the global thermal specifications of the model.

REFERENCE

[1] R. Grundy. (2005) Recommended Data Center Temperature & Humidity Preventing Costly Downtime Caused By Environment Conditions. *AVTECH*.

[2] Q. Chen and W. Xu, "A zero-equation turbulence model for indoor airflow simulation," *Energy and Buildings,* vol. 28, pp. 137-144, 1998.

[3] J. J. McCarthy, "Micro-modeling of cohesive mixing processes," *Powder Technology,* vol. 138, pp. 63-67, 2003.

[4] G. E. Moore, " Cramming More Components onto Integrated Circuits,", *Electron* vol. 38, pp. 114–117, 1965.

[5] B. Agostini, M. Fabbri, J. E. Park, L. Wojtan, J. R. Thome, and B. Michel, "State of the Art of High Heat Flux Cooling Technologies," *Heat Transfer Engineering,* vol. 28, pp. 258-281, 2014/09/01 2007.

[6] Y. Avenas, M. Ivanova, N. Popova, C. Schaeffer, J. L. Schanen, and A. Bricard, "Thermal analysis of thermal spreaders used in power electronics cooling," in *Industry Applications Conference, 2002. 37th IAS Annual Meeting. Conference Record of the*, 2002, pp. 216-221 vol.1.

[7] T. J. Lu, "Thermal management of high power electronics with phase change cooling," *International Journal of Heat and Mass Transfer,* vol. 43, pp. 2245-2256, 7/1/ 2000.

[8] A. Bejan, "Laminar Boundary Layer Flow," in *Convection Heat Transfer*, ed: John Wiley & Sons, Inc., 2013, pp. 30-95.

[9] Y. E. Cengel, *Heat & mass transfer: a practical approach*, Third ed.: McGraw-Hill, 2007.

[10] B. Ghasemi and S. M. Aminossadati, "Numerical simulation of mixed convection in a rectangular enclosure with different numbers and arrangements of discrete heat sources," *The Arabian Journal for Science and Engineering* vol. 33, April 2008.

[11] C. Li, X. Li, Y. Su, and Y. Zhu, "A new zero-equation turbulence model for micro-scale climate simulation," *Building and Environment,* vol. 47, pp. 243-255, 2012.

[12] R. Feurich and N. R. B. Olsen, "Finding Free Surface of Supercritical Flows - Numerical Investigation," *Engineering Applications of Computational Fluid Mechanics,* vol. 6, pp. 307-315, 2012/01/01 2012.

[13] A. Bar-Cohen, "Thermal Management of Electronic Components with Dielectric Liquids," *JSME international journal. Ser. B, Fluids and thermal engineering,* vol. 36, pp. 1-25, 1993.

[14] E. Bergles, Ma, C.-F., "Boiling jet impingement cooling of simulated microelectronic chips," *Heat transfer in electronic equipment* pp. 5-12, November 13-18 1983.

[15] S. V. Garimella, "Advances in mesoscale thermal management technologies for microelectronics," *Microelectron. J.,* vol. 37, pp. 1165-1185, 2006.

[16] F. P. Incropera, J. S. Kerby, D. F. Moffatt, and S. Ramadhyani, "Convection heat transfer from discrete heat sources in a rectangular channel," *International Journal of Heat and Mass Transfer,* vol. 29, pp. 1051-1058, 1986.

[17] T. C. Willingham and I. Mudawar, "Forced-convection boiling and critical heat flux from a linear array of discrete heat sources," *International Journal of Heat and Mass Transfer,* vol. 35, pp. 2879-2890, 1992.

[18] S. Lee and M. M. Yovanovich, "Conjugate Heat Transfer From a Vertical Plate With Discrete Heat Sources Under Natural Convection," *Journal of Electronic Packaging,* vol. 111, pp. 261-267, 1989.

[19] R. Schmidt, "Challenges in Electronic Coolingâ€"Opportunities for Enhanced Thermal Management Techniquesâ€"Microprocessor Liquid Cooled Minichannel Heat Sink," *Heat Transfer Engineering,* vol. 25, pp. 3-12, 2014/08/31 2004.

[20] M. L. Chadwick, B. W. Webb, and H. S. Heaton, "Natural convection from two-dimensional discrete heat sources in a rectangular enclosure," *International Journal of Heat and Mass Transfer,* vol. 34, pp. 1679-1693, 1991.

[21] G. I. Sultan, "Enhancing forced convection heat transfer from multiple protruding heat sources simulating electronic components in a horizontal channel by passing cooling," *Microelectronics Journal* vol. 31, pp. 773-779., 2000.

[22] A. B. McEntire and B. W. Webb, "Local forced convective heat transfer from protruding and flush-mounted two-dimensional discrete heat sources," *International Journal of Heat and Mass Transfer,* vol. 33, pp. 1521-1533, 1990.

[23] C. Y. Choi and A. Ortega, "Mixed convection in an inclined channel with a discrete heat source," in *Thermal Phenomena in Electronic Systems, 1992. I-THERM III, InterSociety Conference on*, 1992, pp. 40-48.

[24] B. Premachandran and C. Balaji, "Conjugate mixed convection with surface radiation from a horizontal channel with protruding heat sources," *International Journal of Heat and Mass Transfer,* vol. 49, pp. 3568-3582, 2006.

[25] T. A. Alves and C. A. C. Altemani, "Convective cooling of three discrete heat sources in channel flow," *Journal of the Brazilian Society of Mechanical Sciences and Engineering,* vol. 30, pp. 245-252, 2008.

[26] A. Yutaka and F. Mohammad, "Three-dimensional heat transfer analysis of arrays of heated square blocks," *International Journal of Heat and Mass Transfer,* vol. 32, pp. 395-405, 1989.

[27] L. T. F. Culham J R, Lee S, Yovanovich MM, "META− A conjugate heat transfer model foe air cooling of circuit boards with arbitrarily heat source
" *Heat Transfer in Electronic Equipment ASME* . vol. 171, 1991.

[28] Y. P. Cheng, T. S. Lee, and H. T. Low, "Numerical analysis of mixed convection in three-dimensional rectangular channel with flush-mounted heat sources based on field synergy principle," *International Journal for Numerical Methods in Fluids,* vol. 52, pp. 987-1003, 2006.

[29] Y. P. Cheng, T. S. Lee, and H. T. Low, "Numerical simulation of conjugate heat transfer in electronic cooling and analysis based on field synergy principle," *Applied Thermal Engineering,* vol. 28, pp. 1826-1833, 2008.

[30] F. C. Hung TC, "Conjugate heat transfer anakysis for the passive enhancement of electronic cooling through geometric modification in a mixed convective

domain," *Numerical Heat Transfer, Part A: Applications,* vol. 35, pp. 519-535, 2014/09/01 1999.

[31] T. A. Alves and C. A. C. Altemani, "An invariant descriptor for heaters temperature prediction in conjugate cooling," *International Journal of Thermal Sciences,* vol. 58, pp. 92-101, 8// 2012.

[32] T. J. Young and K. Vafai, "Convective flow and heat transfer in a channel containing multiple heated obstacles," *International Journal of Heat and Mass Transfer,* vol. 41, pp. 3279-3298, 1998.

[33] Y. Zeng and K. Vafai, "An Investigation of Convective Cooling of an Array of Channel-Mounted Obstacles," *Numerical Heat Transfer, Part A: Applications,* vol. 55, pp. 967-982, 2014/11/11 2009.

[34] M. El Nakla, "Forced Convection Heat Transfer in Two-Dimensional Ribbed Channels with Varying Heat Flux Profiles Using ANSYSâ€™ Software and Modeling," *Arabian Journal for Science and Engineering,* vol. 39, pp. 2157-2164.

[35] Y. Liu, S. Chen, and B. W. Shiu, "An optimum spacing problem for four chips on a horizontal substrate â€“ mixed convection," *Computational Mechanics,* vol. 26, pp. 470-477, 2000-11-01 2000.

[36] S. Chen and Y. Liu, "An optimum spacing problem for three-by-three heated elements mounted on a substrate," *Heat and Mass Transfer,* vol. 39, pp. 3-9, 2002-11-01 2002.

[37] A. K. da Silva, S. Lorente, and A. Bejan, "Optimal distribution of discrete heat sources on a plate with laminar forced convection," *International Journal of Heat and Mass Transfer,* vol. 47, pp. 2139-2148, 2004.

[38] E. Jassim and Y. S. Muzychka, "Optimal Distribution of Heat Sources in Convergent Channels Cooled by Laminar Forced Convection," *Journal of Heat Transfer,* vol. 132, pp. 011701-011701, 2009.

[39] K.-Y. Kim and J.-Y. Choi, "Shape Optimization of a Dimpled Channel to Enhance Turbulent Heat Transfer," *Numerical Heat Transfer, Part A: Applications,* vol. 48, pp. 901-915, 2014/10/14 2005.

[40] K.-Y. Kim and S.-S. Kim, "Shape optimization of rib-roughened surface to enhance turbulent heat transfer," *International Journal of Heat and Mass Transfer,* vol. 45, pp. 2719-2727, 2002.

[41] T. Bello-Ochende, J. P. Meyer, and A. Bejan, "Constructal ducts with wrinkled entrances," *International Journal of Heat and Mass Transfer,* vol. 52, pp. 3628-3633, 2009.

[42] T. Bello-Ochende, J. P. Meyer, and J. Dirker, "Three-dimensional multi-scale plate assembly for maximum heat transfer rate density," *International Journal of Heat and Mass Transfer,* vol. 53, pp. 586-593, 2010.

[43] T. Bello-Ochende, J. P. Meyer, and F. U. Ighalo, "Combined Numerical Optimization and Constructal Theory for the Design of Microchannel Heat Sinks," *Numerical Heat Transfer, Part A: Applications,* vol. 58, pp. 882-899, 2014/10/29.

[44] T. Bello-Ochende, J. P. Meyer, and O. I. Ogunronbi, "Constructal multiscale cylinders rotating in cross-flow," *International Journal of Heat and Mass Transfer,* vol. 54, pp. 2568-2577, 2011.

[45] O. T. Olakoyejo, T. Bello-Ochende, and J. P. Meyer, "Constructal conjugate cooling channels with internal heat generation," *International Journal of Heat and Mass Transfer,* vol. 55, pp. 4385-4396, 2012.

[46] T. Bello-Ochende, J. P. Meyer, and A. Bejan, "Constructal multi-scale pinâ€“fins," *International Journal of Heat and Mass Transfer,* vol. 53, pp. 2773-2779, 2010.

[47] M. R. Hajmohammadi, E. Shirani, M. R. Salimpour, and A. Campo, "Constructal placement of unequal heat sources on a plate cooled by laminar forced convection," *International Journal of Thermal Sciences,* vol. 60, pp. 13-22, 2012.

[48] W. M. H K Versteeg, *An Introduction to Computational Fluid Dynamics: The Finite Volume Method*, Second ed.: Pearson Prentice Hall, 2007.

[49] STAR-CCM+, " USER GUIDE ", 8.02 ed: CD-adapco, 2013.

[50] S. V. Patankar and D. B. Spalding, "A calculation procedure for heat, mass and momentum transfer in three-dimensional parabolic flows," *International Journal of Heat and Mass Transfer,* vol. 15, pp. 1787-1806, 1972.

[51] F. M. White, *Fluid Mechanics*, Sixth Edition ed.: McGraw-Hill, 2007.

[52] F. M. White, *VISCOUS FLUID FLOW*, Third dition ed. Singapore: McGraw-Hill, 2006.

[53] W. M. Kays and M. E. Crawford, *Convective heat and mass transfer*, Second Edition ed.: McGraw-Hill, New York, 1980.

[54] S. Chen, Y. Liu, S. F. Chan, C. W. Leung, and T. L. Chan, "Experimental study of optimum spacing problem in the cooling of simulated electronic package," *Heat and Mass Transfer,* vol. 37, pp. 251-257, 2001.

[55] T. J. Young and K. Vafai, "Experimental and Numerical Investigation of Forced Convective Characteristics of Arrays of Channel Mounted Obstacles," *Journal of Heat Transfer,* vol. 121, pp. 34-42, 1999.

[56] A. Bar-Cohen and A. D. Kraus, *Advances in thermal modeling of electronic components and systems*, 1988.

[57] Y. Liu, N. Phan-Thien, C. W. Leung, and T. L. Chan, "An optimum spacing problem for five chips on a horizontal substrate in a vertically insulated enclosure," *Computational Mechanics,* vol. 24, pp. 310-318, 1999.

[58] Y. L. N. Phan-Thien, "AN OPTIMUM SPACING PROBLEM FOR THREE CHIPS MOUNTED ON A VERTICAL SUBSTRATE IN AN ENCLOSURE," *Numerical Heat Transfer, Part A: Applications,* vol. 37, pp. 613-630, 2000.

[59] Q. Wang and Y. Jaluria, "Instability and heat transfer in a mixed-convection flow in a horinzontal duct with discrete heat sources," *Numerical Heat Transfer, Part A: Applications,* vol. 42, pp. 445-463, 2002.

[60] S. J. Kim and S. W. Lee, *Air cooling technology for electronic equipment*: CRC press, 1996.

[61] A. M. Anderson, "Decoupling Convective and Conductive Heat Transfer Using the Adiabatic Heat Transfer Coefficient," *Journal of Electronic Packaging,* vol. 116, pp. 310-316, 1994.

[62] R. J. Moffat, "What's new in convective heat transfer?," *International Journal of Heat and Fluid Flow,* vol. 19, pp. 90-101, 1998.

[63] J. Rhee, "The Role of Superposition Techniques in Thermal Management," in *Advanced Packaging Materials: Processes, Properties and Interface, 200611th International Symposium on*, 2006, pp. 163-168.

[64] T. J. Young and K. Vafai, "Convective cooling of a heated obstacle in a channel," *International Journal of Heat and Mass Transfer,* vol. 41, pp. 3131-3148, 1998.

[65] R. D. Cess and E. C. Shaffer, "Heat transfer to laminar flow between parallel plates with a prescribed wall heat flux," *Applied Scientific Research, Section A,* vol. 8, pp. 339-344, 1959.

[66] J. Rhee and S. I. Hernandez, "Thermal Management of Electronics in Telecommunications Products: Designing for the Network Equipment Building System (NEBS) Standards," *Journal of Electronic Packaging,* vol. 128, pp. 484-493, 2006.

[67] S. Oktay, R. J. Moffat, A. S. o. M. Engineers, and A. S. o. M. E. H. T. D. K.-. Committee, *Heat transfer in electronic equipment - 1985: presented at the 23rd National Heat Tranfer Conference, Denver, Colorado, August 4-7, 1985*: ASME, 1985.

[68] Snyman, Springer,J.A, *Practical mathematical optimisation: an introduction to basic optimisation theory and classical and new gradient-based algorithms*. New York: Springer, 2005.

[69] HEEDS, "- mdo Getting Started Guide," ed: Red Cedar Technology, 2011.

[70] A. K. da Silva, S. Lorente, and A. Bejan, "Constructal multi-scale structures with asymmetric heat sources of finite thickness," *International Journal of Heat and Mass Transfer,* vol. 48, pp. 2662-2672, 2005.

[71] T. Dias Jr and L. F. Milanez, "Optimal location of heat sources on a vertical wall with natural convection through genetic algorithms," *International Journal of Heat and Mass Transfer,* vol. 49, pp. 2090-2096, 2006.

[72] R. R. Madadi and C. Balaji, "Optimization of the location of multiple discrete heat sources in a ventilated cavity using artificial neural networks and micro genetic algorithm," *International Journal of Heat and Mass Transfer,* vol. 51, pp. 2299-2312, 2008.